



UNICAMP

PATRÍCIA SEVERINO

**“DESENVOLVIMENTO E CARACTERIZAÇÃO
FÍSICO-QUÍMICA DE NANOPARTÍCULAS
LIPÍDICAS SÓLIDAS PARA ENCAPSULAÇÃO DE
PROTEÍNAS”**

CAMPINAS

2012



UNICAMP

UNIVERSIDADE ESTADUAL DE CAMPINAS

FACULDADE DE ENGENHARIA QUÍMICA

PATRÍCIA SEVERINO

**“DESENVOLVIMENTO E CARACTERIZAÇÃO FÍSICO-QUÍMICA DE
NANOPARTÍCULAS LIPÍDICAS SÓLIDAS PARA ENCAPSULAÇÃO DE
PROTEÍNAS”**

Orientador/supervisor: Profa. Dra. Maria Helena Andrade Santana

Tese de Doutorado apresentada a Faculdade de Engenharia Química da Universidade Estadual de Campinas (Unicamp) para obtenção do título de Doutor em Engenharia Química, na área de concentração de Desenvolvimento de Processos Biotecnológicos.

Este exemplar corresponde à versão final da tese de doutorado defendida pela aluna Patrícia Severino, e orientada pela Profa. Dra. Maria Helena Andrade Santana.

Profa. Dra. Maria Helena Andrade Santana

CAMPINAS

2012

FICHA CATALOGRÁFICA ELABORADA PELA
BIBLIOTECA DA ÁREA DE ENGENHARIA E ARQUITETURA - BAE -
UNICAMP

Se83d Severino, Patrícia
Desenvolvimento e caracterização físico-química de nanopartículas lipídicas sólidas para encapsulação de proteínas / Patrícia Severino. --Campinas, SP: [s.n.], 2012.

Orientador: Maria Helena Andrade Santana.
Tese de Doutorado - Universidade Estadual de Campinas, Faculdade de Engenharia Química.

1. Físico-química. 2. Nanopartículas. 3. Lipídios. 4. Encapsulação. I. Santana, Maria Helena Andrade, 1951-. II. Universidade Estadual de Campinas. Faculdade de Engenharia Química. III. Título.

Título em Inglês: Development and physical chemistry characterization of solid lipid nanoparticles for encapsulating proteins

Palavras-chave em Inglês: Physical chemistry , Nanoparticles, Lipids, Encapsulation

Área de concentração: Desenvolvimento de Processos Biotecnológicos

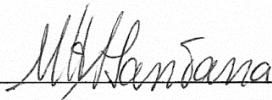
Titulação: Doutora em Engenharia Química

Banca examinadora: Eliana Maria Barbosa Souto, Maria Palmira Daflon Gremião, Adriano Rodrigues Azzoni, Marco Vinicius Chaud

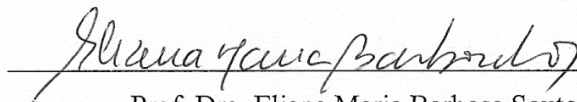
Data da defesa: 06-08-2012

Programa de Pós Graduação: Engenharia Química

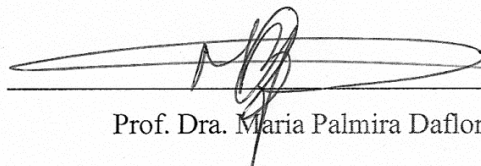
Tese de Doutorado defendida por Patrícia Severino e aprovada em 06 de agosto de 2012
pela banca examinadora constituída pelos doutores:



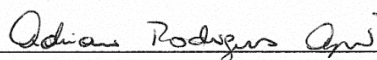
Prof. Dra. Maria Helena Andrade Santana



Prof. Dra. Eliana Maria Barbosa Souto



Prof. Dra. Maria Palmira Daflon Gremião



Prof. Dr. Adriano Rodrigues Azzoni



Prof. Dr. Marco Vinicius Chaud

Dedico este trabalho aos meus pais

Ivone e Dirceu (in memoriam)

Agradecimentos

Eu considero os agradecimentos à parte mais árdua deste trabalho, mas muito gratificante por ter a oportunidade de reconhecer as pessoas que me ajudaram a trilhar este caminho. Perto ou longe, diariamente ou esporadicamente participaram da minha caminhada não somente com contribuições científicas, mas também como amigos que vou levar pela vida.

À Profa. Dra. Maria Helena Santana pela orientação, paciência, atenção e confiança depositadas em meu trabalho.

À Profa. Dra. Eliana Souto pela atenção e disponibilidade em me receber em Portugal.

Agradeço aos meus pais pela dedicação, incentivo e carinho que me fizeram que eu conseguisse alcançar mais essa etapa da vida.

Ao Prof. Dr. Marco V. Chaud por ter despertado meu interesse para a pesquisa na graduação. Obrigado por ter me acompanhado e ajudado a vencer os desafios.

Aos amigos do Laboratório de Desenvolvimento de Processos Biotecnológicos, Andréa, Amanda, Leandra, Caroline, Gabriela, Fernanda, Marina, Tiago, Leandro, Felipe, Carla, Carolina, Fernanda, Rafaela, Viviane, André, Anayla, Absolom, Rafael, Micaela, pelos dias que compartilhamos juntos e pela amizade. Especialmente para nosso técnico Gilson que em todos os momentos me ajudou com grande empenho.

Aos amigos do Laboratório da Universidade Fernando Pessoa, Joana, Tatiana, Rita, Tarek e Ana que me receberam de braços abertos.

Aos amigos do Centro de Biologia Molecular e Engenharia Genética (CBMEG), que foram de extrema parceria e companheiro nos experimentos finais desta tese. Meu

muito obrigado ao Marcelo, Marianna, Clelton, Aline, Julina, Maria Augusta, professor Dr. Adriano Azzoni, Lilian e André.

Ao Rafael Basso pela parceria e aprendizado. Uma pessoa ímpar em amizade, trabalho e carisma.

Aos Classius e ao Araújo pelo companheirismo, sem vocês tudo teria sido mais difícil. Obrigada pelas deliciosas viagens que partilhamos pelo velho mundo.

Aos amigos de todos os momentos Patrícia Zancanella, Cibelem Benites, Mariana Altenhofen da Silva, Marina Miranda, Georgiana Pascotto, Camila, Andréia Padovese, Bruno Mastrocola, Priscila de Oliveira, Alessandra pela amizade e momentos inesquecíveis que passamos juntos.

Aos funcionários e professores da FEQ.

A todas as pessoas que, direta ou indiretamente tornaram esse trabalho agradável e ajudaram com a minha formação pessoal e profissional.

“Há Momentos

Há momentos na vida em que sentimos tanto
a falta de alguém que o que mais queremos
é tirar esta pessoa de nossos sonhos
e abraçá-la.

Sonhe com aquilo que você quiser.
Seja o que você quer ser,
porque você possui apenas uma vida
e nela só se tem uma chance
de fazer aquilo que se quer.

Tenha felicidade bastante para fazê-la doce.
Dificuldades para fazê-la forte.
Tristeza para fazê-la humana.
E esperança suficiente para fazê-la feliz.

As pessoas mais felizes
não têm as melhores coisas.
Elas sabem fazer o melhor
das oportunidades que aparecem
em seus caminhos.

A felicidade aparece para aqueles que choram.
Para aqueles que se machucam.
Para aqueles que buscam e tentam sempre.
E para aqueles que reconhecem
a importância das pessoas que passam por suas vidas.

O futuro mais brilhante
é baseado num passado intensamente vivido.
Você só terá sucesso na vida
quando perdoar os erros
e as decepções do passado.

A vida é curta, mas as emoções que podemos deixar
duram uma eternidade.
A vida não é de se brincar
porque um belo dia se morre”.

Clarice Lispector

Resumo

Nanopartículas Lipídicas Sólidas (NLS) vêm sendo investigadas desde o início dos anos 90. As dispersões de NLS apresentam como característica principal a interação com moléculas dos fármacos ou proteínas resultando em uma liberação sustentada e o transporte do princípio ativo até o alvo terapêutico, aumentando assim a sua eficácia de ação.

Este trabalho teve como objetivo o desenvolvimento de NLS empregando vários tipos de lipídios (Dynasan[®] 114, Dynasan[®] 118, Ácido esteárico, Cetilpalmitato, Softisan[®] 100), misturas de tensoativos (Tween[®] 80, Span[®] 85, Span[®] 80, Lipoid[®] S75) e de metodologias de homogeneização a alta pressão a quente e dupla emulsificação (A/O/A). A caracterização da pré-formulação por realizada por análises térmicas, morfologia e equilíbrio hidrofílico lipofílico (EHL). Os processos de produção empregados foram otimizados com planejamento de experimentos e as NLS produzidas foram caracterizadas quanto ao tamanho, polidispersidade, potencial zeta, eficiência de encapsulação, citotoxicidade, capacidade de transfecção, morfologia e estabilidade. Proteína modelos foi encapsulada em NLS desenvolvidas pela metodologia de dupla emulsificação. As NLS apresentaram baixa toxicidade em estudos celulares, estabilidade em estudos *in vitro*, e morfologia esférica. Adicionalmente, foi acrescentado carga superficial catiônica e ensaios de capacidade de transfecção mostraram satisfatórios. As NLS desenvolvidas neste trabalho apresentaram promissoras para encapsulação de proteínas e possivelmente ácidos nucleicos para administração parenteral.

Abstract

Solid Lipid Nanoparticles (SLN) have been investigated since the early 90s. The SLN dispersions have as main feature the strong interaction with drugs molecule or proteins resulting in a sustained release and target specific delivery increasing the action.

This work aimed at the development of NLS employing various types of lipids (dynasan[®] 114, dynasan[®] 118, stearic acid, cetyl palmitate, softisan[®] 100), mixtures of surfactants (tween[®] 80, span[®] 85, span[®] 80, lipoid[®] S75) and methods for hot high pressure omogenization and double emulsification (w/o/a). The pre formulation characterization was performed by thermal analysis, morphology and Hydrophilic Lipophilic Balance (HLB). The production processes were optimized with factorial design and NLS were characterized by size, polydispersidade, zeta potential, encapsulation efficiency, cytotoxicity, transfection capacity, morphology and stability. Model Protein was encapsulated in NLS developed by double emulsification methodology. The NLS showed low toxicity in cellular studies, stability *in vitro* and spherical morphology. Additionally, was added cationic charge in surface and evaluate capacity of transfection in Hela cells. The NLS developed in this work showed promise for encapsulation of proteins and, possibly, nucleic acids for parenteral administration.

Sumário

Resumo	viii
Abstract	ix
Lista de Figuras	
Lista de Tabelas	
Lista de abreviações	
Introdução	1
Objetivo	6
 <i>Capítulo 1</i>	
Nanopartículas de lipídios sólidos: métodos clássicos de produção laboratorial	7
Crystallinity of Dynasan [®] 114 and Dynasan [®] 118 matrices for the production of stable Miglyol [®] loaded nanoparticles	38
 <i>Capítulo 2</i>	
Current State-of-Art and New Trends on Lipid Nanoparticles (SLN and NLC) for Oral Drug Delivery	61
Polymorphism, crystallinity and hydrophilic–lipophilic balance of stearic acid and stearic acid–capric/caprylic triglyceride matrices for production of stable nanoparticles	97
Optimizing SLN and NLC by 22 full factorial design: Effect of homogenization technique	118
 <i>Capítulo 3</i>	
Development potential solid lipid nanoparticles carrier for vehicle proteins	139
Development Cationic Lipid carrier for transfection cell	165
Conclusões finais	183
Sugestões para próximos trabalhos	185

Lista de Figuras

Capítulo 1

Crystallinity of Dynasan[®] 114 and Dynasan[®] 118 matrices for the production of stable Miglyol[®] loaded nanoparticles

- Figure 1.** WAXD diffractogram after fusion of (a) Dynasan[®]114 and (b) Dynasan[®]118. 48
- Figure 2.** WAXD diffractogram after fusion (a) Dynasan[®]114 and Miglyol[®]812; (b) Dynasan[®]114 and Miglyol[®]840; (c) Dynasan[®]118 and Miglyol[®]812; (d) Dynasan[®]118 e Miglyol[®]840. 50
- Figure 3.** WAXD diffractogram after fusion (a) Dynasan[®]114 and Miglyol[®]812 (b) Dynasan[®]114 and Miglyol[®]840, (c) Dynasan[®]118 and Miglyol[®]812. (d) Dynasan[®]118 and Miglyol[®]840. 53
- Figure 4.** Micrographs obtained by PLM (a) Dynasan[®]114, (b) Dynasan[®]118, (c) Dynasan[®]114 and Miglyol[®]812 (70:30); (b) Dynasan[®]114 and Miglyol[®]840 (70:30); (c) Dynasan[®]118 and Miglyol[®]812 (70:30); (d) Dynasan[®]118 e Miglyol[®]840 (70:30). 55

Capítulo 2

Polymorphism, crystallinity and hydrophilic–lipophilic balance of stearic acid and stearic acid–capric/caprylic triglyceride matrices for production of stable nanoparticles

- Figure 1.** WAXD diffractogram recorded for stearic acid (upper) and stearic acidcapric/caprylic triglycerides (lower) before tempering. Intensity (arbitrary units). 109
- Figure 2.** WAXD diffractogram recorded for stearic acid (upper) and stearic acidcapric/caprylic triglycerides (lower) after tempering. Intensity (arbitrary units). 111
- Figure 3.** Micrographs obtained by PLM of stearic acid (a) and of stearic acidcapric/caprylic triglycerides (b) before tempering; and of stearic 112

acid (c) and stearic acid–capric/caprylic triglycerides (d) after tempering.

Figure 4. Stability of stearic acid–capric/caprylic triglycerides emulsion recorded after 24 h. 113

Optimizing SLN and NLC by 22 full factorial design: Effect of homogenization technique

Figure 1. Influence of HSH intensity on the particle size of the pre-emulsion to produce (a) SLN and (b) NLC. 124

Figure 2. Surface response charts of experimental design SLN (a) particle size; (b) zeta potential; (c) polydispersity index. Color codes stand for the area below the given value. 126

Figure 3. Pareto chart of the standardized effects for SLN (a) particle size; (b) zeta potential; (c) polydispersity index. 127

Figure 4. Surface response charts of experimental design NLC (a) particle size; (b) zeta potential; (c) polydispersity index. Color codes stand for the area below the given value. 130

Figure 5. Pareto chart of the standardized effects for NLC (a) particle size; (b) zeta potential; (c) polydispersity index 131

Capítulo 3

Development potential solid lipid nanoparticles carrier for vehicle proteins

Figure 1. Pareto chart of the standardized effects for SLN (a) size, (b) polydispersity index, (c) zeta potential, (e) encapsulation efficiency. 150

Figure 2. Surface response charts of experimental design of SLN. 151

Figure 3. DSC thermograms (a) Softisan before and after tempering; (b) SLN empty and loading insulin. 153

Figure 4. WAXD diffractogram (a) Softisan[®] 100 before and after tempering, (b) WAXD diffractogram SLN. 155

Figure 5. Cell viability determined by alamar blue[®] assay, after exposition to blank and SLN formulations (concentration 1%, 2%, 5% and 10%) 156

prepared by double emulsion technique. The results are average values (n=3), compared balnk and control cells (unexposed to SLN).

Figure 6. Distribution of R_h for SLN ($6.25 \mu\text{g.mL}^{-1}$) in presence of 45 mg.mL^{-1} HSA dissolved in PBS at various times during 24 hours. 158

Figure 7. R_h vs. time of the SLN in presence of 45 mg.mL^{-1} HSA dissolved in PBS. 158

Figure 8. (a) Transmission electron micrograph (TEM) (b) Scanning electron micrograph (SEM). 159

Development Cationic Lipid carrier for transfection cell

Figure 1. Release profile of protein vs time by double emulsion method (Protein-free: aqueous solution of protein; I-SLN: insulin loaded SLN). The results are average values (n=3). 175

Figure 2. Cell viability determined by WST-1 essay (a) SLN empty after exposition to SLN formulations (concentration 1%, 2%, 5% and 10%) and control prepared by double emulsion technique. The results are average values (n=6). 176

Figure 3. SLN loading Lc8 incubated for 4 h detected by detected by western blot technique. C: control; 1: SLN concentration 1 %, 2: SLN concentration 2 %, 3: SLN concentration 5 %, 4: SLN contraction 10 %. The results are average values (n=3). 177

Figure 4. Transmission electron microscopy images of SLN. 177

Lista de Tabelas

Capítulo 1

Nanopartículas de lipídios sólidos: métodos clássicos de produção laboratorial

Tabela 1. Fármacos incorporados em NLS e sua composição	10
Tabela 2. Estrutura tridimensional das três formas mais comuns de polimorfismo em triacilgliceróis	16
Crystallinity of Dynasan [®] 114 and Dynasan [®] 118 matrices for the production of stable Miglyol [®] loaded nanoparticles	
Table 1. Composition of lipid mixtures % (w/w).	42
Table 2. Composition of solid lipid nanoparticles, values in % (w/w)	43
Table 3. Thermal properties of lipids mixtures	46
Table 4. Thermal properties of lipids mixtures after and before tempering	47

Capítulo 2

Current State-of-Art and New Trends on Lipid Nanoparticles (SLN and NLC) for Oral Drug Delivery

Table 1. Examples of drugs, miscellaneous active ingredients and macrocyclic skeletons incorporated into lipid nanoparticles.	68
Table 2. Lipids used for lipid nanoparticles production.	71
Table 3. Emulsifiers used for the production of lipid nanoparticles.	73
Polymorphism, crystallinity and hydrophilic–lipophilic balance of stearic acid and stearic acid–capric/caprylic triglyceride matrices for production of stable nanoparticles	
Table 1. HLB values obtained for different blends of lipid and surfactant combinations for 7 emulsions (n = 5).	104
Table 2. DSC analysis of stearic acid and stearic acid–capric/caprylic triglycerides, before and after tempering the samples for 1 h at 80 °C.	105
Table 3. DSC analysis of crystallization of stearic acid and stearic acid–capric/caprylic triglycerides, before and after tempering the samples	106

for 1 h at 80 °C.

Optimizing SLN and NLC by 22 full factorial design: Effect of homogenization technique

Table 1. Initial 2-level full factorial design, providing the lower (-1), upper (+1) and (0) central point level values for each variable.	123
Table 2. Influence of pressure and number of homogenization cycles used for the production of SLN.	125
Table 3. Influence of pressure and number of homogenization cycles used for the production of NLC.	128

Capítulo 3

Development potential solid lipid nanoparticles carrier for vehicle proteins

Table 1. Factorial design 2^2 with triplicate of central point.	144
Table 2. Results of design factorial for SLN loading insulin.	149

Development Cationic Lipid carrier for transfection cell

Table 1. Particle size, polydispersity index, zeta potential and entrapment efficiency of SLN formulations, ($n = 3$). SLN: empty SLN; I-SLN: insulin loaded SLN.	174
Table 2. Stability of SLN after lyophilization ($n = 3$). SLN: empty SLN; I-SLN: insulin loaded SLN.	174

Lista de Abreviações

CCD	Central Composite Design
CI	Crystallinity index
CTAB	Brometo de cetil trimetil amônio
DNA	Deoxyribonucleic acide
DSC	Differential scanning calorimetry
EE	Entrapment efficiency
EHL	Equilíbrio Hidrofílico Lipofílico
EP	External aqueous phase
FDA	Food and Drug Administration
GIT	Gastro intestinal tract
GRAS	Generally Recognized As Safe
HAP	Homogeneização a alta pressão
HLB	Hydrophilic-Lipophilic Balance
HPH	High pressure homogenization
HSH	High shear homogenization
IP	Internal aqueous phase
LC	Loading capacity
LCT	Long-chain triglycerides
LL	Liquid lipid
LP	Lipid phase
MCT	Medium-chain triglycerides
MTT	(3-(4,5-Dimethylthiazol-2-yl)-2,5-diphenyltetrazolium bromide
NLC	Nanostructured lipid Carrier
NLS	Nanopartículas lipídicas sólidas
OMS	Organização Mundial da Saúde
PCS	Photon Correlation Spectroscopy
PI	Polidispersity index
PLM	Polarized Light Microscopy
ROS	Reactive oxygen species

SEM	Scanning electron micrograph.
SL	Solid lipid
SLN	Solid lipid nanoparticle
TEM	Transmission Electron Microscope
WAXD	Wide angle X-ray diffraction
z-ave	Size
ZP	Zeta potential

Introdução

Nanopartículas Lipídicas Sólidas (NLS) vem sendo investigadas desde o início dos anos 90. A produção das NLS é baseada no conceito da substituição do centro aquoso de emulsões por lipídios sólidos.

A primeira geração das NLS foi produzida somente com lipídios sólidos e tensoativos e, em seguida, uma segunda geração denominada de carreadores lipídicos nanoestruturados foi desenvolvida utilizando lipídio sólido, líquido e tensoativo. A segunda geração surgiu com o intuito de produzir uma matriz lipídica, menos estruturada em relação à cristalinidade, capaz de obter melhor eficiência de encapsulação e evitar a liberação do fármaco durante a estocagem.

As vantagens das dispersões de NLS são em relação ao custo acessível das matérias primas empregado na produção, insenção do uso de solventes orgânicos, e os lipídios e tensoativos estão de acordo com *Generally Recognized As Safe (GRAS)* e *Food and Drug Administration (FDA)*.

Este trabalho teve como objetivo o desenvolvimento e caracterização físico-química de NLS pelo método de homogeneização a alta pressão e ultra-turrax[®] para encapsulação de proteínas.

O **Capítulo 1** é iniciado com um artigo científico denominado “Nanopartículas de lipídios sólidos: métodos clássicos de produção laboratorial”, o qual aborda os métodos clássicos de produção laboratorial das NLS existentes na literatura que serviu de referência para a produção das NLS neste trabalho.

Na segunda parte deste capítulo em artigo, denominada “Crystallinity of Dynasan[®] 114 e Dynasan[®] 118 matrices for the production of stable Miglyol[®] loaded nanoparticles”. A parte experimental consistiu na caracterização das misturas lipídicas em diferentes concentrações, através das técnicas de Calorimetria Diferencial de Varredura (DSC), Difractometria de raios-X (DRX) e Microscopia de Luz Polarizada (PLM). As matérias primas utilizadas foram triglicerídeos sólidos (Dynasan[®] 114 e Dynasan[®] 118), líquidos (Miglyol[®] 812 e Miglyol[®] 840), e o tensoativo Tween[®] 80. As misturas lipídicas mais promissoras, aquelas que apresentaram maior desordem cristalina, foram também submetidas a um processo denominado temperagem (aquecimento a 80 °C por 1 hora) e reanalisadas pelas mesmas técnicas citadas acima. Em seguida foi realizada a produção das NLS pelo método de Homogeneização a Alta Pressão (HAP). Os resultados obtidos das análises das misturas lipídicas forneceram dados para o início dos ensaios preliminares da produção das NLS, e sua caracterização através de tamanho, índice de polidispersidade e potencial zeta. Logo após obter os primeiros ensaios e obter resultados satisfatórios teve-se dificuldade em realizar a reimportação dos lipídios (Dynasan[®] 114, Dynasan[®] 118, Miglyol[®] 812 e Miglyol[®] 840) previamente selecionados, por isso optou-se por trabalhar com matérias-primas de origem nacional (cetilpalmitato, ácido esteárico e Crodamol[®] GTCC).

O **Capítulo 2** é separado em três partes, o primeiro é uma revisão bibliográfica do uso das NLS para administração oral denominado de “Current State-of-Art and New Trends on Lipid Nanoparticles (SLN and NLC) for oral Drug delivery”.

Na segunda parte, a fase experimental inicia utilizando o ácido esteárico como lipídio sólido, Crodamol[®] GTCC como lipídio líquido e; Tween[®] 80 e Span[®] 85 como tensoativos. A caracterização das misturas de lipídicas através das técnicas de DSC, DRX e PLM foi

realizada antes e após o procedimento de temperagem. Após a caracterização das misturas lipídicas, estudou o cálculo teórico para a determinação do Equilíbrio Hidrofílico Lipofílico (EHL) para produção de NLS estáveis e foi publicado com o título de “Polymorphism, crystallinity and hydrophilic–lipophilic balance of stearic acid and stearic acid–capric/caprylic triglyceride matrices for production of stable nanoparticles”. Estudo semelhante foi realizado com o lipídio sólido cetilpalmitato e publicado nos anais do Congresso Colloids and Materials como “Polymorphic behavior and hydrophile-lipophile balance of lipid nanoparticles for improving drug delivery”.

Na terceira parte foi dada continuidade da parte experimental com a otimização da produção das NLS previamente estudadas. Este estudo foi publicado com o título de “Optimizing SLN and NLC by 2^2 full factorial design: Effect of homogenization technique”, baseou na produção das NLS de ácido estárico ou cetilpalmitato por ultra-turrax e HAP, operando isoladamente, ou em série. No ultra-turrax foi avaliado o efeito da velocidade de agitação e no HAP a pressão de alimentação e o número de passagens. Estes resultados delinearam a região de um planejamento fatorial 2^2 com triplicata no ponto central, para análise do efeito conjunto do processamento em série, nas propriedades das NLS (diâmetro, polidispersidade, potencial zeta).

O **Capítulo 3** foi dividido em 2 partes. A primeira envolveu o desenvolvimento de NLS pelo método de dupla emulsão utilizando o lipídio sólido softisan[®] 100 para encapsulação de proteínas modelos. O softisan[®] 100 apresenta ponto de fusão baixo em comparação com os lipídios empregados anteriormente, evitando altas temperaturas e possível degradação da proteína. A metodologia de dupla emulsão foi escolhida por demandar menor quantidade de matéria-prima e ser uma metodologia menos agressiva para manter a integridade da proteína. No desenvolvimento da NLS foi estudado a concentração dos tensoativos por um

Introdução

planejamento fatorial 2^2 com triplicata no ponto central, o efeito da toxicidade em células de HepG-2 e Caco-3 e estabilidade na presença de albumina *in vitro*. Este trabalho foi concluído e esta em fase de submissão para publicação com o título de “Development potential solid lipid nanoparticles carrier for proteins”.

Finalmente, para completar este estudo foi adicionado brometo de cetil trimetil amônio (CTAB) na formulação das NLS para obter carga positiva e avaliar a capacidade de transfeção em células HeLa empregando proteína modelo, o tempo de estocagem, toxicidade, morfologia e perfil de liberação *in vitro* da formulação. Os resultados mostraram que as NLS foi estável após armazenagem e o processo de liofilização, apresentou liberação controlada, morfologia esférica e capacidade de transfeção em células HeLa. Estes resultados também e em fase de submissão com o título de “Development Cationic Lipid carrier for transfection cell”.

Objetivo

O objetivo deste trabalho foi o desenvolvimento e caracterização físico-química de nanopartículas lipídicas sólidas pelo método de homogeneização a alta pressão e ultraturrax[®] para encapsulação de proteínas.

As metas para alcançar este objetivo foram:

- Seleção das matérias primas lipídicas e tensoativas;
- Estudo prévio da estabilidade das misturas lipídicas com as técnicas de calorimetria diferencial de varredura, difração de raios-X e microscopia de luz polarizada;
- Estudo do Equilíbrio Hidrofílico Lipofílico (EHL) das pré-formulações para produção das nanopartículas lipídicas sólidas;
- Seleção do método de produção e a otimização por planejamento experimental;
- Caracterização físico-química das nanopartículas;
- Modificação da superfície das nanopartículas utilizando brometo de cetil trimetil amônio;
- Avaliação da citotoxicidade em células do tipo Caco-3, HepG-2 e HeLa.
- Avaliação da capacidade de transfecção em células HeLa.
- Avaliação do perfil de liberação e estabilidade *in vitro*.

Capítulo 1

Nanopartículas de lipídios sólidos: métodos clássicos de produção laboratorial

Eliana B. Souto^{1,2}, **Patrícia Severino**^{1,3}, Maria Helena A. Santana³, Samantha C. Pinho⁴

¹Faculdade de Ciências da Saúde, Universidade Fernando Pessoa, 4200-150 Porto

²Instituto de Biotecnologia e Bioengenharia, Centro de Genómica e Biotecnologia, Universidade de Trás-os-Montes e Alto Douro, 5001-801 Vila Real - Portugal

³Departamento de Processos Biotecnológicos, Faculdade de Engenharia Química, Universidade de Campinas, 13083-852 Campinas – SP, Brasil

⁴Departamento de Engenharia de Alimentos, Faculdade de Zootecnia e Engenharia de Alimentos, Universidade de São Paulo, 13635- 900 Pirassununga – SP, Brasil

Artigo publicado na Revista Química Nova, Vol. 34, 10, 1762-1769, 2011.

Abstract

Solid lipid nanoparticles have been extensively investigated as drug delivery systems. These colloidal systems have major advantages compared to others more traditional. Reported advantages include sustained release, ability to solubilize lipophilic drugs, increased physical and chemical stability of labile molecules, decreased unwanted side-effects because they show lower toxicity, and easy to scale up. This paper aims at reviewing the traditional methods of solid lipid nanoparticles production, such as fusion-emulsification (hot and cold), solvent evaporation-emulsification and microemulsion, dealing with the main technological parameters that influence the quality properties of solid lipid nanoparticles.

Keywords: solid lipid nanoparticle, production of methods, technological parameters.

Introdução

Nanopartículas lipídicas sólidas (NLS) foram desenvolvidas em 1991, como um sistema alternativo de encapsulação de princípios ativos em relação aos sistemas coloidais tradicionais, tais como emulsões, lipossomas e nanopartículas poliméricas. O grande diferencial das NLS é a sua excelente estabilidade físico-química que proporciona maior proteção contra a degradação de fármacos lábeis.^{1,2} Na área farmacêutica, as NLS podem ser usadas por todas as vias de administração, como a oral,³ parenteral⁴ e cutânea⁵, devido seu tamanho reduzido, variando de 50 a 1000 nm e biocompatibilidade.^{6,7}

Diferentes métodos de produção de NLS permitem incorporar princípios ativos hidrossolúveis⁸ e lipossolúveis.⁹ No entanto, devido à natureza lipídica da matriz, as NLS são particularmente adequadas para veicular ativos apolares, para os quais evidenciam uma capacidade de carga elevada.¹⁰ A Tabela 1 apresenta alguns exemplos de fármacos, recentemente incorporados em NLS, assim como a composição lipídica dessas partículas. A preparação das NLS pode ser realizada por fusão-emulsificação, por emulsificação-evaporação do solvente, ou a partir de microemulsões.^{2,11}

Tabela 1. Fármacos incorporados em NLS e sua composição.

Fármacos incorporados em NLS	Composição	Referência
Vários	Precirol [®] ATO 5; Compritol [®] 888 ATO;	12
Corticosteróides	Dynasan [®] 114, Dynasan [®] 118, Softisan [®] 142, Tegin [®] 4100	12
Lopinavir	Compritol [®] 888 ATO	13
Carvedilol	Ácido esteárico	14
Luteína	Preceol [®]	15
Saquinavir	Compritol [®] 888 ATO e manteiga de cacau	16
Sinvastatina	Monoestearato de glicerina	17
Gatifloxacina	Compritol [®] ATO 888	18
5-flurouracilo	Dynasan [®] 114 and 118	19
Diazepam	Compritol [®] ATO 888; Imwitor [®] 900K	20
Dexametasona	Compritol [®] 888 ATO	21
Vinpocetine	Monoestearato de glicerina	22
Cetoprofeno	Cera de carnaúba	23
Itraconazol	Tristearina e triolina	24
Budesonida	Compritol [®] 888	25

1. Preparação das NLS por fusão-emulsificação

A preparação de NLS por fusão-emulsificação consiste na fusão prévia do lipídio incorporando o princípio ativo por dissolução ou por dispersão. Para aumentar a estabilidade da emulsão, geralmente é adicionado fosfatidilcolina ao lipídio fundido. Em seguida, esta fase é emulsificada numa fase aquosa, que contém um tensoativo do tipo O/A, como, por exemplo, um polisorbato^{16, 23, 26, 27} ou um polaxamer.¹⁵ No final, a emulsão recém-preparada é mantida à temperatura ambiente para a solidificação do lipídio e obtenção da dispersão aquosa de NLS.²⁸ Para a emulsificação do lipídio fundido com a fase aquosa faz-se uso de ultrassons^{20, 22, 29} ou de agitação mecânica,^{30, 31} podendo ainda proceder-se, adicionalmente, a uma operação complementar de Homogeneização a Alta Pressão (HAP).³²⁻³⁴ Estes procedimentos provocam a ruptura das gotículas lipídicas de maiores dimensões, originando gotículas pequenas, dispersas no meio da fase aquosa.³⁵

Os ultrassons e a agitação mecânica são métodos simples, mas apresentam a desvantagem de originarem NLS com dimensões heterogêneas.³⁶ Além disso, o uso de ultrassons é sempre acompanhado por um risco de contaminação por titânio e pela possibilidade de degradação do princípio ativo, devido à elevada força de cavitação aplicada. Para se obter partículas lipídicas de dimensões nanométricas são requeridos períodos de agitação superiores a 15 minutos e a presença de fosfatidilcolina no lipídio fundido. No entanto, o aumento da concentração desta última provoca uma diminuição da cristalinidade das nanopartículas formadas.³⁵ Além disso, as NLS que contêm uma concentração elevada de tensoativo não são apropriadas para administração intravenosa.³⁷

A HAP constitui um método vantajoso para preparar NLS por fusão-emulsificação, uma vez que não apresenta dificuldades de transposição de escala e permite trabalhar em condições assépticas.³⁸ Para se obter NLS com uma distribuição homogênea de tamanhos,

toda a dispersão deverá ser sujeita à mesma intensidade de energia. Caso contrário, as gotículas localizadas em diferentes volumes da amostra estarão expostas a diferentes forças de dispersão, originando NLS com dimensões muito heterogêneas. A HAP caracteriza-se pela aplicação da mesma tensão de corte a toda a amostra, devido às dimensões reduzidas do orifício de saída do homogeneizador ($\leq 25\text{-}30\ \mu\text{m}$).^{38, 39}

A concentração lipídica das emulsões destinadas à preparação de NLS por fusão-emulsificação varia, em regra, entre 5 e 10% (m/m), [26, 40] podendo, no entanto, atingir valores compreendidos entre 30 e 50%.⁴¹

A HAP pode ser realizada a uma temperatura superior ou inferior à temperatura de fusão do lipídio.⁴²⁻⁴⁴ Na primeira situação denomina-se HAP realizada a quente e na segunda HAP realizada a frio. Na HAP a quente, o lipídio é previamente fundido a uma temperatura de cerca de 5 a 10°C acima do seu ponto de fusão, incorporando-se, em seguida, o princípio ativo.⁴⁵

A preparação de NLS por HAP a quente,³⁸ é realizada fundido o lipídio, contendo o princípio ativo, seguindo-se a sua dispersão por agitação mecânica⁴⁶ ou por ultrassons,^{32, 33, 47} numa solução aquosa, aquecida à mesma temperatura, que contém um tensoativo do tipo O/A. Obtém-se, desta forma, uma “pré-emulsão”, que, em seguida, é submetida a HAP, realizada a uma temperatura compreendida entre 70 e 90°C, resultando uma nanoemulsão do tipo O/A. No final, a nanoemulsão é resfriada a uma temperatura igual ou inferior à temperatura ambiente (entre 20 e 25°C),^{26, 48} seguindo-se a solidificação do lipídio e a obtenção da dispersão aquosa de NLS. A etapa de homogeneização pode ser repetida várias vezes. No entanto, deve ter-se em conta que a HAP, por si só, aumenta a

temperatura da amostra em cerca de 10 a 20°C a cada ciclo de homogeneização. Em muitos casos, são suficientes 2 a 5 ciclos de homogeneização, a 500-1500 bar.³⁵

A HAP pode ser realizada com o lipídio no estado sólido. A preparação de NLS por HAP a frio consiste em fundir previamente o lipídio, onde se incorpora rapidamente o princípio ativo, promovendo, em seguida, o resfriamento em gelo seco ou nitrogênio líquido. Uma velocidade de resfriamento elevada favorece a distribuição homogênea do princípio ativo no interior da matriz lipídica.⁴⁹ Após solidificação, o material é fragmentado, recorrendo-se, por exemplo, a um almofariz ou moinho.^{50, 51} Deste processo resultam micropartículas com dimensões compreendidas entre 50 e 100 µm,⁴⁵ as quais se dispersam numa solução aquosa resfriada, contendo um tensoativo do tipo O/A, de modo a formar uma “pré-suspensão”. Uma vez obtida, esta pré-suspensão é submetida à HAP à temperatura ambiente ou abaixo desta, obtendo-se uma dispersão aquosa de NLS. A realização da HAP a baixas temperaturas aumenta a fragilidade do lipídio, facilitando a obtenção de partículas lipídicas de menores dimensões.⁴⁹

Em comparação com a HAP a quente, a HAP realizada a frio requer um maior número de ciclos de homogeneização (em regra 10 ciclos) e origina NLS de dimensões superiores e mais heterogêneas.^{45, 49} Como a HAP aumenta a temperatura da amostra em cerca de 10 a 20°C, em cada ciclo, a diferença entre o ponto de fusão do lipídio e a temperatura de homogeneização tem que ser suficientemente elevada, de modo a garantir a não ocorrência da fusão do lipídio durante o processo de HAP.⁵² As características físico-químicas das NLS obtidas por fusão-emulsificação são afetadas por um conjunto de parâmetros tecnológicos, que incluem a solubilidade do princípio ativo, o polimorfismo do lipídio, a

natureza e concentração do lipídio e do tensoativo, a temperatura, a força de cisalhamento e o número de ciclos de homogeneização efetuados.

Solubilidade do princípio ativo

O princípio ativo pode ser incorporado no lipídio fundido, dissolvendo-se ou dispersando-se, independente de ser lipossolúvel ou hidrossolúvel. Durante a preparação das NLS por HAP realizada a quente, o princípio ativo encontra-se dissolvido no lipídio fundido, numa concentração próxima da saturação, observando-se a sua difusão para a fase externa aquosa. Este fenômeno é tanto mais acentuado quanto maior for a hidrossolubilidade do princípio ativo, a temperatura da fase aquosa e a concentração do tensoativo nesta fase.³⁵ Após a homogeneização cria-se uma região de sobressaturação do princípio ativo à volta das gotículas de lipídio fundido recém-formadas. Durante o resfriamento do sistema, a solubilidade do princípio ativo na fase externa aquosa diminui, sendo, em consequência, redistribuída na superfície das NLS, antes de o lipídio recristalizar completamente. Formam-se, assim, NLS constituídas por um núcleo lipídico revestido por uma parede contendo princípio ativo.

Devido à natureza aquosa da fase externa da “pré-emulsão”, a preparação das NLS se realiza por HAP a quente obtém-se uma eficiência de encapsulação e uma capacidade de carga mais elevadas para princípios ativos hidrófobos. Estes princípios ativos têm menor tendência para abandonar o lipídio fundido, difundindo-se para a fase externa aquosa, contrariamente ao que sucede com os princípios ativos hidrofílicos.³⁵ Para se aumentar a eficiência de encapsulação das substâncias hidrossolúveis, promove-se o aumento da sua solubilidade no lipídio fundido, por conjugação com pares iônicos,⁵³ ou adicionando-se ao

lipídio fundido um tensoativo, como a fosfatidilcolina, ou ainda recorrendo-se a lipídios com propriedades solubilizantes (como os mono e os diacilgliceróis) para formar a matriz lipídica sólida. A HAP realizada a frio proporciona um aumento da incorporação dos princípios ativos hidrofílicos nas NLS.⁴⁹ Durante a homogeneização, o lipídio encontra-se no estado sólido, pelo que é minimizada a difusão do princípio ativo da matriz lipídica sólida para a fase externa aquosa, contrariamente ao que sucede com a HAP realizada a quente. A mobilidade das moléculas dos princípios ativos é menor na matriz lipídica sólida do que no lipídio fundido, pelo que, durante a HAP realizada a frio, menor será a quantidade de ativos que se perde para a fase aquosa. Além disso, esta fase pode ser substituída por outros líquidos, como os polietilenoglicóis de massa molar baixa, nos quais o princípio ativo evidencia menor difusão e solubilidade, o que contribui para a sua retenção na matriz lipídica sólida.⁴⁵

Polimorfismo do lipídio

O processo de preparação de NLS inicia-se com a fusão do lipídio seguida do resfriamento para originar NLS. Ao iniciar o processo de solidificação, a viscosidade do lipídio fundido aumenta progressivamente, tornando-se mais difícil acomodar as moléculas lipídicas, o que origina, no final, cristais lipídicos com diferentes graus de organização tridimensional, isto é, com diferentes formas polimórficas.⁵⁴ Este fenómeno é habitualmente conhecido por recristalização do lipídio. O grau de cristalinidade das NLS recém-formadas depende da organização tridimensional das cadeias hidrocarbonadas das moléculas na matriz lipídica solidificada.⁵⁵

Os lipídios podem apresentar polimorfismo, isto é, se cristalizar em formas distintas formando estruturas diferenciadas, alterando a liberação do princípio ativo encapsulado. Essas formas polimórficas podem ser identificadas por padrões de difração de raios X, onde os espaçamentos longos fornecem informações sobre a distância entre os cristais planos (comprimento de cadeia), enquanto os espaçamentos curtos dão informações sobre a estrutura da sub-célula (distância entre cadeias).⁵⁶ Os lipídios podem cristalizar em estruturas tridimensionais do tipo α , β' , β . A forma α (hexagonal) é a menos estável com menor ponto de fusão e calor latente. A forma β (tricíclica) é a mais estável com maior ponto de fusão e maior calor latente. As transformações de α , para β' (ortorrômbica) e desta para β ocorrem nesta ordem e são irreversíveis.^{57, 58} Desta forma, para uma aplicação industrial das partículas lipídicas sólidas é necessário controlar este polimorfismo. A estrutura polimórfica tem influência direta na eficiência de encapsulação e na expulsão do ativo durante o processo de estocagem sendo, muito importante a sua caracterização.^{54, 59} Os espaços dessas moléculas estão descritas, conforme a Tabela 2.

Tabela 2. Estruturas tridimensionais das três formas mais comuns de polimorfismo em triacilgliceróis.

Modificações	α	β'	β
cristal	Hexagonal (H)	Ortorrômbica perpendicular ($O \perp$)	Tricíclica paralela (T//)
subcélulas	Ortorrômbica 0,415 – 0,42 nm	Ortorrômbica 0,42 - 0,43 nm 0,37 – 0,40 nm	Tricíclica 0,46 nm

A organização tridimensional que a matriz lipídica adquire durante a solidificação, depende da velocidade de resfriamento do lipídio e da sua composição, e constitui um fator muito importante para a incorporação do princípio ativo nas NLS. Quando a velocidade de resfriamento é lenta, as cadeias hidrocarbonadas dos lipídios podem rearranjar-se numa forma mais ordenada e estável. Pelo contrário, quando a velocidade de resfriamento é elevada, a solidificação da matriz ocorre também rapidamente, rearranjando-se numa forma polimórfica mais instável. Assim, na preparação de NLS por HAP realizada a quente, como a velocidade de resfriamento é elevada, as partículas recém-formadas adquirem, preferencialmente, a forma polimórfica β .⁶⁰ No que se refere à composição lipídica, as matrizes com um conteúdo elevado de diacilgliceróis (> 50%) cristalizam na forma polimórfica metaestável β' ,⁶¹ que se caracteriza por alguma imperfeição na sua estrutura tridimensional. As matrizes lipídicas formadas por triacilgliceróis, esterificados com um único tipo de ácido graxo, cristalizam, normalmente, no polimorfo mais estável β , que se caracteriza por um grau de organização elevado. Adicionalmente, são encontradas outras formas polimórficas em misturas de acilgliceróis, que são habitualmente referidas como formas β_i .⁵⁵

A estabilidade termodinâmica das NLS e o seu grau de empacotamento lipídico aumentam, enquanto a incorporação do princípio ativo diminui na seguinte ordem: forma polimórfica α , forma polimórfica β' , forma polimórfica β . Em regra, as moléculas lipídicas apresentam maior mobilidade quando se encontram em configurações termodinamicamente mais instáveis, como, por exemplo, a forma polimórfica α . Por esta razão, estas configurações apresentam um grau de empacotamento lipídico menor, sendo maior a sua capacidade para incorporar os princípios ativos.⁶⁰ Portanto, para a preparação de NLS com capacidade de carga elevada, em particular quando se pretende incorporar ativos hidrofílicos, o lipídio

deverá cristalizar, preferencialmente, na forma polimórfica mais instável, isto é, na forma α , que deverá manter-se durante o armazenamento.^{62, 63}

As transformações polimórficas podem ocorrer durante o armazenamento promovendo a instabilidade da dispersão coloidal, uma vez que estão associadas ao aumento do tamanho das partículas lipídicas. Durante o armazenamento, a ocorrência de transformações polimórficas é acompanhada por alterações na forma das partículas, designadamente das formas esféricas (α) para as formas achatadas (β).^{64, 65}

O problema associado às modificações do lipídio não é sempre resolvido com a manipulação das formas α , β e β' . A complexidade do sistema aumenta devido às subespécies polimórficas e às interações do lipídio com os agentes tensoativos. Para preparar NLS com capacidade de carga elevada utilizando formas polimórficas instáveis, é necessário o desenvolvimento de estratégias que previnam a transformação das formas instáveis para as formas mais estáveis, durante o armazenamento.⁶⁶

Natureza e concentração do lipídio

A maioria dos lipídios utilizados na preparação de NLS consiste em misturas de vários compostos químicos. A natureza química dos lipídios selecionados e a sua concentração influenciam a incorporação dos princípios ativos e tamanho das NLS.

Os lipídios que dão origem a partículas altamente cristalinas, como os triacilgliceróis constituídos por um tipo de ácido gordo, originam estruturas organizadas, com poucos locais para acomodar as moléculas de princípios ativos, induzindo a sua expulsão da matriz lipídica sólida.⁶⁷ Os lipídios de composição mais complexa – como as misturas de mono, di e triacilgliceróis e as misturas de diferentes ácidos graxos formam cristais com muitas

imperfeições, oferecendo mais espaço para acomodar as moléculas de princípio ativo.⁶⁸

Por esta razão, as misturas de acilgliceróis proporcionam uma capacidade de carga maior do que os lipídios puros.

Para se obter NLS com dimensões reduzidas, recorre-se a misturas de mono e diacilgliceróis, os quais apresentam propriedades tensoativas (EHL 2-5).²⁰ Ahlin *et al.* observaram que o tamanho médio das NLS de Witepsol[®] W35 (constituído por ácidos graxos de cadeia curta e quantidades elevadas de mono e diacilgliceróis) era significativamente menor ($117,0 \pm 1,8$ nm) do que o das NLS de Dynasan[®] 118 (constituído por triestearina) ($175,1 \pm 3,5$ nm).⁶⁹ Utilizando a HAP a quente, Siekmann e Westesen demonstraram que o tamanho médio das NLS aumenta com o aumento da temperatura de fusão dos lipídios usados para a preparação, devido o aumento da viscosidade da fase interna da emulsão.⁷⁰

O aumento da concentração lipídica aumenta as dimensões das NLS, devido o aumento da viscosidade da “pré-emulsão”, tornando mais difícil a sua emulsificação na fase aquosa.⁷¹

Portanto, são formadas NLS de dimensões maiores. Como as emulsões contêm cerca de 5 a 10% (m/m) de lipídio, a sua viscosidade é suficientemente reduzida para serem homogeneizadas por HAP, obtendo-se NLS com dimensões reduzidas e com uma distribuição homogênea de tamanhos. Acima de 10% (m/m) de lipídio resultam NLS de dimensões mais elevadas e uma distribuição mais heterogênea de tamanhos.⁵²

Natureza e concentração do tensoativo

A escolha do tensoativo e da sua concentração são fatores que influenciam diretamente as características das NLS, designadamente as suas dimensões, a retenção do princípio ativo e a eficiência de encapsulação.⁶⁵ Na preparação de NLS por HAP a quente, é frequente

incorporar fosfolipídeos (como a fosfatidilcolina)⁷² no lipídio fundido e um estabilizante estereoquímico (por exemplo, um polaxamer) na fase aquosa externa.⁷³ Deste modo, forma-se uma barreira mecânica e/ou elétrica que impede a coalescência das partículas durante a sua formação, e também a sua agregação durante o armazenamento. A carga elétrica da superfície das partículas provoca a repulsão, mantendo o sistema num estado termodinâmico mais estável. Se a fase interna da nanoemulsão O/A for suficientemente estável, as NLS obtidas após a recristalização do lipídio apresentarão menores dimensões e maior estabilidade durante o armazenamento, em comparação com formulações que contêm apenas um tensoativo incluído na fase aquosa.^{74, 75}

Se o aumento da concentração de fosfatidilcolina for acompanhado pelo aumento do tamanho das NLS, este deve-se, provavelmente, à formação de múltiplas camadas de fosfatidilcolina à sua superfície ou à formação de lipossomas na fase aquosa. É de notar que as moléculas de fosfolipídio em excesso na fase interna deslocam-se para a superfície das partículas lipídicas e/ou para a fase aquosa organizando-se em bicamadas. As concentrações elevadas de tensoativo reduzem a tensão interfacial, aumentam a área de superfície e, em consequência, originam NLS de menores dimensões.⁷⁶ No entanto, quando a fase aquosa externa contém moléculas de tensoativo em excesso podem formar-se outras espécies coloidais (como, por exemplo, lipossomas), que podem incorporar moléculas de princípios ativos e diminuir a sua eficiência de encapsulação nas NLS.²⁶

Temperatura

Na preparação de NLS por HAP realizada a quente, as temperaturas elevadas conduzem a uma diminuição do tamanho das partículas, uma vez que promovem uma diminuição da

viscosidade da fase interna, originando também uma distribuição mais homogênea de tamanhos.⁷⁷ Para iniciar a recristalização do lipídio, é necessário resfriar a nanoemulsão O/A a uma temperatura que depende da natureza do lipídio. Quando se utilizam acilgliceróis formados por ácidos graxos de cadeia curta, e com baixo ponto de fusão (próximo da temperatura ambiente), a recristalização deve ocorrer a um valor inferior a esta. Em alternativa, a recristalização do lipídio pode ser iniciada submetendo a nanoemulsão a liofilização.

Tensão de cisalhamento e número de ciclos de homogeneização

Na preparação de NLS por HAP realizada a quente, para se reduzir as dimensões das gotículas de fase interna da “pré-emulsão” pode aumentar-se a tensão aplicada ou o número de ciclos de homogeneização.⁷⁷ No entanto, o excesso de ciclos, o aumento da tensão aplicada ou do número de ciclos origina NLS de dimensões mais elevadas, devido à coalescência das gotículas lipídicas, que ocorre em virtude do aumento da energia cinética.

38

Na preparação de NLS por HAP realizada a frio, o lipídio encontra-se no estado sólido, pelo que se torna necessária uma tensão superficial mais elevada e um maior número de ciclos de homogeneização para se obter partículas com dimensões nanométricas.⁴⁹

Problemas inerentes à preparação de NLS por fusão-emulsificação

Os problemas inerentes à preparação de NLS por fusão-emulsificação estão relacionados com o risco potencial de degradação do lipídio e/ou do princípio ativo e com a possível ocorrência do fenómeno de recristalização do lipídio.

Degradação do lipídio e/ou do princípio ativo

O risco de ocorrência de degradação do lipídio e/ou do princípio ativo durante a HAP está associado às elevadas temperaturas e tensões de cisalhamento aplicadas durante o processo. No caso de princípios ativos termo-sensíveis, a HAP realizada a frio tem vantagens, uma vez que o impacto térmico é apenas aplicado no início do processo, para promover a fusão do lipídio.⁴⁹ No entanto, a HAP, por si só, aumenta a temperatura da amostra, pelo que, quando se processa a frio, deve garantir-se que a temperatura é suficientemente reduzida para evitar a fusão do lipídio.⁵¹

A HAP pode também ser responsável pela redução da massa molar do lipídio, já que uma tensão de cisalhamento elevada parece ser a principal causa para a formação de radicais livres, responsáveis pela peroxidação lipídica.^{45, 49} A massa molar e a estrutura molecular do princípio ativo são os parâmetros mais importantes para avaliar a sua possível degradação pela aplicação de tensões de cisalhamento elevadas. Os princípios ativos de massa molar elevada e com cadeias longas são as mais sensíveis. Com efeito, a HAP parece causar a degradação do DNA (*deoxyribonucleic acide*) da albumina. No entanto, para a maior parte dos princípios ativos incorporados em NLS, a HAP não apresenta qualquer problema.

Recristalização do lipídio

Para preparar NLS por HAP a quente, a nanoemulsão O/A previamente obtida deverá ser resfriada, de modo a recristalizar o lipídio e, em consequência, originar a formação de partículas lipídicas solidificadas. Devido à quantidade elevada de moléculas de tensoativo, necessária para estabilizar a dispersão coloidal, e à complexidade química da mistura lipídica, a cristalinidade do lipídio sob a forma de NLS, pode diferir consideravelmente do

lipídio como matéria-prima. Devido à mistura complexa de lipídios, a diferença de temperatura entre os pontos de fusão e de cristalização da matriz lipídica (intervalo de resfriamento) pode atingir entre 30 e 40°C nas dispersões lipídicas. Por exemplo, a temperatura de fusão da trilaurina é superior a 40°C. No entanto, nas NLS formadas por um sistema de tensoativos constituído por um fosfolipídio e tiloxapol, o lipídio recristaliza a temperaturas inferiores ao ponto de congelação da água.⁶⁵ A estabilidade das dispersões coloidais de NLS está, portanto, condicionada pela ocorrência de fusões super-resfriadas e pelas transformações polimórficas que o lipídio sofre aquando da sua recristalização sob a forma de partículas sólidas e durante o armazenamento.

Fusões super-resfriadas

Na sequência de uma HAP realizada a quente podem resultar fusões super-resfriadas, em vez de dispersões aquosas de NLS. As fusões super-resfriadas são sistemas heterogêneos semelhantes a emulsões do tipo O/A, uma vez que o lipídio se mantém no estado líquido e disperso na fase aquosa, embora a preparação seja armazenada a uma temperatura inferior ao ponto de fusão do lipídio. Estes sistemas resultam da recristalização do lipídio ser consideravelmente retardada, após a realização da HAP à quente, devido ao baixo ponto de fusão e à composição complexa da mistura lipídica utilizada. Se a recristalização não for induzida artificialmente, as dispersões lipídicas podem permanecer super-resfriadas durante vários meses. A ocorrência de fusões super-resfriadas aumenta com a diminuição das dimensões das gotículas de lipídio fundido emulsificadas na fase aquosa. Para o lipídio iniciar a recristalização é necessária a existência de um determinado número de núcleos de cristalização presentes na emulsão. A formação desses núcleos é menor com a diminuição

das dimensões das gotículas e, como consequência, é retardado o processo de recristalização.

O aumento da temperatura e da tensão de cisalhamento aplicada podem originar fusões super-resfriadas, devido à formação de gotículas lipídicas de dimensões reduzidas. Pode verificar-se também um atraso na recristalização com o aumento da concentração de tensoativo e com a diminuição da concentração do lipídio na formulação.

Em comparação com as formas polimórficas que o lipídio pode adquirir (α , β' ou β), a estabilidade termodinâmica e o grau de empacotamento lipídico são mais baixos nas fusões super-resfriadas.⁵⁴ Por esta razão, estas últimas não conseguem imobilizar as moléculas de princípio ativo tão fortemente quanto às partículas sólidas, não podendo, por isso, ser utilizadas para modificar a cedência *in vivo* das moléculas incorporadas. Além disso, mesmo que fosse possível recristalizar o lipídio e formar NLS a partir das fusões super-resfriadas, após a administração *in vivo* ocorreria a sua fusão, uma vez que a temperatura corporal é superior ao ponto de fusão do lipídio.

2. Preparação por emulsificação-evaporação do solvente

A preparação de NLS por emulsificação-evaporação do solvente consiste na preparação de uma fase orgânica, constituída pelo lipídio dissolvido num solvente orgânico imiscível com a água, como, por exemplo, a acetona, o diclorometano⁷⁸ ou clorofórmio.⁷⁹ Nesta fase é incorporado o princípio ativo, por dissolução ou por dispersão, e adicionada a fosfatidilcolina para aumentar a estabilidade termodinâmica da emulsão preparada. A fase orgânica é depois emulsificada numa fase aquosa, que contém um tensoativo do tipo O/A como, por exemplo, o polaxamer 188,¹⁵ obtendo-se uma emulsão do tipo O/A.

Para se proceder à evaporação do solvente orgânico, a emulsão obtida é diluída num volume elevado de fase aquosa e submetida à agitação a uma temperatura compreendida entre 0 e 2°C, podendo decorrer a pressão reduzida. As NLS formam-se em consequência da precipitação do lipídio na fase externa aquosa. A evaporação do solvente orgânico deve realizar-se o mais rapidamente possível, de modo a evitar a agregação das NLS recém-formadas. Os princípios ativos hidrossolúveis, em vez de serem dispersos na fase orgânica podem, como alternativa, ser dissolvidos numa fase aquosa, que, posteriormente, vai constituir a fase interna de uma emulsão múltipla A/O/A.⁸⁰ Este processo é particularmente adequado para a incorporação de peptídios e proteínas em NLS. Neste caso, como a fase aquosa interna tem tendência para coalescer durante a agitação, a presença de um tensoativo na fase orgânica é essencial para aumentar a estabilidade da emulsão primária A/O e, em consequência, da emulsão múltipla A/O/A.⁸¹

Em comparação com o processo de preparação das NLS por fusão-emulsificação, a emulsificação-evaporação do solvente origina partículas com dimensões mais reduzidas, devido à menor viscosidade da fase interna, que resulta do lipídio se encontrar dissolvido num solvente orgânico em lugar de fundido. Este método apresenta a vantagem de evitar a exposição dos princípios ativos a temperaturas elevadas, apresentando, no entanto, o inconveniente relacionado com o uso de solventes orgânicos.⁸

As características físico-químicas das NLS obtidas por emulsificação-evaporação do solvente são afetadas por um conjunto de parâmetros tecnológicos, que incluem a solubilidade do princípio ativo, o polimorfismo do lipídio e ainda a natureza e concentração do lipídio e do agente tensoativo.

Solubilidade do princípio ativo

Os princípios ativos hidrofóbicos dissolvem-se na fase interna orgânica da emulsão e não sofrem difusão para a fase externa aquosa, obtendo-se, por isso, uma incorporação elevada. No caso dos princípios ativos hidrofílicos, estas evidenciam uma tendência elevada para abandonar a fase interna orgânica, pelo que a sua eficiência de encapsulação é significativamente reduzida. Para ultrapassar este problema, estas substâncias, em particular, os peptídios e as proteínas, podem ser dissolvidas numa fase aquosa interna, formando-se uma emulsão múltipla A/O/A, com a qual se preparam as NLS. Em comparação com o método de fusão-emulsificação anteriormente descrito, a emulsificação-evaporação do solvente origina NLS com eficiência de encapsulação menores para os princípios ativos hidrossolúveis. Neste caso, a fase interna é menos viscosa, uma vez que o lipídio se encontra dissolvido num solvente orgânico, enquanto no método de fusão-emulsificação, o lipídio está fundido, contribuindo para reduzir a difusão do princípio ativo para a fase externa aquosa.

Polimorfismo do lipídio

Devido à difusão lenta do solvente orgânico através da fase aquosa, a solidificação das NLS obtidas por emulsificação-evaporação do solvente é mais lenta, em comparação com as preparadas por fusão-emulsificação. Em consequência, as moléculas lipídicas podem rearranjar-se numa forma termodinâmica mais estável, adquirindo a forma polimórfica β , à qual está associada uma menor capacidade para incorporar os princípios ativos.

Natureza e concentração do lipídio

A natureza do lipídio influencia também as características físico-químicas das NLS preparadas por emulsificação-evaporação do solvente. Com efeito, os lipídios de composição complexa, como as misturas de mono, di e triacilgliceróis, e os que contêm ácidos graxos com cadeia de diferentes comprimentos, originam NLS com muitas imperfeições, oferecendo mais espaço para acomodar as moléculas do princípio ativo. O tamanho médio das NLS aumenta com o aumento da concentração lipídica na emulsão, devido ao aumento da viscosidade da fase interna. Em regra, são utilizadas concentrações compreendidas entre 0,5 e 2,5% (m/v). Para se obter NLS de dimensões menores são utilizadas concentrações lipídicas inferiores a 5% (m/v).⁸⁰

Natureza e concentração do tensoativo

O tamanho médio das NLS e a extensão de incorporação dos princípios ativos por emulsificação-evaporação do solvente dependem do tipo de agentes tensoativos utilizados. A presença de um agente tensoativo do tipo O/A na fase externa aquosa é fundamental para a formação da emulsão O/A. O aumento da sua concentração provoca uma diminuição da tensão interfacial entre ambas as fases, contribuindo para diminuir as dimensões das NLS. Verifica-se, igualmente, uma redução das dimensões das NLS, quando se usa um sistema de tensoativos, em que um está incluído na fase interna, como um fosfolipídio; e outro na fase externa, como um sal biliar.^{76, 82} Quando o princípio ativo se encontra disperso, em lugar de dissolvido, na fase orgânica, a sua tendência para se difundir para a fase aquosa é maior, reduzindo a sua incorporação nas NLS. A utilização de um agente tensoativo na fase

interna aumenta a molhabilidade das partículas sólidas do princípio ativo, contribuindo para a sua permanência nesta fase e permitindo aumentar a eficiência de encapsulação.

3. Preparação a partir de microemulsões

As microemulsões são sistemas heterogêneos termodinamicamente estáveis, que podem ser formados espontaneamente devido a uma tensão interfacial reduzida entre uma fase interna e uma fase externa. Para se preparar a microemulsão, o lipídio é inicialmente fundido, incorporando-se depois o princípio ativo por dissolução ou por dispersão, consoante esta é lipossolúvel ou hidrossolúvel. Simultaneamente, prepara-se, à mesma temperatura, uma fase aquosa, contendo um agente tensoativo do tipo O/A. Em seguida, submete-se à emulsificação do lipídio fundido na fase aquosa, sob agitação mecânica intensa, obtendo-se uma microemulsão O/A termodinamicamente estável.⁸³

A microemulsão O/A, em regra aquecida a uma temperatura compreendida entre 60 e 70°C,⁸⁴⁻⁸⁶ é diluída sob agitação mecânica, num volume elevado de água⁸⁷ ou de uma solução aquosa resfriada a uma temperatura compreendida entre 2 e 3°C. A razão entre os volumes da microemulsão e da solução aquosa está compreendida entre 1:2 e 1:100 (v/v). Desta forma, assegura-se que as dimensões reduzidas das NLS são devidas à precipitação do lipídio na solução aquosa resfriada e não induzidas mecanicamente pelo processo de agitação. Devido à etapa de diluição, a concentração lipídica da microemulsão é consideravelmente mais baixa, em comparação com a das emulsões obtidas no método de fusão-emulsificação.⁸³ As características físico-químicas das NLS obtidas a partir de microemulsões são afetadas, não somente pelos fatores que interferem na preparação da microemulsão, mas também pelas condições experimentais a que decorre a sua diluição na solução aquosa, designadamente pela temperatura desta última e pelo seu volume e ainda

pelo modo como se processa a diluição. Os principais parâmetros que afetam a eficiência de encapsulação, a capacidade de carga e as dimensões das NLS.

Temperatura e volume da solução aquosa

As NLS são formadas devido ao contato rápido entre a microemulsão aquecida e a solução aquosa resfriada, pelo que a diferença de temperatura entre ambas e o volume da solução aquosa são parâmetros que afetam as dimensões das partículas. A diferença de temperatura entre a microemulsão recém-preparada e a solução aquosa resfriada é o principal parâmetro que afeta as dimensões das NLS. Uma diferença elevada facilita a recristalização rápida do lipídio e previne a agregação das NLS recém-formadas. Por esta razão, são obtidas NLS com menores dimensões quando é maior a diferença de temperatura entre a microemulsão aquecida e a solução aquosa resfriada.⁸³ Um volume mais elevado de solução aquosa resfriada diminui o risco de agregação das NLS recém-formadas, enquanto um menor volume poderá não ser suficiente para dispersar a totalidade da microemulsão, obtendo-se NLS de maiores dimensões.⁸⁷ A diluição microemulsão O/A numa solução aquosa resfriada processa-se sob agitação mecânica. Embora a agitação não seja o fator responsável pelas dimensões reduzidas das NLS obtidas, este processo pode não ser adequado para o controle das dimensões das partículas devido à agregação que podem sofrer, originando uma distribuição mais heterogênea de tamanhos. A utilização de dispositivos capilares constitui uma alternativa vantajosa para o controle das dimensões das NLS, já que proporciona uma diluição gradual e controlada da microemulsão.

Marengo et al. desenvolveram um aparelho para a preparação industrial de NLS, que permite a diluição de um volume superior a 100 ml de microemulsão líquida aquecida

numa solução aquosa resfriada.⁸⁸ A microemulsão é colocada numa câmara de alumínio, revestida por uma parede termostalizada, e esterilizada por filtração através uma membrana filtrante com 0,22 µm de abertura do poro. Posteriormente, a microemulsão é conduzida através de uma agulha, diretamente para a solução aquosa resfriada, sob agitação magnética a 300 rpm. O diâmetro médio e a distribuição de tamanhos das NLS estão condicionados pelo diâmetro da agulha utilizada, pela temperatura e pelo volume da solução aquosa.⁸⁸ Para um determinado valor de temperatura e volume de solução, o aumento do diâmetro da agulha origina NLS maiores, uma vez que as gotículas emulsificadas são também maiores.

Conclusões

As NLS podem ser usadas para as mesmas finalidades das nanopartículas poliméricas. Por esta razão, têm sido igualmente objeto de estudo, considerando a sua administração por vias não parenterais (sob a forma de comprimidos, pellets, cápsulas, hidrogéis e cremes) e por vias parenterais. Após a administração oral, pode conseguir-se uma liberação modificada dos princípios ativos para a mucosa gastrointestinal e reduzir a variabilidade da absorção devido à natureza lipídica da sua matriz. A absorção pode ser melhorada, em comparação com as nanopartículas poliméricas, devido às propriedades adesivas da matriz lipídica à mucosa gastrointestinal. Além disso, os lipídios das NLS podem ser processados e absorvidos, tal como os lipídios provenientes da alimentação. Assim, os princípios ativos podem ser absorvidos juntamente com os lipídios com aumento da sua biodisponibilidade. A maior vantagem das NLS para administração tópica reside no fato de protegerem dos princípios ativos contra a degradação química e modularem a sua liberação para camadas particulares da pele. Em muitos casos, para se conseguir uma formulação para a administração tópica é necessária à incorporação das dispersões aquosas de NLS em

hidrogéis ou em cremes. No que se referem à administração parenteral, as NLS têm sido estudadas para o direcionamento de princípios ativos para os pulmões, baço e cérebro. As propriedades físico-químicas das NLS dependem do método de preparação utilizado, o qual, por sua vez, é influenciado por vários parâmetros tecnológicos. Como a matriz destes sistemas é de natureza lipídica, os métodos de preparação ocorrem em meio orgânico e evidenciam melhores resultados para princípios ativos de natureza hidrofóbica. Devido ao fenômeno de recristalização do lipídio, necessário para a solidificação da matriz e formação das nanopartículas, as propriedades físico-químicas das NLS estão condicionadas pela ocorrência de transformações polimórficas, que dependem do tipo de lipídio utilizado. O tipo de forma polimórfica que o lipídio adquire condiciona a capacidade de carga das NLS. Os lipídios que cristalizam em formas altamente organizadas, como os triacilgliceróis, constituídos por um único tipo de ácido gordo, originam sistemas com poucos locais para acomodar os princípios ativos, induzindo a sua expulsão da matriz lipídica sólida. Os lipídios de composição mais complexa, como as misturas de mono, di e triacilgliceróis, formam estruturas com muitas imperfeições, originando NLS com maior capacidade para incorporar os princípios ativos. As NLS podem ser preparadas a partir de métodos que se baseiam na fusão-emulsificação, sendo particularmente importantes aqueles que recorrem à HAP realizada a quente ou a frio. Os parâmetros que concorrem para a otimização das formulações incluem, para além da natureza e concentração do lipídio e do tensoativo, a temperatura, a tensão de superficial e o número de ciclos de homogeneização. Este método apresenta o inconveniente associado ao risco de degradação do lipídio e/ou do princípio ativo devido às elevadas temperaturas e tensões superficiais aplicadas durante o processo, bem como ao risco de ocorrência de transformações polimórficas durante o armazenamento das NLS. A preparação por emulsificação-*evaporação* do solvente é realizada no meio de

emulsões do tipo O/A ou A/O/A, sendo particularmente adequado para incorporar substâncias termosensíveis, uma vez que, durante o processo de preparação não se aplicam temperaturas elevadas. Este método apresenta o inconveniente relacionado com a utilização de solventes orgânicos, nos quais deve ser solubilizado o material lipídico. Finalmente, a preparação de NLS a partir de microemulsões requer a utilização de um dispositivo apropriado para dispersar a microemulsão aquecida numa solução aquosa resfriada, sendo, por isso, um método influenciado pela temperatura e pelo volume da solução aquosa e pelas dimensões do dispositivo capilar utilizado. Neste método, as dimensões reduzidas das NLS são devidas à precipitação do lipídio na solução aquosa resfriada e não induzidas mecanicamente pelo processo de agitação.

Agradecimentos

Os autores agradecem à Fundação para a Ciência e a Tecnologia (FCT) do Ministério da Ciência e Tecnologia (PTDC/SAU-FAR/113100/2009), à Fundação de Amparo à Pesquisa do Estado de São Paulo (FAPESP/Brasil) e à Coordenação de Aperfeiçoamento de Pessoal de Nível Superior (Capes, Brasil).

Referências

1. Trevaskis, N.L.; Charman, W.N.; Porter, C.J.; *Adv. Drug Deliv. Rev.* **2008**, 60, 702.
2. Souto, E.B.; *Tese de Mestrado*, Faculdade de Farmácia do Porto, Portugal, 2003.
3. Rawat, M.K.; Jain, A.; Singh, S.; *J. Pharm. Sci.* **2011**, 100, 2406.
4. Nayak, A.P.; Tiyaboonchai, W.; Patankar, S.; Madhusudhan, B.; Souto, E.B.; *Colloids Surf. B Biointerfaces.* **2010**, 81, 263.

5. Zhang, J.; Smith, E.; *J. Pharm. Sci.* **2011**, 100, 896.
6. Araujo, J.; Gonzalez-Mira, E.; Egea, M.A.; Garcia, M.L.; Souto, E.B.; *Int. J. Pharm.* **2010**, 393, 167-175.
7. Muchow, M.; Maincent, P.; Muller, R.H.; *Drug Dev. Ind. Pharm.* **2008**, 34, 1394.
8. Singh, S.; Dobhal, A.K.; Jain, A.; Pandit, J.K.; Chakraborty, S.; *Chem. Pharm. Bull. (Tokyo)*. **2010**, 58, 650.
9. Bunjes, H.; *J. Pharm. Pharmacol.* **2010**, 62, 1637.
10. Wang, T.; Wang, N.; Zhang, Y.; Shen, W.; Gao, X.; Li, T.; *Colloids Surf. B Biointerfaces*. **2010**, 79, 254.
11. Souto, E.B.; *Tese de Doutorado*, Faculdade de Farmácia do Porto, Portugal, 2003.
12. Jensen, L.B.; Magnusson, E.; Gunnarsson, L.; Vermehren, C.; Nielsen, H.M.; *Int. J. Pharm.* **2009**, 390, 53.
13. Aji Alex, M.R.; Chacko, A.J.; Jose, S.; Souto, E.B.; *Eur. J. Pharm. Sci.* **2011**, 18, 11.
14. Chakraborty, S.; Shukla, D.; Vuddanda, P.R.; Mishra, B.; Singh, S.; *Colloids Surf. B Biointerfaces*. **2010**, 81, 563.
15. Yoo, J.H.; Shanmugam, S.; Thapa, P.; Lee, E.S.; Balakrishnan, P.; Baskaran, R.; Yoon, S.K.; Choi, H.G.; Yong, C.S.; Yoo, B.K.; Han, K.; *Arch. Pharm. Res.* **2010**, 33, 417.
16. Kuo, Y.C.; Chen, H.H.; *Int. J. Pharm.* **2009**, 365, 206.
17. Shah, M.; Pathak, K.; *AAPS Pharm. Sci. Tech.* **2010**, 11, 489.
18. Kalam, M.A.; Sultana, Y.; Ali, A.; Aqil, M.; Mishra, A.K.; Chuttani, K.; *J. Drug Target.* **2010**, 18, 191.
19. Yassin, A.E.; Anwer, M.K.; Mowafy, H.A.; El-Bagory, I.M.; Bayomi, M.A.; Alsarra, I.A. *Int. J. Med. Sci.* **2010**, 7, 398.
20. Abdelbary, G.; Fahmy, R.H.; *AAPS Pharm. Sci. Tech.* **2009**, 10, 211.

21. Chen, G.; Hou, S.X.; Hu, P.; Hu, Q.H.; Guo, D.D.; Xiao, Y.; *Nan Fang Yi Ke Da Xue Xue Bao.* **2008**, 28, 1022.
22. Luo, Y.; Chen, D.; Ren, L.; Zhao, X.; Qin, J.; *J. Control. Release.* **2006**, 114, 53.
23. Kheradmandnia, S.; Vasheghani-Farahani, E.; Nosrati, M.; Atyabi, F.; *Nanomedicine.* **2010**, 6, 753.
24. Kim, J.K.; Park, J.S.; Kim, C.K.; *Int. J. Pharm.* **2010**, 383, 209.
25. Mezzena, M.; Scalia, S.; Young, P.M.; Traini, D.; *AAPS J.* **2009**, 11, 771.
26. Helgason, T.; Awad, T.S.; Kristbergsson, K.; McClements, D.J.; Weiss, J.; *J. Colloid Interface Sci.* **2009**, 334, 75.
27. Doroud, D.; Vatanara, A.; Zahedifard, F.; Gholami, E.; Vahabpour, R.; Rouholamini, N.A, Rafati, S.; *J. Pharm. Pharm. Sci.* **2010**, 13, 320.
28. Siddiqui, A.; Patwardhan, G.A.; Liu, Y.Y.; Nazzal, S.; *Int. J. Pharm.* **2010**, 400, 251.
29. Yang, L.; Geng, Y.; Li, H.; Zhang, Y.; You, J.; Chang, Y.; *Pharmazie.* **2009**, 64, 86.
30. Jain, S.K.; Chourasia, M.K.; Masuriha, R.; Soni, V.; Jain, A.; Jain, N.K.; Gupta, Y. *Drug Deliv.* **2005**, 12, 207.
31. Igartua, M.; Saulnier, P.; Heurtault, B.; Pech, B.; Proust, J.E.; Pedraz, J.L.; Benoit, J.P.; *Int. J. Pharm.* **2002**, 233, 149.
32. Hu, L.; Xing, Q.; Meng, J.; Shang, C.; *AAPS Pharm. Sci. Tech.* **2010**, 11, 582.
33. Hu, L.; Jia, H.; Luo, Z.; Liu, C.; Xing, Q.; *Pharmazie.* **2010**, 65, 110.
34. Attama, A.A.; Reichl, S.; Muller-Goymann, C.C.; *Curr. Eye Res.* **2009**, 34, 698.
35. Muller, R.H.; Mader, K.; Gohla, S.; *Eur. J. Pharm. Biopharm.* **2000**, 50, 161.
36. Eldem, T.; Speiser, P.; Hincal, A.; *Pharm. Res.* **1991**, 8, 47.
37. Zur Muhlen, A.; Schwarz, C.; Mehnert, W.; *Eur. J. Pharm. Biopharm.* **1998**, 45, 149.
38. Shegokar, R.; Singh, K.K.; Muller, R.H.; *Int. J. Pharm.* **2010**, in press.

39. Seo, M.; Gorelikoy, I.; Williams, R.; Matsuura, N.; *Langmuir*. **2010**, 26, 13855.
40. Yang, C.R.; Zhao, X.L.; Hu, H.Y.; Li, K.X.; Sun, X.; Li, L.; Chen, D.W.; *Chem. Pharm. Bull.* **2010**, 58, 656.
41. Lippacher, A.; Mäder, K.; *Int. J. Pharm.* **2000**, 196, 227.
42. Jennings, V.; Lippacher, A.; Gohla, S.H.; *J. Microencapsul.* **2002**, 19, 1.
43. Souto, E.B.; Müller, R.H. *J. Microencapsul.* **2006**, 23, 377.
44. Wang, D.; Zhao, P.; Cuia, F.; Li, X.; *J. Pharm. Sci. Technol.* **2007**, 61, 110.
45. Gohla, S.H.; Dingler, A.; *Pharmazie*. **2001**, 56, 61.
46. Wang, W.; Zhao, X.; Hu, H.; Chen, D.; Gu, J.; Deng, Y.; Sun, J.; *Drug Deliv.* **2010**, 17, 114.
47. Wang, D.; Wang, X.; li, X.; Ye, L., *PDA J. Pharm. Sci. Technol.* **2008**, 62, 56.
48. Bhalekar, M.R.; Pokharkar, V.; Madgulkar, A.; Patil, N.; Patil, N.; *AAPS PharmSciTech.* **2009**, 10, 289.
49. Dingler, A.; Gohla, S.; *J. Microencapsul.* **2002**, 19, 11.
50. You, J.; Wan, F.; De Cui, F.; Sun, Y.; Du, Y.Z.; Hu, F.Q.; *Int. J. Pharm.* **2007**, 343, 270.
51. Wan, F.; You, J., Sun, Y.; Zhang, X.G.; Cui, F.D.; Du, Y.Z., Yuan, H.; Hu, F.Q.; *Int. J. Pharm.* **2008**, 359, 104.
52. Lippacher, A., Müller, R.H.; Mäder, K.; *Eur. J. Pharm. Biopharm.* **2002**, 53, 155.
- 53.. Freitas, C.; Müller, R.H. *J. Microencapsul.* **1999**, 16, 59.
54. Souto, E.B.; Mehnert, W.; Müller, R.H.; *J. Microencapsul.* **2006**, 23, 417.
55. Jennings, V.; Gohla, S.; *Int. J. Pharm.* **2000**, 196, 219.
56. Kumar, V.V.; Chandrasekar, D.; Ramakrishna, S.; Kishan, V.; Rao, Y.M.; Diwan, P.V.; *Int. J. Pharm.* **2007**, 335, 167.

57. Schubert, M.A.; Harms, M.; Muller-Goymann, C.C.; *Eur. J. Pharm. Sci.* **2006**, 27, 226.
58. Attama, A.A.; Schicke, B.C.; Muller-Goymann, C.C.; *Eur. J. Pharm. Biopharm.* **2006**, 64, 294.
59. Larsson, K. *Acta Chem. Scandinavia.* **1966**, 20, 2255.
60. Freitas, C.; Müller, R.H. *Eur. J. Pharm. Biopharm.* **1999**, 47, 125.
61. Windbergs, M.; Strachan, C.J.; kleinebudde, P.; *AAPS PharmSciTech.* **2009**, 10, 1224.
62. Bummer, P.M.; *Crit. Rev. Ther. Drug Carrier Syst.* **2004**, 21, 1.
63. Müller, R.H.; Keck, C.M.; *J. Biotechnol.* **2004**, 113, 151.
64. Rosenblatt, K.M.; Bunjes. *Mol. Pharm.* **2009**, 6, 105.
65. Bunjes, H.; Koch, M.H.; Westesen, K. *J. Pharm. Sci.* **2003**, 92, 1509.
66. Bunjes, H.; Unruh, T. *Adv. Drug Deliv. Rev.* **2007**, 59, 379.
67. Anantachaisilp, S.; Smith, S.M.; Treetong, A.; Pratontep, S.; Puttipipatkachom, S.; Ruktanonchai, U.R.; *Nanotechnology.* **2010**, 21, 1251.
68. Paliwal, R.; Vaidya, B.; khatri, K.; Goyal, A.K.; Mishra, N.; Mehta, A.; Vyas, S.P.; *Nanomedicine.* **2009**, 5, 184.
69. Ahlin, P.; Kristl, L.; Sentjurc, M.; Strancar, J.; Pecar, S.; *Int. J. Pharm.* **2000**, 196, 241.
70. Siekmann, B.; Bunjes, H.; Koch, M.H.; Westesen, K.; *Int. J. Pharm.* **2002**, 244, 33-43.
71. Yassin, A.E.; Anwer, M.K.; Mowafy, H.A.; El-Bagory, I.M.; Bayomi, M.A.; Alsarra, I.A.; *Int. J. Med. Sci.* **2010**, 7, 398.
72. Liu, M.; Chen, J.H.; Dong, F.R.; Liu, Y. *Nan Fang Yi Ke Da Xue Xue Bao.* **2008**, 28, 700.
73. Chen, H.; Chang, X.; Du, D.; Liu, W.; Liu, J.; Weng, T.; Yang, Y.; Xu, H.; Yang, X. *J. Control. Release.* **2006**, 110, 296.

74. Yang, S.C.; Lu, L.F.; Cai, Y.; Zhu, J.B.; Liang, B.W.; Yang, C.Z. *J. Control. Release.* **1999**, *59*, 299.
75. Yang, Y.; Feng, J.F.; Zhang, H.; Luo, J.Y. *Zhongguo Zhong Yao Za Zhi.* **2006**, *31*, 650.
76. Schmidts, T.; Dobler, D.; Nissing, C.; Runkel, F.; *J. Colloid Interface Sci.* **2009**, *338*, 184.
77. Varia, J.K.; Dodiya, S.S.; Sawant, K.K.; *Curr. Drug Deliv.* **2008**, *5*, 64.
76. Jores, K.; Mehnert, W.; Drechsler, M.; Bunjes, H.; Johann, C.; Mader, K.; *J. Control. Release.* **2004**, *95*, 217.
78. Varshosaz, J.; Tabbakhian, M.; Mohammadi, M.Y.; *J. Liposome Res.* **2010**, *20*, 286.
79. Zhu, R.R.; Qin, L.L.; Wang, M.; Wu, S.M.; Wang, S.L.; Zhang, R.; Liu, Z.X.; Sun, X.Y.; Yao, S.D.; *Nanotechnology.* **2009**, *20*, 055702.
80. Yang, R.; Gao, R.C.; Li, F.; He, H.; Tang, X.; *Drug Dev. Ind. Pharm.* **2010** (In press).
81. Yang, R.; Gao, R.C.; Cai, C.F.; Xu, H.; Li, F.; He, H.B.; Tang, X.; *Chem. Pharm. Bull.* **2010**, *58*, 1195.
82. Tirnaksiz, F.; Kalsin, O.; *J. Pharm. Pharm. Sci.* **2005**, *8*, 299.
83. Gasco, M.R.; Priano, L.; Zara, G.P.; *Prog. Brain. Res.* **2009**, *180*, 181.
84. Caboi, F.; Lazzari, P.; Pani, L.; Monduzzi, M.; *Chem. Phys. Lipids.* **2005**, *135*, 147.
85. Mao, S.R.; Wang, Y.Z.; Ji, H.Y.; Bi, D.Z.; *Yao Xue Xue Bao.* **2003**, *38*, 624.
86. Kristl, J.; Volk, B.; Gasperlin, M.; Sentjurc, M.; Jurkovic, P.; *Eur. J. Pharm. Sci.* **2003**, *19*, 181.
87. Shah, K.A.; Joshi, M.D.; Patravale, V.B.; *J. Biomed. Nanotechnol.* **2009**, *5*, 396.
88. Marego, E.; Cavalli, R.; Caputo, O.; Rodriguez, L.; Gasco, M.R.; *Int. J. Pharm.* **2000**, *205*, 3.

Crystallinity of Dynasan[®] 114 and Dynasan[®] 118 matrices for the production of stable Miglyol[®] loaded nanoparticles

Patrícia Severino^{1,2}, Samantha C. Pinho³, Eliana B. Souto^{2,4}, Maria Helena A. Santana¹

¹Departamento de Processos Biotecnológicos, Faculdade de Engenharia Química, Universidade de Campinas, 13083-852 Campinas – SP, Brasil

²Faculdade de Ciências da Saúde, Universidade Fernando Pessoa, 4200-150 Porto, Portugal

³Departamento de Engenharia de Alimentos, Faculdade de Zootecnia e Engenharia de Alimentos, Universidade de São Paulo, 13635- 900 Pirassununga – SP, Brasil

⁴Instituto de Biotecnologia e Bioengenharia, Centro de Genómica e Biotecnologia, Universidade de Trás-os-Montes e Alto Douro, 5001-801 Vila Real, Portugal

Paper published in Journal of Thermal Analysis and Calorimetry, p. 101-108, 2011.

DOI: 10.1007/s10973-011-1613-7

Abstract

This work focuses on the physicochemical characterization of lipid materials useful for the production of the so-called solid lipid nanoparticle (SLN) and nanostructured lipid carriers (NLC). The chosen lipids were Dynasan[®]114 and Dynasan[®]118 (as solid lipids (SL), melting above 80°C, and Miglyol[®]812 and Miglyol[®]840 as liquid lipids (LL), crystallizing below -15°C. Raw lipids (pure or SL:LL mixtures) were analyzed by Differential Scanning Calorimetry (DSC), Wide Angle X-ray Diffraction (WAXD) and Polarized Light Microscopy (PLM), before and after tempering at 100°C for 1 hour. The selected SL:LL combination was 70% (Dynasan[®]812 and 840) and 30% (Miglyol[®]812 and 840) for the production of SLN and NLC by High Pressure Homogenization (HPH). Particles with a mean size of 200 nm (polydispersity index <0.329) and zeta potential of -15mV were obtained, and their long-term stability was confirmed for 3 months of storage at 7°C.

Keywords: Dynasan[®]114, Dynasan[®]118, Miglyol[®]812, Miglyol[®]840, Differential Scanning Calorimetry, Wide Angle X-ray Diffraction, Polarized Light Microscopy, Lipid nanoparticles

1. Introduction

Nanoparticles have become a rapidly growing field with potential applications in health and drug therapy [1]. Examples include solid lipid nanoparticles (SLN) [2], nanostructure lipid carrier (NLC) [3], liposomes [4], polymeric nanoparticles [5] and dendrimers [6], provided by their extraordinary physical and chemical properties resulting from the nano size effect [7]. Lipid nanoparticles are considered the least toxic among all the other nanoparticles for *in vivo* applications. SLN and NLC have been proposed as alternative drug carriers because of their physiological lipid composition, the variety of possible administration routes (e.g. intravenous, oral and topical), large scale production by HPH, and the relatively low costs of excipients. A number of studies have recently been published focusing on the production of SLN and NLC, and their physicochemical characterization, release profile, including the feasibility of incorporation of lipophilic and hydrophilic drugs [7,8].

Lipids employed for the production of nanoparticles include triglycerides and their mixtures, fatty acids and waxes [9]. It is however required that matrix maintains the solid state at room temperature and for this, the selection of lipids requires the evaluation of their polymorphism, crystallinity, miscibility and physicochemical structure. For large production, the control of polymorphism is a demand due to its influence on the encapsulation efficiency and on the drug expulsion during storage [10]. The lipid crystallization is also an important characteristic, since the crystalline structures of triglycerides (e.g. Dynasan[®]114 and Dynasan[®]118) can occur in different polymorphism forms (α , β' , β). The α -form (hexagonal) is the least stable with a lower melting point and latent heat, whereas the β -form (triclinic) is more stable with higher melting point and higher latent heat. The transformation of α to β' (orthorhombic) and β is irreversible, and occurs towards a more hydrodynamic stable system [11].

In the pharmaceutical field, lipid nanoparticles can be used for all administration routes because of their small particle size, ranging from 50 to 1000 nm [12-16]. Until today, a variety of techniques have been employed for lipid nanoparticle production [17]. The most promising technique to achieve higher drug loading in nanoparticles is the HPH. This process is easy to scale up, it does not use organic solvents, produced particle with small diameter [18-20] and low polydispersity index ²¹. High shear homogenization followed by the HPH can modulate the mean nanoparticle size. Furthermore, different lipid combinations can be tested to obtain the desired release profile [22-23]. HPH has been used for more than fifty years for the production of emulsions for parenteral nutrition, such as Intralipid[®] and Lipofundin[®] [15].

The aim of this study was to evaluate the polymorphism and crystallinity of triglycerides commonly used in the production of SLN and NLC, such as trimiristin (Dynasan[®]114) and tristearin (Dynasan[®]118), and the binary mixture of solid and liquid lipids caprylic/capric triglyceride (Miglyol[®]812) and propylene glycol dicaprylate/dicaprate (Miglyol[®]840).

2. Material and methods

2.1 Material

Trimyristin (Dynasan[®]114), Tristearin (Dynasan[®]118), Caprylic/Capric Triglycerides (Miglyol[®]812) and Propylene Glycol Dicaprylate/Dicaprate (Miglyol[®]840) were obtained from Sasol Olefins & Surfactants (Germany). Polysorbate 80 (Tween[®]80) was obtained from Synth (Brazil). Double distilled water was used after filtration in a Millipore systems (home supplied).

2.2 Methods

2.2.1 Lipid Screening and Thermal Treatment of Lipid Materials

The solid lipid (Dynasan[®]114 and Dynasan[®]118) and the binary mixture of solid and liquid lipids (Miglyol[®]812 and Miglyol[®]840) were combined in different ratios and analysed separately. Samples were analysed before and after tempering at 80°C for 1 h. This process consisted of melting at 80°C on a thermostatic bath (Marconi, MA 127/BD, Brazil), following tempering by sample incubation in the thermostatic bath for 1 h at 80°C²⁴. Samples were then kept at room temperature until complete cooling and solidification, to check for the creation of polymorphic forms. Most production processes of SLN and NLC require heating; thus, tempering was performed to mimic the production procedure carried out for lipid nanoparticles production.

Table 1. Composition of lipid mixtures % (w/w).

Sample	Dynasan [®] 114	Dynasan [®] 118	Miglyol [®] 812	Miglyol [®] 840
D4M812 (90:10)	90		10	
D4M812 (80:20)	80		20	
D4M812 (70:30)	70		30	
D4M840 (90:10)	90			10
D4M840 (80:20)	80			20
D4M840 (70:30)	70			30
D8M812 (90:10)		90	10	
D8M812 (80:20)		80	20	
D8M812 (70:30)		70	30	
D8M840 (90:10)		90		10
D8M840 (80:20)		80		20
D8M840 (70:30)		70		30

2.2.2 Preparation of nanoparticles and characterization

Solid lipid nanoparticles was prepared by HPH (NiroSoavi, Panda, Italy) [25]. The experimental protocol was to melt the lipid or its mixtures 10°C above the melting point of solid lipid and, simultaneously, an aqueous solution containing the surfactant was heated at the same temperature. The melted lipid phase was dispersed in aqueous surfactant solution applying high shear homogenization (Ultra-Turrax[®] T25, USA) at 15.000 rpm for 3 minutes to obtain a microemulsion. Then, the microemulsion was passed 3 times at 500 bar through the hot HPH. After that, formulation was cooled in ice bath to allow lipid recrystallization until reaching the temperature of 20°C. Table 1 shows the developed formulation.

Table 2. Composition of solid lipid nanoparticles, values in % (w/w)

Phase	Formulation	1	2	3	4
oil	Dynasan [®] 114	2.1		2.1	
	Dynasan [®] 118		2.1		
	Miglyol [®] 812	0.9	0.9		
	Miglyol [®] 840			0.9	0.9
Aqueous	Tween [®] 80	3	3	3	3
	Water	200	200	200	200

2.2.3 Differential Scanning Calorimetry (DSC)

Thermal behavior of lipid matrices was analysed by DSC (Mettler Toledo, FP90 Central Processor, São Paulo, Brazil). A volume of sample containing approximately 5-10 mg of lipid mass was weighed in an aluminum pan and sealed hermetically, under inert atmosphere (N₂). The analysis was performed at a heating and cooling rate of 5 K/min,

using an empty pan as reference. The samples were heated up from 10°C to 100°C, following cooling down to 10°C.

2.2.4 Wide Angle X-ray Diffraction (WAXD)

To study the polymorphism and crystalline properties of the lipids and their mixtures, WAXD was carried out in a diffractometer X-ray (Philips, model X'pert, Pennsylvania, USA), using copper anode which delivered X-ray of wavelength, $\lambda = 0.154056$ nm. WAXD measurements were taken from 5° to 33° in 0.015° steps (1s per step). The interlayer spacings were calculated from the reflections using Bragg's equation:

$$d = \frac{\lambda}{\text{sen}2\theta}$$

where λ is the wavelength of the incident X-ray beam and θ is the scattering angle. The parameter d , otherwise called the interlayer spacing, is the separation between a particular set of planes of the crystal lattice structure. Data of the scattered radiation were recorded with a blend local-sensible detector using an anode voltage of 40 kV, a current of 25 mA and a scan rate of 0.5° per minute. The samples were mounted on a thin glass capillary being fastened to a brass pin without any previous sample treatment.

2.2.5 Polarized Light Microscopy (PLM)

PLM is used to check for lipid microstructures and to monitor their melting transitions and fusion. Micrographs of crystallizing lipid mixtures were examined with a photomicroscope (LEICA, model Leitz DMRXE, Bensheim, Germany coupled with a software Motic Images Advanced 3.2. and using cross polarizer. Samples were evaluated 24 h after production and analyzed with increase of 20.000x.

2.2.6 Particle size and zeta potential analysis

The particle size of nanoparticle was determined through dynamic light scattering (DLS, Zetasizer Nano NS, Malvern Instruments, Malvern, UK). DLS, sometimes referred to as Photon correlation spectroscopy (PCS), is a non-invasive, well established technique for measuring the size of molecules and particles typically in the submicron region ²⁶. This instrument also allows determining the electrophoretic mobility to assess the surface electrical charge of particles. The samples were diluted with ultra-purified water to weaken the opalescence before measuring the particle mean diameter and polydispersity index. Zeta potential of lipid nanoparticles was also measured in purified water adjusting conductivity (50 $\mu\text{S}/\text{cm}$) with potassium chloride solution (0.1%, w/v). The zeta potential was determined from the electrophoretic mobility using the Helmholtz–Smoluchowski equation [27]. The processing was done by the software included within the system.

3. Results

Polymorphic behaviour is often shown by long-chain compounds, in general, those compounds crystallize in two or three different phases, α and β' , or α , β' and β , respectively. DSC was employed to study the melting temperature and crystallization behaviour of lipids [28]. For this study 12 samples were analyzed using different ratios of Dynasan[®]114 Dynasan[®]118 as solid lipid and Miglyol[®]812 and Miglyol[®]840 as liquid lipids, according to Table 1.

According to the results obtained after DSC analysis (Table 3), Dynasan[®]114 and Dynasan[®]118 depicted a melting event at 60.7°C and 73.8°C, respectively, and the onset temperature at 57.0°C and 60.9°C. The difference between the melting and the onset temperatures is the range at which the melting event of the lipid occurs, and the greater the

difference the greater the disorder of the crystals. After adding the liquid lipid (Miglyol[®]812 or Miglyol[®]840) to the solid lipid (Dynasan[®]114 or Dynasan[®]118), this difference increased as observed for samples D4M812 (70:30); D4M812 (70:30); D8M812 (70:30) and D8M840 (70:30).

Using 30% of liquid lipid, major differences between the temperatures were recorded, favouring a less orderly and lipid matrix containing imperfections in their structure, capable of accommodating a larger amount of drug, to minimize its expulsion during storage, also to modelate their release pattern [9-29]. In colloidal systems, for *in vivo* use it is desired to work with lipids having onset temperatures above 40°C, to avoid melting of the nanoparticles when administered [30].

Table 3. Thermal properties of lipids mixtures.

Sample	Onset Temperature (°C)	Melting Peak (°C)	ΔH Melting Enthalpy (J/g)	ΔT (T _{melting} -T _{onset})
D4M812 (90:10)	53.7	59.2	130.0	5.5
D4M812 (80:20)	51.8	56.3	113.0	4.5
D4M812 (70:30)	52.8	58.2	106.0	5.4
D4M840 (90:10)	53.1	58.0	124.0	4.9
D4M840 (80:20)	49.0	55.8	106.0	6.8
D4M840 (70:30)	47.1	54.1	94.4	7.0
D8M812 (90:10)	68.2	72.2	147.0	4.0
D8M812 (80:20)	67.3	71.4	125.0	4.1
D8M812 (70:30)	64.9	69.4	110.0	4.5
D8M840 (90:10)	67.3	71.9	141.0	4.6
D8M840 (80:20)	62.1	68.1	84.5	6.0
D8M840 (70:30)	60.3	67.2	90.2	6.9

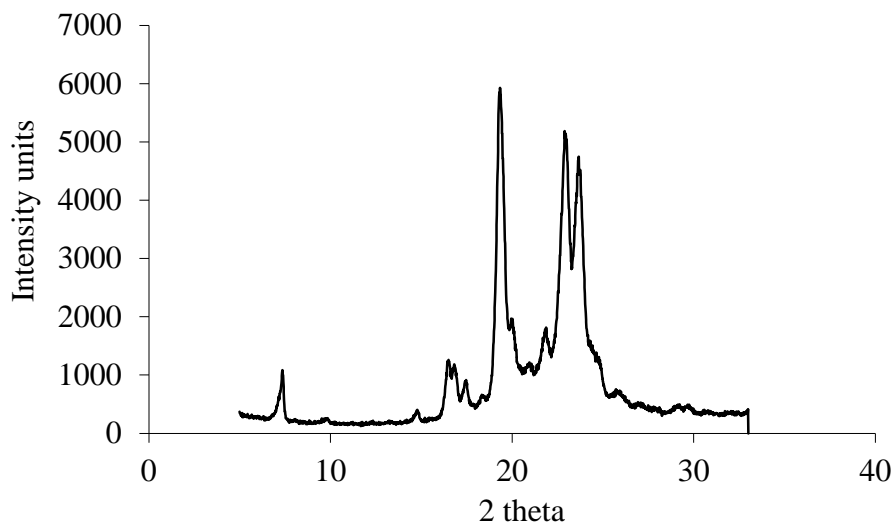
The samples chosen to undergo tempering are presented in Table 4, which also shows the melting temperatures and onset temperature, before and after the tempering process, and the differences among them. The melting and the onset temperatures fusion of each lipid mixture subjected to tempering was obtained from the DSC thermograms. Comparing the differences between the melting and onset temperatures, before and after tempering, the differences increased after tempering. These results show that structures exhibit susceptibility to clutter after processing for production of lipid nanoparticles. This disruption facilitates the encapsulation of drugs and increase particle stability during storage. After tempering, the obtained melting temperatures were higher than 40°C, which represents an important property, because it ensures the integrity of the particles for parenteral use [31,32].

Table 4. Thermal properties of lipids mixtures after and before tempering.

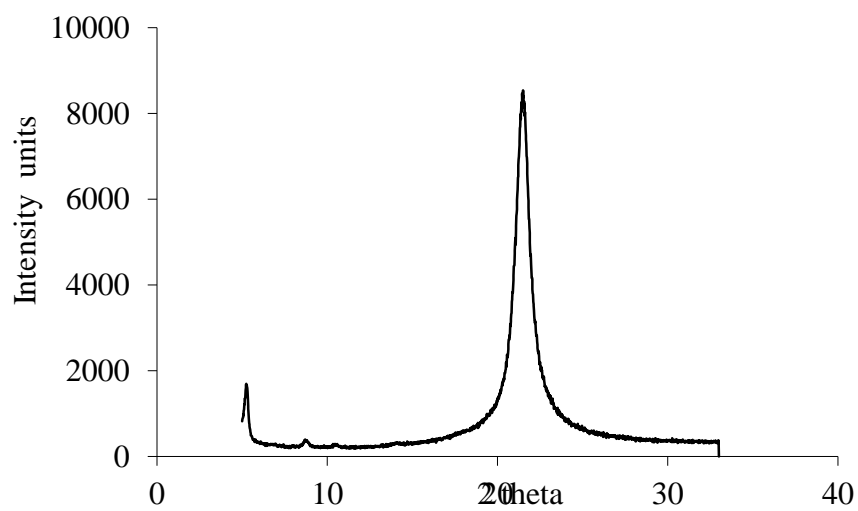
Sample	Before			After		
	Tonset	Tmelting	ΔT	Tonset	Tmelting	ΔT
D4M812 (70:30)	52.8	58.2	5.4	51.4	58.1	6.7
D4M840 (70:30)	47.1	54.1	7.0	47.0	56.4	9.4
D8M812 (70:30)	64.9	69.4	4.5	66.9	72.1	5.2
D8M840 (70:30)	60.3	67.2	6.9	64.5	70.8	6.3

In general, the lipids crystallize in two or three different phases, α and β 'or α , β and β' '. To analyse these different polymorphic forms, DSC was carried out and for a more precise identification of the phases WAXD is employed since it allows for a better differentiation of each phase. In addition, WAXD is used to investigate the arrangement of the layers of lipid molecules and their crystallinity. Figure 1 shows the X-ray diffraction patterns of solid

lipids, Dynasan[®]114 and Dynasan[®]118. In Figure 1 (a) the phases α , β and β'/β are well defined, showing that Dynasan[®]114 exists in a crystalline state (Figure 1 (b)) only one peak at 21.53 (2θ) was recorded typical of the β -form.

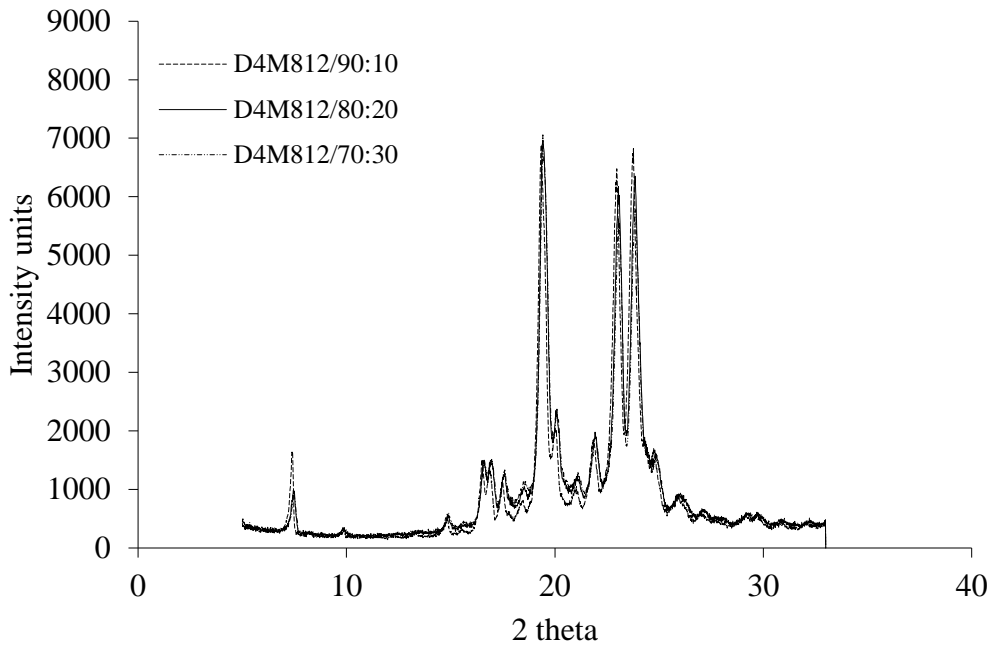


(a)

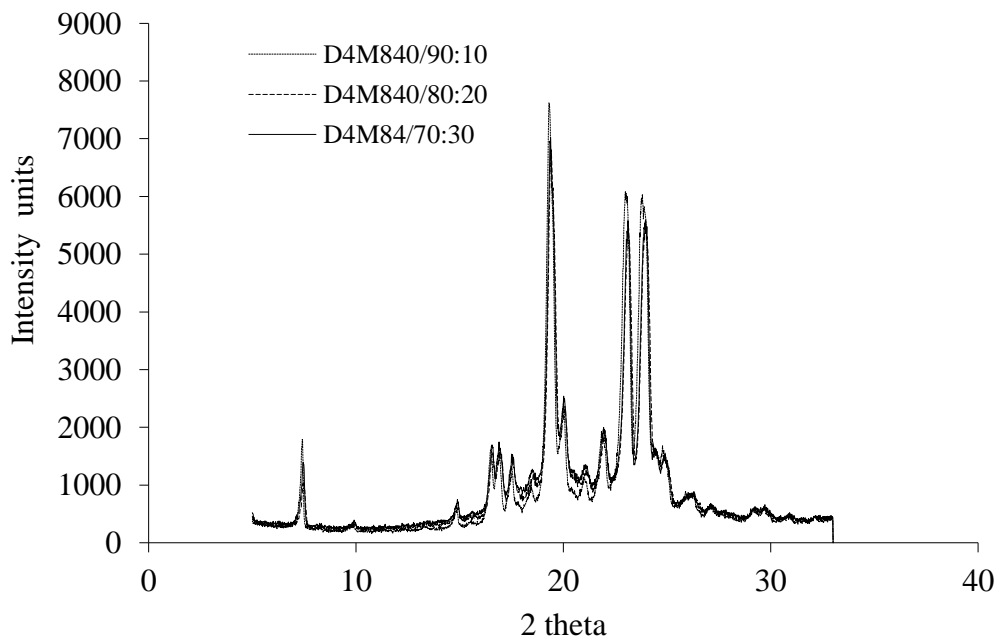


(b)

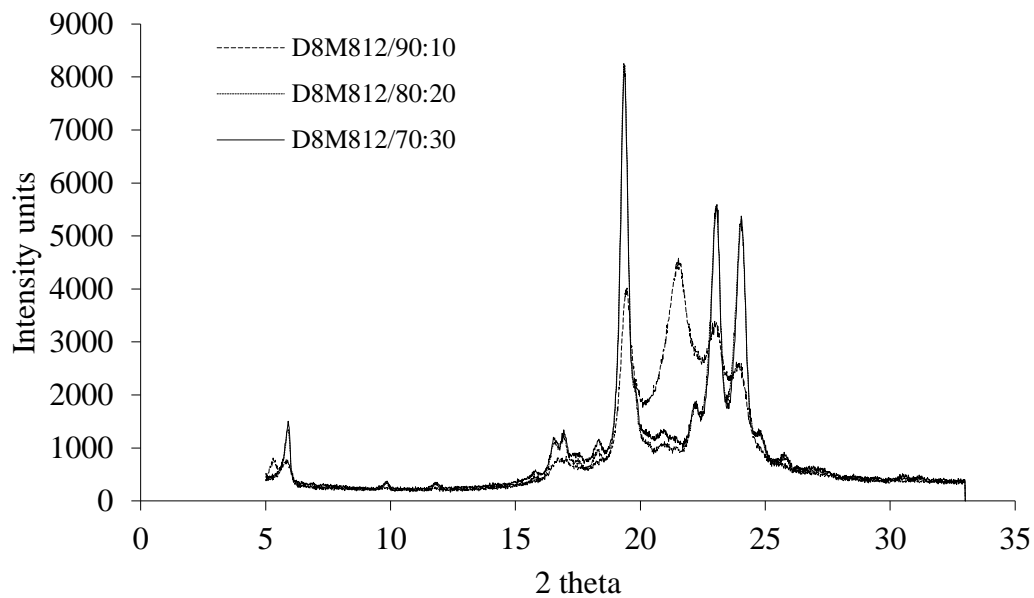
Figure 1. WAXD diffractogram after fusion of (a) Dynasan[®]114 and (b) Dynasan[®]118.



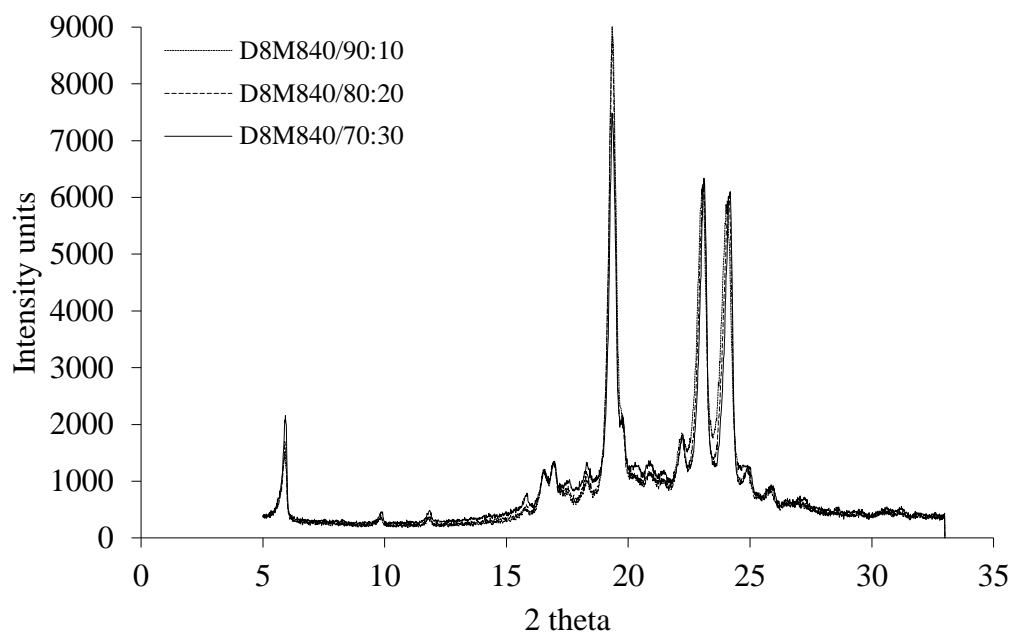
(a)



(b)



(c)

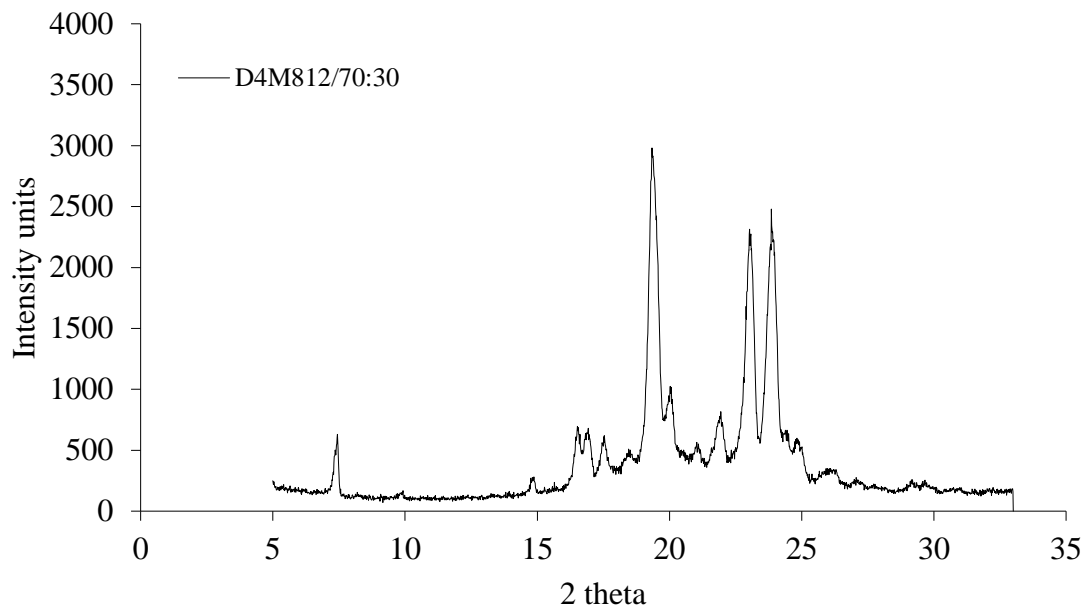


(d)

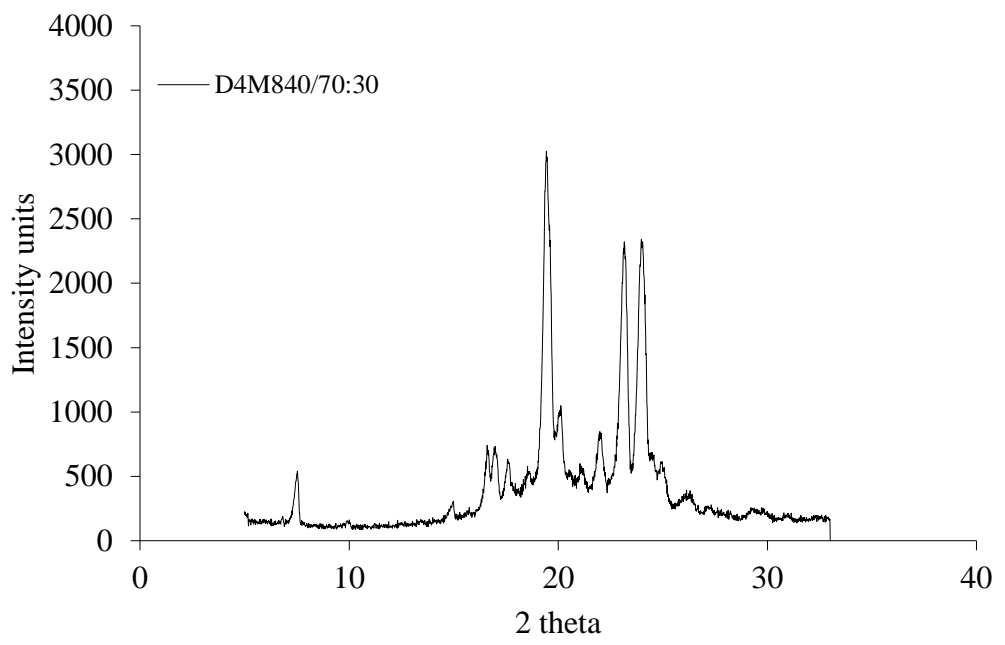
Figure 2. WAXD diffractogram after fusion (a) Dynasan[®]114 and Miglyol[®]812; (b) Dynasan[®]114 and Miglyol[®]840; (c) Dynasan[®]118 and Miglyol[®]812; (d) Dynasan[®]118 e Miglyol[®]840.

The WAXD diffractogram of Figure 2 corresponds to the lipid mixtures containing a solid lipid with different ratios of liquid lipid, according to Table 1. It is clearly in all cases the presence of three phases crystalline (α , β and β'/β). In the specific case of Dynasan[®]118, which as a bulk material shows only one phase (Figure 1 (b)), in liquid mixture with the lipids (Figure 2 (a) and (b)) showed the three distinct typical phases.

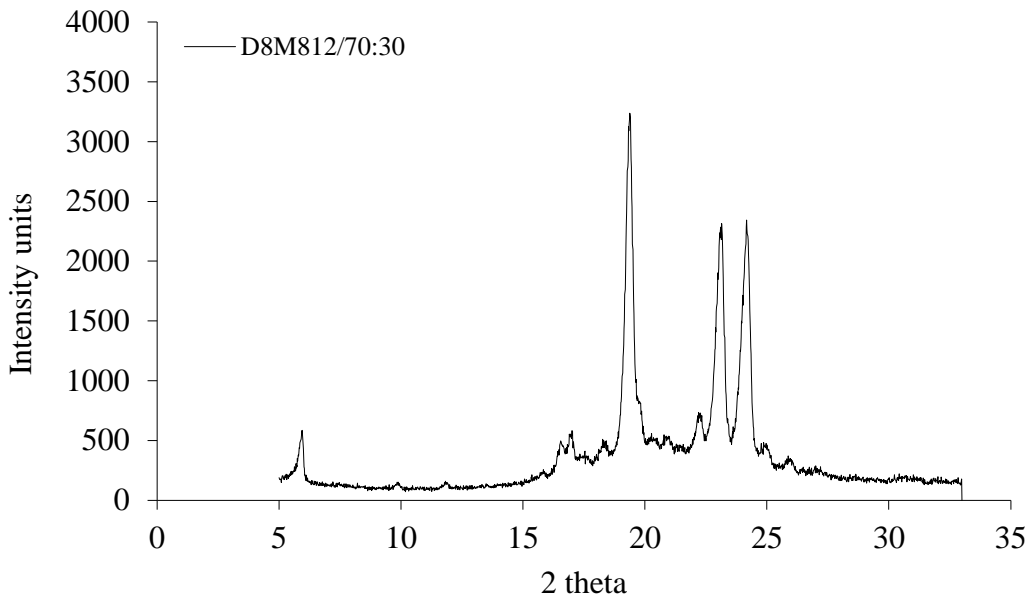
Comparing the baseline (trend linearity) of solid lipid (Figure 1) with the baselines of the lipid mixtures in Figure 2, it was also shown that the addition of liquid lipid (Miglyol[®]812 or Miglyol[®]840) promoted disorder. From the obtained results, to develop NLC have chosen the ratio 70:30 (SS:SL), i.e. that responsive for a greater disorder of the matrix. Therefore, system stability and ability for doing loading. The WAXD diffractogram patterns of Figure 3 show that after the tempering process of lipid mixtures containing 30% liquid lipid, the intensity of the peaks. It is observed that the peak was reduced. The peak width was maintained, although not as well defined as before the treatment.



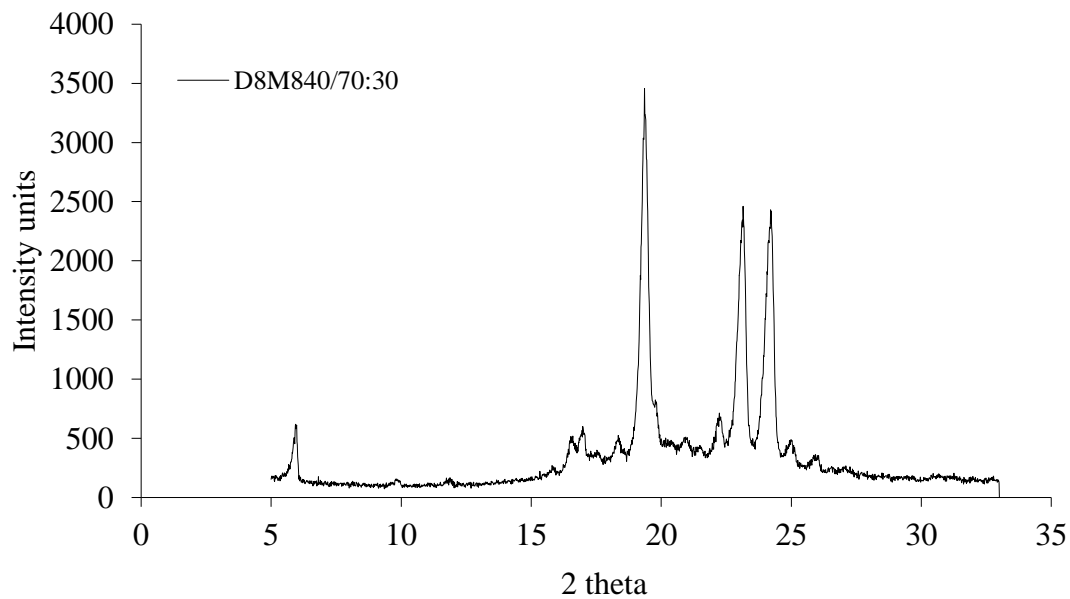
(a)



(b)



(c)



(d)

Figure 3. WAXD diffractogram after fusion (a) Dynasan[®]114 and Miglyol[®]812 (b) Dynasan[®]114 and Miglyol[®]840, (c) Dynasan[®]118 and Miglyol[®]812. (d) Dynasan[®]118 and Miglyol[®]840.

Correlating the data obtained by DSC and WAXD after the tempering process, consistent outcomes were observed. The decrease of the melting temperature was followed by the decrease of intensity of WAXD peaks, suggesting the presence of more unorganized structures. This phenomenon is desired for drug loading and to increase the thermodynamic stability during storage.

PLM analysis compared the morphological characteristics of lipid mixtures with samples of solid lipid content 30% liquid lipid liquid (Figure 4). The results show the presence of crystalline structures in equilibrium with liquid crystalline lipids. Dynasan[®]114 and Dynasan[®]118 are in the form of irregular crystals of varying sizes. Addition liquid lipid (30%) created more amorphous structures.

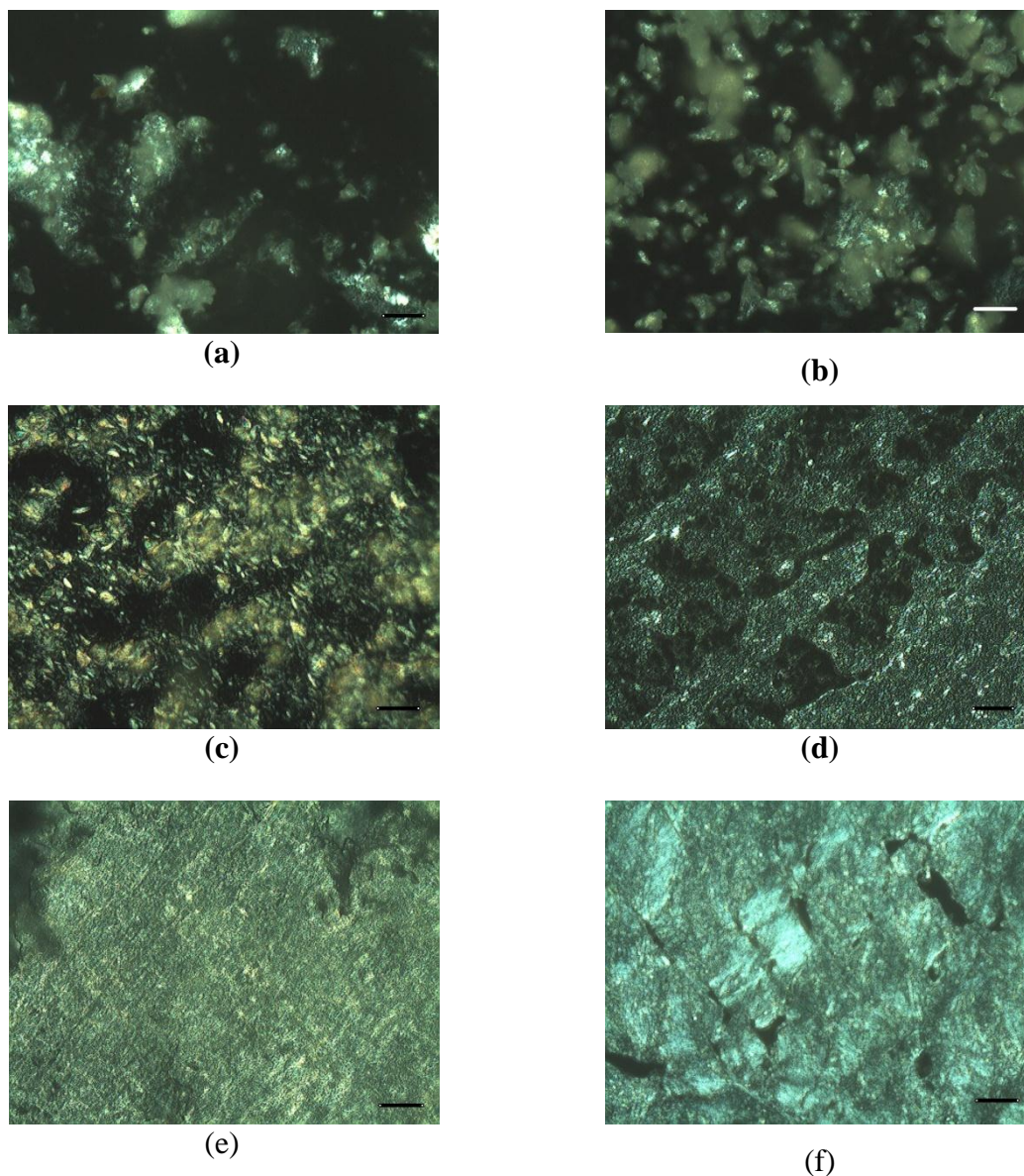


Figure 4. Micrographs obtained by PLM (a) Dynasan[®]114, (b) Dynasan[®]118, (c) Dynasan[®]114 and Miglyol[®]812 (70:30); (b) Dynasan[®]114 and Miglyol[®]840 (70:30); (c) Dynasan[®]118 and Miglyol[®]812 (70:30); (d) Dynasan[®]118 e Miglyol[®]840 (70:30).

Physicochemical characterization of a lipid nanoparticles produced by hot HPH is shown in Table 4. All formulations were obtained with an average hydrodynamic diameter around 200 nm and polydispersity index of 0.329, with the presence of one population. The zeta potential was -19.26 to +0.25 mV for all formulation with standard deviation of about 0.20

to 0.66. The zeta potential zeta range can be explain by coating of polysorbate 80 in structure of SLN and NLC. This values reveals the particles stability as a result of their interaction with electrolytes and rheology of colloidal suspensions. While less than $|30 \text{ mV}|$, the nanoparticles showed a good level of electrostatic instability, i.e. the electrostatic repulsion prevents aggregation of particles. Other strategies may be added to increase colloidal stability. The values obtained are of adequate size for pharmaceutical and cosmetic use.

4. Conclusion

This work was focused on the characterization of lipid mixtures in different concentrations, by DSC, WAXD and PLM. The results of characterization of the lipid mixtures show that mixtures containing 30% lipid liquid, both for Miglyol[®]812 and Miglyol[®]840 were the most promising for the production of the NLC, due to the presence of a more disordered crystal, results that are consistent while the employed technology. The lipid nanoparticles showed size, polydispersity index and zeta potential promising for drug loading for pharmaceutical and cosmetic use.

Acknowledgements

The authors wish to acknowledge the sponsorship of the FAPESP (Fundação de Amparo e Pesquisa do Estado de São Paulo) and CAPES (Coordenação de Aperfeiçoamento de Pessoal de Nível Superior).

5. References

1. Sahoo SK, Parveen S, Panda JJ. The present and future of nanotechnology in human health care. *Nanomedicine*. 2007;3(1):20-31.
2. Aji Alex MR, Chacko AJ, Jose S, Souto EB. Lopinavir loaded solid lipid nanoparticles (SLN) for intestinal lymphatic targeting. *Eur J Pharm Sci*. 2011;42(1-2):11-8.
3. Gonzalez-Mira E, Egea MA, Garcia ML, Souto EB. Design and ocular tolerance of flurbiprofen loaded ultrasound-engineered NLC. *Colloids Surf B Biointerfaces*. 2010;81(2):412-421.
4. Heney M, Alipour M, Vergidis D, Omri A, Mugabe C, Th'ng J, Suntres Z. Effectiveness of liposomal paclitaxel against MCF-7 breast cancer cells. *Can J Physiol Pharmacol*. 2010;88(12):1172-1180.
5. Wang J, Liu W, Tu Q, Song N, Zhang Y, Nie N. Folate-Decorated Hybrid Polymeric Nanoparticles for Chemically and Physically Combined Paclitaxel Loading and Targeted Delivery. *Biomacromolecules*. 2011;12(1):228-234.
6. Barata TS, Shaunak S, Teo I, Zloh M, Brocchini S. Structural studies of biologically active glycosylated polyamidoamine (PAMAM) dendrimers. *J Mol Model*. 2010 (In press).
7. Yassin AE, Anwer MK, Mowafy HA, El-Bagory IM, Bayomi MA, Alsarra IA. Optimization of 5-fluorouracil solid-lipid nanoparticles: a preliminary study to treat colon cancer. *Int J Med Sci*. 2010;7(6):398-408.
8. Souto EB, Müller RH. Lipid nanoparticles: effect on bioavailability and pharmacokinetic changes. *Handb Exp Pharmacol*. 2010;197:115-141.
9. Muller RH, Mader K, Gohla. Solid lipid nanoparticles (SLN) for controlled drug delivery - a review of the state of the art. *Eur J Pharm Biopharm*. 2000;50(1):161-177.

10. Jores K, Mehnert W, Drechsler M, Bunjes H, Johann C, Mader K. Investigations on the structure of solid lipid nanoparticles (SLN) and oil-loaded solid lipid nanoparticles by photon correlation spectroscopy, field-flow fractionation and transmission electron microscopy. *J Control Release*. 2004;95(2):217-227.
11. Jores K, Mehnert W, Drechsler M, Bunjes H, Johann C, Mader K. Investigations on the structure of solid lipid nanoparticles (SLN) and oil-loaded solid lipid nanoparticles by photon correlation spectroscopy, field-flow fractionation and transmission electron microscopy. *J Control Release*. 2004;95(2):217-227.
12. Bondi ML, Craparo EF, Giammona G, Drago F. Brain-targeted solid lipid nanoparticles containing riluzole: preparation, characterization and biodistribution. *Nanomedicine (Lond)*. 2010;5(1):25-32.
13. Bondi ML, Craparo EF, Giammona G, Drago F. Brain-targeted solid lipid nanoparticles containing riluzole: preparation, characterization and biodistribution. *Nanomedicine*. 2010;5(1):25-32.
14. Souto EB, Muller RH. Investigation of the factors influencing the incorporation of clotrimazole in SLN and NLC prepared by hot high-pressure homogenization. *J Microencapsulation*. 2006;23(4):377-388.
15. Muller R, Mehnert W, Lucks J, Schwarz C, Zurmuhlen A, Weyhers H, Freitas C, Ruhl D. Solid lipid nanoparticle (SLN) - An alternative colloidal carrier system for controlled drug-delivery. *Eur J Pharm Biopharm*. 1995; 41(1):62-69.
16. Ali H, Shirode AB, Sylvester PW, Nazzal S. Preparation and in vitro antiproliferative effect of tocotrienol loaded lipid nanoparticles. *Colloids Surf A Physicochem Eng Asp*. 2010;353(1):43-51.

17. Wissing SA, Kayser O, Muller RH. Solid lipid nanoparticles for parenteral drug delivery. *Adv Drug Deliv Reviews*. 2004;56(9):1257-1272.
18. Muchow M, Maincent P, Muller RH. Lipid nanoparticles with a solid matrix (SLN, NLC, LDC) for oral drug delivery. *Drug Dev Ind Pharm*. 2008;34(12):1394-1405.
19. Mehnert W, Mader K. Solid lipid nanoparticles - Production, characterization and applications. *Adv Drug Deliv Reviews*. 2001;47(2-3):165-196.
20. Muchow M, Maincent P, Muller RH. Lipid Nanoparticles with a Solid Matrix (SLN, NLC, LDC) for Oral Drug Delivery. *Drug Dev Ind Pharm*. 2008;34(12):1394-1405.
21. Lippacher A, Muller RH, Mader K. Preparation of semisolid drug carriers for topical application based on solid lipid nanoparticles. *Int J Pharm*. 2001;214(1-2):9-12.
22. Muller RH, Radtke M, Wissing SA. Nanostructured lipid matrices for improved microencapsulation of drugs. *Int J Pharm*. 2002;242(1-2):121-128.
23. Muller RH, Radtke M, Wissing SA. Solid lipid nanoparticles (SLN) and nanostructured lipid carriers (NLC) in cosmetic and dermatological preparations. *Adv Drug Deliv Reviews*. 2002;54:S131-S155.
24. Souto EB, Mehnert W, Muller RH. Polymorphic behaviour of Compritol (R) 888 ATO as bulk lipid and as SLN and NLC. *J Microencapsul*. 2006;23(4):417-433.
25. Potta SG, Minemi S, Nukala RK, Peinado C, Lamprou DA, Urquhart A, Douroumis D. Preparation and characterization of ibuprofen solid lipid nanoparticles with enhanced solubility. *J Microencapsul*. 2011;28(1):74-81.
26. Luykx D, Peters RJB, van Ruth SM, Bouwmeester H. A review of analytical methods for the identification and characterization of nano delivery systems in food. *J Agric Food Chem*. 2008;56(18):8231-8247.

27. Deshiikan SR, Papadopoulos KD. Modified Booth equation for the calculation of zeta potential. *Colloid Polym Sci.* 1998;276(2):117-124.
28. Jenning V, Thunemann AF, Gohla SH. Characterisation of a novel solid lipid nanoparticle carrier system based on binary mixtures of liquid and solid lipids. *Int J Pharm.* 2000;199(2):167-177.
29. Muller RH, Radtke M, Wissing SA. Nanostructured lipid matrices for improved microencapsulation of drugs. *Int J Pharm.* 2002;242(1-2):121-128.
30. Mezzena M, Scalia S, Young PM, Traini D. Solid lipid budesonide microparticles for controlled release inhalation therapy. *AAPS J.* 2009;11(4):771-778.
31. Kim JK, Park JS, Kim CK. Development of a binary lipid nanoparticles formulation of itraconazole for parenteral administration and controlled release. *Int J Pharm.* 2010;383(1-2):209-215.
32. Attama AA, Muller-Goymann CC. Investigation of surface-modified solid lipid nanocontainers formulated with a heterolipid-templated homolipid. *Int J Pharm.* 2007;334(1-2):179-189.

Capítulo 2

Current State-of-Art and New Trends on Lipid Nanoparticles (SLN and NLC) for Oral Drug Delivery

Patrícia Severino^{1,2}, Tatiana Andreani^{2,3,4}, Ana Sofia Macedo², Joana F. Figueiro²,
Maria Helena A. Santana¹, Amélia M. Silva^{3,4} and Eliana B. Souto^{2,5}

¹Department of Biotechnological Processes, School of Chemical Engineering, State University of Campinas (UNICAMP), 13083-970 Campinas, SP, Brazil

²Faculty of Health Sciences, Fernando Pessoa University (FCS-UEP), Rua Carlos da Maia, 296, 4200-150 Porto, Portugal

³Department of Biology and Environment, University of Trás-os Montes e Alto Douro, 5001-801 Vila Real, Portugal

⁴Centre for Research and Technology of Agro-Environmental and Biological Sciences, 5001-801 Vila Real, Portugal

⁵Institute of Biotechnology and Bioengineering, Centre of Genomics and Biotechnology, University of Trás-os-Montes and Alto Douro (CGB-UTAD/IBB), P.O. Box 1013, 5001-801 Vila Real, Portugal

Paper published in Journal of Drug Delivery, 2012.

DOI: 10.1155/2012/750891

Abstract

Lipids and lipid nanoparticles are extensively employed as oral-delivery systems for drugs and other active ingredients. These have been exploited for many features in the field of pharmaceutical technology. Lipids usually enhance drug absorption in the gastrointestinal tract (GIT), and when formulated as nanoparticles, these molecules improve mucosal adhesion due to small particle size and increasing their GIT residence time. In addition, lipid nanoparticles may also protect the loaded drugs from chemical and enzymatic degradation and gradually release drug molecules from the lipid matrix into blood, resulting in improved therapeutic profiles compared to free drug. Therefore, due to their physiological and biodegradable properties, lipid molecules may decrease adverse side effects and chronic toxicity of the drug-delivery systems when compared to other of polymeric nature. This paper highlights the importance of lipid nanoparticles to modify the release profile and the pharmacokinetic parameters of drugs when administrated through oral route.

1. Introduction

The use of lipid particles in pharmaceutical technology has been reported for several years. The first approach of using lipid microparticles was described by Eldem et al. [1], reporting the production by high-speed stirring of a melted lipid phase in a hot surfactant solution obtaining an emulsion. Solid microparticles are formed when this emulsion is cooled to room temperature, and the lipid recrystallizes. The obtained products were called “lipid nanopellets”, and they have been developed for oral administration [2]. Lipospheres were described by Domb applying a sonication process [3–5]. To overcome the drawbacks associated to the traditional colloidal systems [6], such as emulsions [7], liposomes [8], and polymeric nanoparticles [9], solid lipid nanoparticles (SLN) [10, 11] have been developed for similar purposes [12].

SLN are biocompatible and biodegradable and have been used for controlled drug delivery and specific targeting. These colloidal carriers consist of a lipid matrix that should be solid at both room and body temperatures, having a mean particle size between 50 nm and 1000 nm [13, 14]. A clear advantage of the use of lipid particles as drug carrier systems is the fact that the matrix is composed of physiological components, that is, excipients with generally recognized as safe (GRAS) status for oral and topical administration, which decreases the cytotoxicity. SLN have been already tested as site-specific carriers particularly for drugs that have a relatively fast metabolism and are quickly eliminated from the blood, that is, peptides and proteins [15].

The cytotoxicity of SLN can be attributed to nonionic emulsifiers and preservative compounds which are used in the production of these systems [16]. SLN prepared up to concentrations of 2.5% lipid do not exhibit any cytotoxic effects *in vitro* [17]. Even concentrations higher than 10% of lipid have been shown a viability of 80% in culture of

human granulocytes [18]. In contrast, some polymeric nanoparticles showed complete cell death at concentrations of 0.5%. In addition, a high loading capacity for a broad range of drugs can be achieved, especially if they have lipophilic properties [12, 19].

Due to their physiological and biodegradable properties, SLN have been tested for several administration routes [20, 21], including the oral [22, 23] and peroral [24, 25] routes. SLN can be obtained by exchanging the liquid lipid (oil) of the o/w nanoemulsions by a solid lipid [19]. In general, a solid core offers many advantages in comparison to a liquid core [26]. Emulsions and liposomes usually show lack of protection of encapsulated drugs, and drug release as a burst (emulsions) or noncontrolled (from liposomes). SLN possess a solid lipid matrix identical to polymeric nanoparticles. In addition, SLN are of low cost [27], the excipients and production lines are relatively cheap, and the production costs are not much higher than those established for the production of parenteral emulsions [28]. At the turn of the millennium, modifications of SLN, the so-called nanostructured lipid carriers (NLCs), have been introduced to the literature, and these NLC represent nowadays the second generation of lipid nanoparticles. These carrier systems overcome observed limitations of conventional SLN [29]. The main difference between SLN and NLC is the fact that the concept of these latter is performed by nanostructuring the lipid matrix, in order to increase the drug loading and to prevent its leakage, giving more flexibility for modulation of drug release. This approach is achieved by mixing solid lipids with liquid lipids in NLC instead of highly purified lipids with relatively similar molecules in SLN. This mixture has to be solid at least at 40°C. The result is a less-ordered lipid matrix with many imperfections, which can accommodate a higher amount of drug [11].

2. Role of Lipids in Oral Delivery

A limiting factor for *in vivo* performance of poorly water-soluble drugs for oral administration is their resistance of being wetted and dissolved into the fluid in the GIT (apart from potential drug degradation in the gut). Thus, the increase in the dissolution rate of poorly water-soluble drugs is relevant for optimizing bioavailability. Over the last 10 years, poorly water-soluble compounds are formulated in lipid nanoparticles for drug administration [30]. The features of lipid nanoparticles for oral and peroral delivery are related with their adhesive properties. Once adhered to the GIT wall, these particles are able to release the drug exactly where it should be absorbed. In addition, the lipids are known to have absorption-promoting properties not only for lipophilic drugs, such as Vitamin E, repaglinide [22], and puerarin [23].

Hydrophilic drugs can also be incorporated in SLN; nevertheless, the affinity between the drug and the lipid needs to be analysed. Therefore, loading hydrophilic drugs in SLN is a challenge due to the tendency of partitioning the encapsulated molecules in the water during the production process of nanoparticles [31]. Successful examples are zidovudine [31], insulin [32], tretinoin [33], and diminazene [34].

There are even differences in the lipid absorption enhancement depending on the structure of the lipids. For example, medium-chain triglycerides (MCT) lipids are more effective than long-chain triglycerides (LCT) [35]. Basically, the body is taking up the lipid and the solubilized drug at the same time. It can be considered as a kind of “Trojan horse” effect [36, 37].

Oral administration of SLN is possible as aqueous dispersion [38] or alternatively transformed into a traditional dosage forms such as tablets, pellets, capsules, or powders in sachets [25, 39]. For this route, all the lipids and surfactants used in traditional dosage forms can be exploited. In addition, all compounds of GRAS status or accepted GRAS

status can be employed as well as from the food industry [40]. Since the stomach acidic environment and high ionic strength favour the particle aggregation, aqueous dispersions of lipid nanoparticles might not be suitable to be administered as dosage form. In addition, the presence of food will also have a high impact on their performance [41].

The packing of SLN in a sachet for redispersion in water or juice prior to administration will allow an individual dosing by volume of the reconstituted SLN. For the production of tablets, the aqueous SLN dispersions can be used instead of a granulation fluid in the granulation process. Alternatively, SLN can be transferred to a powder (by spray-drying or lyophilization) and added to the tableting powder mixture. In both cases, it is beneficial to have a higher solid content to avoid the need of having to remove too much water. For cost reasons, spray drying might be the preferred method for transforming SLN dispersions into powders, with the previous addition of a protectant [42]. For the production of pellets, the SLN dispersion can be used as a wetting agent in the extrusion process. SLN powders can also be used for the filling of hard gelatine capsules.

Alternatively, SLN can be produced directly in liquid PEG 600 and put into soft gelatine capsules. Advantages of the use of SLN for oral and peroral administration are the possibility of drug protection from hydrolysis, as well as the possible increase of drug bioavailability. Prolonged plasma levels has also been postulated due to a controlled, optimized released [22] in combination with general adhesive properties of small particles [43]. The advantage of colloidal drug carriers described above is that they are generally linked to their size in the submicron range. Therefore, the preservation of particle size of colloidal carrier systems after peroral administration is a crucial point. The gastric environment (ionic strength, low pH) may destabilize the SLN and potentially lead to

aggregation. However, it is possible to produce stable SLN dispersions by optimizing the surfactant/mixture for each lipid *in vitro* [44].

The drug release from SLN in the GIT is also dependent on the lipase/colipase activity for the GIT digestion of the lipid matrix. The lipase/colipase complex leads to a degradation of food lipids as a prestep of the absorption. *In vitro* degradation assay based on pancreas lipase/colipase complex have been developed to obtain basic information about the degradation velocity of SLN as a function of lipid and surfactant used in the production process [45, 46].

Lipid nanoparticles show great promise to enhance oral bioavailability of some of the most poorly soluble drugs. The physical/chemical characteristics of lipid particulate systems are highly complex due to the existence of a variety of lipid assembly morphologies, the morphology-dependent solubility of drug, the interconversion of assembly morphology as a function of time and chemical structure, and the simultaneous lipid digestion [47].

3. Lipid Nanoparticles as Drug Carriers

Lipid nanoparticles show interesting features concerning therapeutic purposes. Their main characteristic is the fact that they are prepared with physiologically well-tolerated lipids [48]. During the last ten years, different substances have been entrapped into lipid nanoparticles (Table 1), ranging from lipophilic [23, 49] and hydrophilic molecules, including labile compounds, such as proteins and peptides [50].

Table 1. Examples of drugs, miscellaneous active ingredients and macrocyclic skeletons incorporated into lipid nanoparticles.

Incorporated drug or substance	Lipid	Advantageous	System	References
3_-Azido-3_-deoxythymidine palmitate	Trilaurin	Stable after autoclaving, and can be lyophilized and rehydrated	SLN	[51]
5-Fluorouracil	Dynasa 114 and Dynasan 118	Prolonged release in simulated colonic medium	SLN	[52]
Apomorphine	Glyceryl monostearate, polyethylene glycol monostearate	Enhanced the bioavailability in rats	SLN	[20]
Ascorbyl palmitate	Imwitor 900 and Labrafil M1944	Viscoelastic measurements is appropriate for topical/dermal application	NLC	[53]
Baclofen	Stearic acid	Significantly higher drug concentrations in plasma	SLN	[54]
Benzyl nicotinate	Dynasan 116	Increased oxygenation in the skin	SLN	[55]
Calcitonin	Trimyristin	Improvement of the efficiency of such carriers for oral delivery of proteins	SLN	[56]
Camptothecin	Monostearin and Soybean Oil 788	Stable and high performance delivery system	NLC	[57, 58]
Clozapine	Trimyristin, tripalmitin,	Improvement of bioavailability	SLN	[59]

Cyclosporin A	and tristearin glyceryl monostearate, and glyceryl palmitostearate	Controlled release	SLN	[60, 61]
Dexamethasone	Compritol 888 ATO	Drug delivery topical use	SLN	[62]
Diazepam	Compritol ATO 888 and Imwitor 900 K	Prolonged release	SLN	[63]
Doxorubicin	Glyceryl caprate	Enhanced apoptotic death	SLN	[64]
Gonadotropin release hormone	Monostearin	Prolonged release	SLN	[65]
Hydrocortisone	Monoglyceride, chain length of the fatty acid moiety	stable release properties	SLN	[66]
Ibuprofen	stearic acid, triluarin, tripalmitin	Stable formulation and negligible cell cytotoxicity	SLN	[67]
Idarubicin	Emulsifying wax	Potential to deliver anticancer drugs	SLN	[68]
Insulin	Stearic acid, octadecyl alcohol, cetyl palmitate, glyceryl monostearate, glyceryl palmitostearate, glyceryl tripalmitate, glyceryl behenate	Promising for oral delivery of proteins	SLN	[50]
Ketoprofen	mixture of beeswax and carnauba wax	SLN with beeswax content exhibited faster drug release as	SLN	[69]

Lopinavir	Compritol 888 ATO	888	compared carnauba wax Bioavailability enhanced	SLN	[70]
Nimesulide	Glyceryl behenate, palmitostearate, glyceryl tristearate		Sustained drug release	SLN	[71]
Penciclovir	Glyceryl monostearate		Provide a good skin targeting	SLN	[72]
Progesterone	Monostearin, stearic acid and oleic acid		Potential drug delivery system for oral administration	NLC	[73, 74]
Repaglinide	Glycerol monostearate and tristearin		Toxicity study indicated that the SLN were well tolerated	SLN	[22, 49]
Salbutamol sulphate	Monostearin and PEG2000		Formulation accelerate release of hydrophilic small molecule drugs	SLN	[75]
Tetracycline	glyceryl monostearate and stearic acid		Sustained release	SLN	[76]

3.1. Lipid Materials for Oral Administration.

The term lipid is used here in a broader sense and includes triglycerides, partial glycerides, fatty acids, steroids, and waxes. However, it is required that matrix maintains the solid state at room temperature, and for this purpose, the selection of lipids is based on the evaluation of their polymorphic, crystallinity, miscibility, and physicochemical structure [11].

Table 2 shows the main lipids employed for the preparation of lipid nanoparticles. Furthermore, the use of mono- and diglycerides as lipid matrix composition might increase drug solubility compared to highly pure lipids, such as monoacid triglycerides. Naturally occurring oils and fats comprise mixtures of mono-, di-, and triglycerides, containing fatty acids of varying chain length and degree of unsaturation [25, 86].

Table 2: Lipids used for preparation of SLN and NLC.

Lipids	References
Triacylglycerols	
Trimyristin (Dynasan [®] 114)	(11)
Tripalmitin (Dynasan [®] 116)	(77)
Tristearin (Dynasan [®] 118)	(11)
Mono, di and triacylglycerols mixtures	
Witeposol [®] bases	(78)
Glyceryl monostearate (Imwitor [®] 900)	(22)
Glyceryl behenate (Compritol [®] 888 ATO)	(79)
Glyceryl palmitostearate (Precirol [®] ATO 5)	(80)
Waxes	
Beeswax	(81)
Cetyl palmitate	(82)
Hard fats	
Stearic acid	(10)
Palmitic acid	(83)
Behenic acid	(84)

Other lipids

Miglyol [®] 812	(11)
Parafin	(85)

The melting point of these lipids increases with the length of the fatty acid chain and decreases with the degree of unsaturation. The chemical nature of the lipid is also important, because lipids which form highly crystalline particles with a perfect lattice (e.g., monoacid triglycerides) lead to drug expulsion during storage time. Physicochemically stable lipid nanoparticles will be obtained only when the right surfactant and adjusted concentration have been employed [25].

3.2. Determination of Optimal Hydrophile-Lipophile Balance (HLB) values for Lipid Nanoparticles Dispersions.

Emulsifiers are essential to stabilize lipid nanoparticles dispersions and prevent particle agglomeration [87]. The choice of the ideal surfactant for a particular lipid matrix is based on the surfactant properties such as charge, molecular weight, chemical structure, and respective hydrophile-lipophile balance (HLB). All these properties affects the stability of the emulsion [10]. The HLB of an emulsifier is given by the balance between the size and strength of the hydrophilic and the lipophilic groups. All emulsifiers consist of a molecule that combines both hydrophilic and lipophilic groups.

Griffin [88] defined the lipophilic emulsifiers as low HLB values (below 9), and hydrophilic emulsifiers as high HLB values (above 11). Those in the range of 9–11 are intermediate [89].

The HLB system is a useful method to choose the ideal emulsifier or blend of emulsifiers for the system, that is, if its required an oil-in-water (o/w), water-in-oil (w/o) [90], or a double (w/o/w) emulsion. Matching the HLB value of the surfactant with the lipid will provide a suitable *in vitro* performance [91].

Table 3 depicts the mainly surfactants employed in the production of lipid nanoparticles.

Severino et al. [10] determined the HLB value for stearic acid and stearic acid capric/caprylic triglycerides to reach the best combination of surfactants (trioleate sorbitan and polysorbate 80) to obtain a stable lipid nanoparticles emulsion.

Table 3: Emulsifiers used for preparation of SLN and NLC.

Emulsifiers/Coemulsifiers	HLB	References
lecithin	4-9	(92, 93)
Poloxamer 188	29	(94)
Poloxamer 407	21.5	(56, 95)
Tyloxapol	13	(96)
Polysorbate 20	16.7	(92)
Polysorbate 60	14.9	(97)
Polysorbate 80	15	(10, 11)
Sodium cholate	18	(98)
Sodium glycocholate	14.9	(99)
Taurodeoxycholic acid sodium salt	13-14	(100)
Butanol and Butyric acid	7-9	(101)

Cetylpyridinium chloride	~15	(102)
Sodium dodecyl sulphate	40	(104)
Sodium oleate	18	(99)
Polyvinyl alcohol	15-19	(104)
Cremophor EL	12-14	(105)

The HLB value obtained for stearic acid was 15 and for stearic acid capric/caprylic triglycerides was 13.8. Sorbitan trioleate has an HLB value of 1.8 and polysorbate 80 of 15, when used in the ratio 10:90, respectively. The surfactant mixtures prepared with different ratios provided well-defined HLB values. Polysorbate 80 is often used in combination with sorbitan trioleate due to their appropriate compatibility attributed to the similar chemical structure (same hydrocarbon chain length) for the production of stable emulsions.

4. Biopharmaceutic and Pharmacokinetic Aspects

Pharmacokinetic behaviour of drugs loaded in lipid nanoparticles need to differentiate if the drug is present as the released free form or as the associated form with lipid nanoparticles [106]. However, the poor aqueous solubility of some drugs turns difficult the design of pharmaceutical formulations and leads to variable bioavailability [107].

Xie et al. [108] reported a significant increase in the bioavailability and extended the systemic circulation of ofloxacin formulated in SLN, which could be attributed to a large surface area of the particles, improving the dissolution rate and level of ofloxacin in the presence of GIT fluids [109, 110], leading to shorter T_{max} and higher peak plasma concentration.

In addition, lipid nanoparticles may adhere to the GIT wall or enter the intervillar spaces due to their small particle size, increasing their residence time [111]. Moreover, nanoparticles could protect the drug from chemical and enzymatic degradation and gradually release drug from the lipid matrix into blood, [112] resulting in a several-fold increase mean residence time compared with native drug.

Han et al. [113] demonstrated that 5 oral doses of tilmicosin loaded in lipid nanoparticles administered every 10 days provided an equivalent therapeutic benefit to 46 daily doses of oral free drugs. *In vitro* release profile demonstrated that tilmicosin loaded in lipid nanoparticles followed a sustained release profile, and *in vivo* results showed that nanoparticles remained effective for a longer period of time, which was attributed to sustained release of the drug and also to enhanced antibacterial activity by the SLN.

Pandita et al. [114] developed paclitaxel loaded in SLN with the aim at improving the oral bioavailability of this antineoplastic drug. *In vitro* studies of SLN formulation exhibited an initial low burst effect within 24 h followed by a slow and sustained release. Statistical analysis of *in vivo* experiments concluded that the oral bioavailability of paclitaxel loaded in SLN was significantly higher than the control group.

Yuan et al. [115] produced stearic acid-SLN with a fluorescence marked for evaluation of *in vivo* pathway by oral administration. About 30% of SLN transport was efficient, where particles were absorbed following linear mechanism in the GIT. The release profile in plasma increased with the increasing of dosage depicting two concentration peaks. The first peak of SLN in blood took place during 1-2 h, attributed to the fast uptake of SLN from the GIT into systematic circulation. Drug concentration began to decrease attributed to the uptake by and the distribution of SLN among particular organs. The second peak occurred at about 6–8 h, and the maximum concentrations were lower than that of the first peak.

5. Toxicology

Lipid nanoparticles are well tolerated in living systems, since they are made from physiological compounds leading to the metabolic pathways [22, 28]. For this purpose, studies focusing on nanotoxicology comprise cytotoxicity and genotoxicity analysis [116]. However, such effects often occur first at rather in high concentrations and the subtler effects that arise at lower concentrations, without necessarily causing cell death, also need to be considered. One the most important effect is DNA damage, since an increased genetic instability is associated with cancer development [117]. The interaction with proteins and cells are an essential focus in assessing and understanding compatibility and toxicity.

Cell and nanoparticle reactions of interest include cellular uptake and processing of nanoparticle in various routes, effects on cell signalling, membrane perturbations, influence on the cellular electron transfer cascades, production of cytokines, chemokines, and reactive oxygen species (ROS), transcytosis and intercellular transport, gene regulation overt toxic reactivity, no observable toxicity, and cell necrosis or apoptosis. *In vitro* culture of cell lines or primary cells on plastic plates are employed in a wide varieties of assays and reflect the variety of possible physiologic responses to nanoparticles *in vivo* and all possible cell processing routes and natural reactions [118].

Silva et al. [119] studied the toxicity of SLN and risperidone loaded SLN with Caco-2 cells by (4,5-dimethylthiazol-2-yl)2,5-diphenyl-tetrazolium bromide (MTT) assay. The results suggest that all formulations evaluated are biocompatible with Caco-2 cells and well tolerated by the GIT.

Similar results have been reported elsewhere [120, 121]. This test evaluates the mitochondrial function as a measurement of cell viability, which allows the detection of

dead cells before they lose their integrity and shape. The amount of viable cells after SLN exposure was performed by the MTT assay with Caco-2 cell models, which are a well-established *in vitro* model that mimics the intestinal barrier and is often used to assess the permeability and transport of oral drugs [122]. Other authors have also reported that SLN show biocompatibility, which increase their attractiveness for drug-delivery applications [120].

6. Marketed Products and Current Studies

Since early nineties, researchers turned their attention to lipid nanoparticles because of their nontoxicity and cost/effectiveness relationship [12]. In spite of the advantages, formulating with lipid nanoparticles has been suffering some drawbacks. Because of the GIT conditions, most of promising drugs do not reach clinical trials. The stability of particles must be comprehensively tested due to pH changes and ionic strength as well as the drug release upon enzymatic degradation [123]. Lipid nanoparticles absorption through GIT occurs via transcellular (through M cells or enterocytes) or paracellular (diffusion between cells). If the major drug uptake occurs through M cells, the portal vein to the liver is bypassed, resulting in higher drug concentrations to the lymph rather than to plasma [124]. Despite the low number of lipid nanoparticles formulations on the market for drug delivery, Mucosolvan retard capsules (Boehringer-Ingelheim) is a story of success [125]. Mucosolvan retard capsules was the first generation. It was produced by highspeed stirring of a melted lipid phase in a hot surfactant solution obtaining an emulsion. This emulsion was then cooled down to room temperature obtaining the so-called “lipid nanopellets for oral administration” [126].

Successful *in vivo* studies also include rifampicin, isoniazid, and pyrazinamide that are used in tuberculosis treatment. These drugs achieved higher bioavailability when incorporated into SLN compared to the free solutions.

Rifampicin has poor cellular penetration which requires high doses to reach effective concentrations. Rifamsolin is a rifampicin-loaded SLN under preclinical phase by AlphaRx. The methodology employed for production is acceptable by the regulatory agencies and has been addressed by various papers and patents [127].

Poor water-soluble drugs, as camptothecin, vinpocetine, and fenofibrate, can have their solubilization improved if incorporated into SLN [124, 128]. Another example is insulin, commonly administered parenterally in the treatment of diabetes mellitus. Injections are often painful and must be administered daily, which result in low patient compliance [129]. Unfortunately, oral administration of insulin, produced by solvent emulsification-evaporation method based on a w/o/w double emulsion, has limitations such as low bioavailability due to degradation in the stomach, inactivation and degradation by proteolytic enzymes, and low permeability across the intestinal epithelium because of lack of lipophilicity and high molecular weight [124, 129]. The main advantages of incorporate insulin into SLN would be the enhancement of transmucosal transport and protection from the degradation in the GIT.

7. Conclusions

Lipids and lipid nanoparticles are promising for oral and peroral administration route for drugs, proteins, and peptides. These matrices are able to promoting controlled release of drugs in GIT and reducing absorption variability. In addition, these matrices can be absorption as food lipids together with drugs improving the bioavailability. These systems

present several advantages, including drug protection and excipients of GRAS status, which decreases the danger of acute and chronic toxicity. In addition, the oral administration of lipids nanoparticles is possible as aqueous dispersion or alternatively transformed into a traditional dosage forms such as tablets, pellets, capsules, or powders in sachets.

Acknowledgments

The authors wish to acknowledge *Fundação para a Ciência e Tecnologia do Ministério da Ciência e Tecnologia*, under reference no. ERA-Eula/0002/2009. Sponsorship of P. Severino was received from CAPES (Coordenação Aperfeiçoamento de Pessoal de Nivel Superior) and FAPESP (Fundação de Amparo a Pesquisa). Sponsorship of T. Andreani was received from Fundação para Ciência e Tecnologia (SFRH/ BD/60640/2009).

References

- [1] T. Eldem, P. Speiser, and A. Hinkal, “Optimization of spraydried and congelated lipid micropellets and characterization of their surface morphology by scanning electron microscopy,” *Pharmaceutical Research*, vol. 8, pp. 47–54, 1991.
- [2] P. Speiser, EP 0167825, assignee. Lipid nanopellets als Tragersystem fur Arzneimittel zur peroralen Anwendung, 1990.
- [3] A. J. Domb, “Long acting injectable oxytetracycline-liposphere formulations,” *International Journal of Pharmaceutics*, vol. 124, no. 2, pp. 271–278, 1995.
- [4] A. J. Domb, “Lipospheres for controlled delivery of substances,” 1993.
- [5] A. J. Domb, “Liposphere parenteral delivery system,” *Proceedings of the Controlled Release Society*, no. 20, pp. 121–122, 1993.

- [6] K. Manjunath, J. S. Ready, and V. Venkateswarlu, “Solid lipid nanoparticles as drug delivery systems,” *Methods and Findings in Experimental and Clinical Pharmacology*, vol. 27, no. 2, pp. 127–144, 2005.
- [7] X. Qi, L. Wang, and J. Zhu, “Water-in-oil-in-water double emulsions: an excellent delivery system for improving the oral bioavailability of pidotimod in rats,” *Journal of Pharmaceutical Sciences*, vol. 100, no. 6, pp. 2203–2211, 2011.
- [8] M. J. Morilla, D. M. Gomez, P. Cabral et al., “Mcells prefer archaeosomes: an in vitro/in vivo snapshot upon oral gavage in rats,” *Current Drug Delivery*, vol. 8, no. 3, pp. 320–329, 2011.
- [9] C. F. Da Silva, P. Severino, F. Martins, M. V. Chaud, and M.H. A. Santana, “The intestinal permeation of didanosine from granules containing microspheres using the everted gut sac model,” *Journal of Microencapsulation*, vol. 26, no. 6, pp. 523–528, 2009.
- [10] P. Severino, S. C. Pinho, E. B. Souto, and M. H. A. Santana, “Polymorphism, crystallinity and hydrophilic-lipophilic balance of stearic acid and stearic acid-capric/caprylic triglyceride matrices for production of stable nanoparticles,” *Colloids and Surfaces B*, vol. 86, no. 1, pp. 125–130, 2011.
- [11] P. Severino, S. C. Pinho, E. B. Souto, and M. H. A. Santana, “Crystallinity of Dynasan114 and Dynasan118 matrices for the production of stable Miglyol-loaded nanoparticles,” *Journal of Thermal Analysis and Calorimetry*. In press.
- [12] R. H. Müller, W. Mehnert, J. S. Lucks et al., “Solid lipid nanoparticles (SLN)—an alternative colloidal carrier system for controlled drug delivery,” *European Journal of Pharmaceutics and Biopharmaceutics*, vol. 41, no. 1, pp. 62–69, 1995.
- [13] R. H. Müller and J. S. Lucks, “Azneistoffträger aus festen Lipidteilchenfeste Lipid Nanosphären (SLN),” Germany, 1996.

- [14] M. R., inventor Gasco, “Method for producing solid lipid microspheres having a narrow size distribution,” Italy, 1993.
- [15] M. Trotta, M. E. Carlotti, M. Gallarate, G. P. Zara, E. Muntoni, and L. Battaglia, “Insulin-loaded SLN prepared with the emulsion dilution technique: in vivo tracking of nanoparticles after oral administration to rats,” *Journal of Dispersion Science and Technology*, vol. 32, no. 7, pp. 1041–1045, 2011.
- [16] E. B. Souto and R. H. Müller, “Lipid nanoparticles—effect on bioavailability and pharmacokinetics changes,” in *Handbook of Experimental Pharmacology—Novel Drug Delivery Approaches*, M. Schafer-Korting, Ed., vol. 197, pp. 115–141, Springer, Berlin, Germany, 2009.
- [17] M. A. Schubert and C. C. Müller-Goymann, “Characterisation of surface-modified solid lipid nanoparticles (SLN): influence of lecithin and nonionic emulsifier,” *European Journal of Pharmaceutics and Biopharmaceutics*, vol. 61, pp. 77–86, 2005.
- [18] R. H. Müller, S. Maaßen, H. Weyhers, F. Specht, and J. S. Lucks, “Cytotoxicity of magnetite-loaded polylactide, polylactide/glycolide particles and solid lipid nanoparticles,” *International Journal of Pharmaceutics*, vol. 138, no. 1, pp. 85–94, 1996.
- [19] R. H. Müller, K. Mäder, and S. Gohla, “Solid lipid nanoparticles (SLN) for controlled drug delivery—a review of the state of the art,” *European Journal of Pharmaceutics and Biopharmaceutics*, vol. 50, no. 1, pp. 161–177, 2000.
- [20] M. J. Tsai, Y. B. Huang, P. C. Wu et al., “Oral apomorphine delivery from solid lipid nanoparticles with different monostearate emulsifiers: pharmacokinetic and behavioral evaluations,” *Journal of Pharmaceutical Sciences*, vol. 100, no. 2, pp. 547–557, 2011.

- [21] S. Mukherjee, S. Ray, and R. S. Thakur, "Solid lipid nanoparticles: a modern formulation approach in drug delivery system," *Indian Journal of Pharmaceutical Sciences*, vol. 71, no. 4, pp. 349–358, 2009.
- [22] M. K. Rawat, A. Jain, and S. Singh, "In vivo and cytotoxicity evaluation of repaglinide-loaded binary solid lipid nanoparticles after oral administration to rats," *Journal of Pharmaceutical Sciences*, vol. 100, no. 6, pp. 2406–2417, 2011.
- [23] C.-F. Luo, M. Yuan, M.-S. Chen et al., "Pharmacokinetics, tissue distribution and relative bioavailability of puerarin solid lipid nanoparticles following oral administration," *International Journal of Pharmaceutics*, vol. 410, no. 1-2, pp. 138–144, 2011.
- [24] L. Hu, Q. Xing, J. Meng, and C. Shang, "Preparation and enhanced oral bioavailability of cryptotanshinone-loaded solid lipid nanoparticles," *AAPS PharmSciTech*, vol. 11, no.2, pp. 582–587, 2010.
- [25] E. B. Souto and R. H. Müller, "Lipid nanoparticles: effect on bioavailability and pharmacokinetic changes," *Handbook of Experimental Pharmacology*, vol. 197, pp. 115–141, 2010.
- [26] B.W. K. Siekmann, "Submicron lipid suspensions (solid lipid nanoparticles) versus lipid nanoemulsions: similarities and differences," Amsterdam, The Netherlands, 1998.
- [27] R. H.Müller, W.Mehnert, and E. B. Souto, "Solid lipid nanoparticles (SLN) and nanostructured lipid carriers (NLC) for dermal delivery," Hong-Kong, 2005.
- [28] S. A.Wissing, O. Kayser, and R. H.Müller, "Solid lipid nanoparticles for parenteral drug delivery," *Advanced Drug Delivery Reviews*, vol. 56, no. 9, pp. 1257–1272, 2004.
- [29] S. Das and A. Chaudhury, "Recent advances in lipid nanoparticle formulations with solid matrix for oral drug delivery," *AAPS PharmSciTech*, vol. 12, no. 1, pp. 62–76, 2010.

- [30] H. Bunjes, “Lipid nanoparticles for the delivery of poorly water-soluble drugs,” *Journal of Pharmacy and Pharmacology*, vol. 62, no. 11, pp. 1637–1645, 2010.
- [31] S. Singh, A. K. Dobhal, A. Jain, J. K. Pandit, and S. Chakraborty, “Formulation and evaluation of solid lipid nanoparticles of a water soluble drug: zidovudine,” *Chemical and Pharmaceutical Bulletin*, vol. 58, no. 5, pp. 650–655, 2010.
- [32] J. F. Fangueiro, E. Gonzalez-Mira, P. Martins-Lopes, M. A. Egea, M. L. Garcia, and S. B. Souto, “A novel lipid nanocarrier for insulin delivery: production, characterization and toxicity testing,” *Pharmaceutical Development and Technology*. In press.
- [33] S. Das, W. K. Ng, P. Kanaujia, S. Kim, and R. B. H. Tan, “Formulation design, preparation and physicochemical characterizations of solid lipid nanoparticles containing a hydrophobic drug: effects of process variables,” *Colloids and Surfaces B*, vol. 88, no. 1, pp. 483–489, 2011.
- [34] C. Olbrich, A. Gessner, O. Kayser, and R. H. Müller, “Lipid drug-conjugate (LDC) nanoparticles as novel carrier system for the hydrophilic antitrypanosomal drug diminazenediacetate,” *Journal of Drug Targeting*, vol. 10, no. 5, pp. 387–396, 2002.
- [35] L. Sek, C. J. H. Porter, A.M. Kaukonen, and W. N. Charman, “Evaluation of the in-vitro digestion profiles of long and medium chain glycerides and the phase behaviour of their lipolytic products,” *Journal of Pharmacy and Pharmacology*, vol. 54, no. 1, pp. 29–41, 2002.
- [36] R. H. Müller and C. M. Keck, “Challenges and solutions for the delivery of biotech drugs—a review of drug nanocrystal technology and lipid nanoparticles,” *Journal of Biotechnology*, vol. 113, no. 1–3, pp. 151–170, 2004.
- [37] E. B. Souto, S. Doktorovova, and P. Boonme, “Lipid nanocarriers-based semisolids: review on materials and end product formulations,” *Journal of Drug Delivery Science and*

Technology, vol. 21, pp. 43–54, 2011.

[38] C. Liu, D. Liu, F. Bai, J. Zhang, and N. Zhang, “In vitro and in vivo studies of lipid-based nanocarriers for oral N3-o-toluyflfluorouracil delivery,” *Drug Delivery*, vol. 17, no. 5, pp. 352–363, 2010.

[39] D. Shukla, S. Chakraborty, S. Singh, and B. Mishra, “Lipid based oral multiparticulate formulations-advantages, technological advances and industrial applications,” *Expert Opinion on Drug Delivery*, vol. 8, no. 2, pp. 207–224, 2011.

[40] H. Weyhers, S. Ehlers, H. Hahn, E. B. Souto, and R. H. Müller, “Solid lipid nanoparticles (SLN)—Effects of lipid composition on in vitro degradation and in vivo toxicity,” *Pharmazie*, vol. 61, no. 6, pp. 539–544, 2006.

[41] W. Mehnert and K. Mäder, “Solid lipid nanoparticles: production, characterization and applications,” *Advanced Drug Delivery Reviews*, vol. 47, no. 2-3, pp. 165–196, 2001.

[42] V. Jenning, A. F. Thünemann, and S. H. Gohla, “Characterisation of a novel solid lipid nanoparticle carrier system based on binary mixtures of liquid and solid lipids,” *International Journal of Pharmaceutics*, vol. 199, no. 2, pp. 167–177, 2000.

[43] M. J. Montisci, A. Dembri, G. Giovannuci, H. Chacun, D. Duchêne, and G. Ponchel, “Gastrointestinal transit and mucoadhesion of colloidal suspensions of *Lycopersicon esculentum* L. and *Lotus tetragonolobus* lectin-PLA microsphere conjugates in rats,” *Pharmaceutical Research*, vol. 18, no. 6, pp. 829–837, 2001.

[44] E. Zimmermann and R. H. Müller, “Electrolyte- and pHstabilities of aqueous solid lipid nanoparticle (SLN) dispersions in artificial gastrointestinal media,” *European Journal of Pharmaceutics and Biopharmaceutics*, vol. 52, no. 2, pp. 203–210, 2001.

- [45] H. Reithmeier, J. Herrmann, and A. Göpferich, "Development and characterization of lipid microparticles as a drug carrier for somatostatin," *International Journal of Pharmaceutics*, vol. 218, no. 1-2, pp. 133–143, 2001.
- [46] J. Kristl, B. Volk, P. Ahlin, K. Gombač, and M. Šentjurc, "Interactions of solid lipid nanoparticles with model membranes and leukocytes studied by EPR," *International Journal of Pharmaceutics*, vol. 256, no. 1-2, pp. 133–140, 2003.
- [47] P. M. Bummer, "Physical chemical considerations of lipidbased oral drug delivery—solid lipid nanoparticles," *Critical Reviews in Therapeutic Drug Carrier Systems*, vol. 21, no. 1, pp. 1–19, 2004.
- [48] V. Kakkar, S. Singh, D. Singla, and I. P. Kaur, "Exploring solid lipid nanoparticles to enhance the oral bioavailability of curcumin," *Molecular Nutrition and Food Research*, vol. 55, no. 3, pp. 495–503, 2011.
- [49] M. K. Rawat, A. Jain, and S. Singh, "Studies on binary lipid matrix based solid lipid nanoparticles of repaglinide: in vitro and in vivo evaluation," *Journal of Pharmaceutical Sciences*, vol. 100, no. 6, pp. 2366–2378, 2011.
- [50] R. Yang, R. Gao, F. Li, H. He, and X. Tang, "The influence of lipid characteristics on the formation, in vitro release, and in vivo absorption of protein-loaded SLN prepared by the double emulsion process," *Drug Development and Industrial Pharmacy*, vol. 37, no. 2, pp. 139–148, 2011.
- [51] H. Heiati, R. Tawashi, and N. C. Phillips, "Drug retention and stability of solid lipid nanoparticles containing azidothymidine palmitate after autoclaving, storage and lyophilization," *Journal of Microencapsulation*, vol. 15, no. 2, pp. 173–184, 1998.
- [52] A. E. B. Yassin, M. D. Khalid Anwer, H. A. Mowafy, I. M. El-Bagory, M. A. Bayomi, and I. A. Alsarra, "Optimization of 5-fluorouracil solid-lipid nanoparticles: a preliminary

study to treat colon cancer,” *International Journal of Medical Sciences*, vol. 7, no. 6, pp. 398–408, 2010.

[53] V. Teeranachaideekul, E. Souto, R. Müller, and V. B. Junyaprasert, “Physicochemical characterization and in vitro release studies of ascorbyl palmitate-loaded semi-solid nanostructured lipid carriers (NLC gels),” *Journal of Microencapsulation*, vol. 25, no. 2, pp. 111–120, 2008.

[54] L. Priano, G. P. Zara, N. El-Assawy et al., “Baclofen-loaded solid lipid nanoparticles: preparation, electrophysiological assessment of efficacy, pharmacokinetic and tissue distribution in rats after intraperitoneal administration,” *European Journal of Pharmaceutics and Biopharmaceutics*, vol. 79, no. 1, pp. 135–141, 2011.

[55] M. Krzic, M. Sentjurec, and J. Kristl, “Improved skin oxygenation after benzyl nicotinate application in different carriers as measured by EPR oximetry in vivo,” *Journal of Controlled Release*, vol. 70, no. 1-2, pp. 203–211, 2001.

[56] S. Martins, A. C. Silva, D. C. Ferreira, and E. B. Souto, “Improving oral absorption of salmon calcitonin by trimyristin lipid nanoparticles,” *Journal of Biomedical Nanotechnology*, vol. 5, no. 1, pp. 76–83, 2009.

[57] X. Zhang, W. Pan, L. Gan, C. Zhu, Y. Gan, and S. Nie, “Preparation of a dispersible PEGylate nanostructured lipid carriers (NLC) loaded with 10-hydroxycamptothecin by spray-drying,” *Chemical and Pharmaceutical Bulletin*, vol. 56, no. 12, pp. 1645–1650, 2008.

[58] Z. R. Huang, S. C. Hua, Y. L. Yang, and J. Y. Fang, “Development and evaluation of lipid nanoparticles for camptothecin delivery: a comparison of solid lipid nanoparticles, nanostructured lipid carriers, and lipid emulsion,” *Acta Pharmacologica Sinica*, vol. 29, no. 9, pp. 1094–1102, 2008.

- [59] K. Manjunath and V. Venkateswarlu, "Pharmacokinetics, tissue distribution and bioavailability of clozapine solid lipid nanoparticles after intravenous and intraduodenal administration," *Journal of Controlled Release*, vol. 107, no. 2, pp. 215–228, 2005.
- [60] J. K. Varia, S. S. Dodiya, and K. K. Sawant, "Cyclosporine a loaded solid lipid nanoparticles: optimization of formulation, process variable and characterization," *Current Drug Delivery*, vol. 5, no. 1, pp. 64–69, 2008.
- [61] R. H. Müller, S. A. Runge, V. Ravelli, A. F. Thünemann, W. Mehnert, and E. B. Souto, "Cyclosporine-loaded solid lipid nanoparticles (SLN): drug-lipid physicochemical interactions and characterization of drug incorporation," *European Journal of Pharmaceutics and Biopharmaceutics*, vol. 68, no. 3, pp. 535–544, 2008.
- [62] G. Chen, S. X. Hou, P. Hu, Q. H. Hu, D. D. Guo, and Y. Xiao, "In vitro dexamethasone release from nanoparticles and its pharmacokinetics in the inner ear after administration of the drug-loaded nanoparticles via the round window," *Journal of Southern Medical University*, vol. 28, no. 6, pp. 1022–1024, 2008.
- [63] G. Abdelbary and R. H. Fahmy, "Diazepam-Loaded solid lipid nanoparticles: design and characterization," *AAPS PharmSciTech*, vol. 10, no. 1, pp. 211–219, 2009.
- [64] K. W. Kang, M. K. Chun, O. Kim et al., "Doxorubicin-loaded solid lipid nanoparticles to overcome multidrug resistance in cancer therapy," *Nanomedicine*, vol. 6, no. 2, pp. 210–213, 2010.
- [65] F. Q. Hu, Y. Hong, and H. Yuan, "Preparation and characterization of solid lipid nanoparticles containing peptide," *International Journal of Pharmaceutics*, vol. 273, no. 1-2, pp. 29–35, 2004.

- [66] L. B. Jensen, E. Magnusson, L. Gunnarsson, C. Vermehren, H. M. Nielsen, and K. Petersson, “Corticosteroid solubility and lipid polarity control release from solid lipid nanoparticles,” *International Journal of Pharmaceutics*, vol. 390, no. 1, pp. 53–60, 2010.
- [67] S. G. Potta, S. Minemi, R. K. Nukala et al., “Preparation and characterization of ibuprofen solid lipid nanoparticles with enhanced solubility,” *Journal of Microencapsulation*, vol. 28, no. 1, pp. 74–81, 2011.
- [68] P. Ma, X. Dong, C. L. Swadley et al., “Development of idarubicin and doxorubicin solid lipid nanoparticles to overcome Pgp-mediated multiple drug resistance in leukemia,” *Journal of Biomedical Nanotechnology*, vol. 5, no. 2, pp. 151–161, 2009.
- [69] S. Kheradmandnia, E. Vasheghani-Farahani, M. Nosrati, and F. Atyabi, “Preparation and characterization of ketoprofenloaded solid lipid nanoparticles made from beeswax and carnauba wax,” *Nanomedicine*, vol. 6, no. 6, pp. 753–759, 2010.
- [70] M. R. Aji Alex, A. J. Chacko, S. Jose, and E. B. Souto, “Lopinavir loaded solid lipid nanoparticles (SLN) for intestinal lymphatic targeting,” *European Journal of Pharmaceutical Sciences*, vol. 42, no. 1-2, pp. 11–18, 2011.
- [71] V. B. Patravale and A. V. Ambarkhane, “Study of solid lipid nanoparticles with respect to particle size distribution and drug loading,” *Pharmazie*, vol. 58, no. 6, pp. 392–395, 2003.
- [72] Q. Lv, A. Yu, Y. Xi et al., “Development and evaluation of penciclovir-loaded solid lipid nanoparticles for topical delivery,” *International Journal of Pharmaceutics*, vol. 372, no. 1-2, pp. 191–198, 2009.
- [73] H. Yuan, L. L. Wang, Y. Z. Du, J. You, F. Q. Hu, and S. Zeng, “Preparation and characteristics of nanostructured lipid carriers for control-releasing progesterone by meltemulsification,” *Colloids and Surfaces B*, vol. 60, no. 2, pp. 174–179, 2007.

- [74] R. Cavalli, E. Peira, O. Caputo, and M. R. Gasco, “Solid lipid nanoparticles as carriers of hydrocortisone and progesterone complexes with β -cyclodextrins,” *International Journal of Pharmaceutics*, vol. 182, no. 1, pp. 59–69, 1999.
- [75] Y. Hong, F. Q. Hu, and H. Yuan, “Effect of PEG2000 on drug delivery characterization from solid lipid nanoparticles,” *Pharmazie*, vol. 61, no. 4, pp. 312–315, 2006.
- [76] X.-M. Xu, Y.-S. Wang, R.-Y. Chen et al., “Formulation and pharmacokinetic evaluation of tetracycline-loaded solid lipid nanoparticles for subcutaneous injection in mice,” *Chemical and Pharmaceutical Bulletin*, vol. 59, no. 2, pp. 260–265, 2011.
- [77] E. Bas,aran, M. Demirel, B. Sirmag“ul, and Y. Yazan, “Cyclosporine a incorporated cationic solid lipid nanoparticles for ocular delivery,” *Journal of Microencapsulation*, vol. 27, no. 1, pp. 37–47, 2010.
- [78] K. Vivek, H. Reddy, and R. S. R. Murthy, “Investigations of the effect of the lipid matrix on drug entrapment, in vitro release, and physical stability of olanzapine-loaded solid lipid nanoparticles,” *AAPS PharmSciTech*, vol. 8, no. 4, article no.83, 2007.
- [79] M. Shah, K. Chuttani, A. K. Mishra, and K. Pathak, “Oral solid compritol 888 ATO nanosuspension of simvastatin: optimization and biodistribution studies,” *Drug Development and Industrial Pharmacy*, vol. 37, no. 5, pp. 526–537, 2011.
- [80] A. del Pozo-Rodr‘iguez, D. Delgado, M. A. Solin‘is et al., “Solid lipid nanoparticles as potential tools for gene therapy: in vivo protein expression after intravenous administration,” *International Journal of Pharmaceutics*, vol. 385, no. 1-2, pp. 157–162, 2010.

- [81] J. Zhang and E. Smith, "Percutaneous permeation of betamethasone 17-valerate incorporated in lipid nanoparticles," *Journal of Pharmaceutical Sciences*, vol. 100, no. 3, pp. 896–903, 2011.
- [82] L. Montenegro, A. Campisi, M. G. Sarpietro et al., "In vitro evaluation of idebenone-loaded solid lipid nanoparticles for drug delivery to the brain," *Drug Development and Industrial Pharmacy*, vol. 37, no. 6, pp. 737–746, 2011.
- [83] S. Xie, L. Zhu, Z. Dong, Y. Wang, X. Wang, and W. Zhou, "Preparation and evaluation of ofloxacin-loaded palmitic acid solid lipid nanoparticles," *International Journal of Nanomedicine*, vol. 6, pp. 547–555, 2011.
- [84] L. Battaglia, M. Gallarate, R. Cavalli, and M. Trotta, "Solid lipid nanoparticles produced through a coacervation method," *Journal of Microencapsulation*, vol. 27, no. 1, pp. 78–85, 2010.
- [85] N. Schöler, H. Hahn, R. H. Müller, and O. Liesenfeld, "Effect of lipid matrix and size of solid lipid nanoparticles (SLN) on the viability and cytokine production of macrophages," *International Journal of Pharmaceutics*, vol. 231, no. 2, pp. 167–176, 2002.
- [86] D. J. Hauss, "Oral lipid-based formulations," *Advanced Drug Delivery Reviews*, vol. 59, no. 7, pp. 667–676, 2007.
- [87] T. M. Goppert and R. H. Müller, "Polysorbate-stabilized solid lipid nanoparticles as colloidal carriers for intravenous targeting of drugs to the brain: comparison of plasma protein adsorption patterns," *Journal of Drug Targeting*, vol. 13, no. 3, pp. 179–187, 2005.
- [88] W. C. Griffin, "Classification of surface-active agents by HLB," *Journal of the Society of Cosmetic Chemists*, vol. 1, p. 311, 1949.

- [89] R. Kinget, "Classification of the most important surface active agents being used for the formulation of drugs and cosmetic products," *Farmaceutisch Tijdschrift voor België*, vol. 75, no. 4, pp. 3–15, 1998.
- [90] W. C. Griffin, "Calculation of HLB values of nonionic surfactants," *Journal of the Society of Cosmetic Chemists*, vol. 5, pp. 249–256, 1954.
- [91] T. Schmidts, D. Dobler, C. Nissing, and F. Runkel, "Influence of hydrophilic surfactants on the properties of multiple W/O/W emulsions," *Journal of Colloid and Interface Science*, vol. 338, no. 1, pp. 184–192, 2009.
- [92] J. Varshosaz, M. Tabbakhian, and M. Y. Mohammadi, "Formulation and optimization of solid lipid nanoparticles of buspirone HCl for enhancement of its oral bioavailability," *Journal of Liposome Research*, vol. 20, no. 4, pp. 286–296, 2010.
- [93] S. Jain, S. Jain, P. Khare, A. Gulbake, D. Bansal, and S. K. Jain, "Design and development of solid lipid nanoparticles for topical delivery of an anti-fungal agent," *Drug Delivery*, vol. 17, no. 6, pp. 443–451, 2010.
- [94] M. A. Kalam, Y. Sultana, A. Ali, M. Aqil, A. K. Mishra, and K. Chuttani, "Preparation, characterization, and evaluation of gatifloxacin loaded solid lipid nanoparticles as colloidal ocular drug delivery system," *Journal of Drug Targeting*, vol. 18, no. 3, pp. 191–204, 2010.
- [95] T. M. Göppert and R. H. Müller, "Adsorption kinetics of plasma proteins on solid lipid nanoparticles for drug targeting," *International Journal of Pharmaceutics*, vol. 302, no. 1-2, pp. 172–186, 2005.
- [96] J. Kristl, K. Teskac, M. Milek, and I. Mlinaric-Rascan, "Surface active stabilizer Tyloxapol in colloidal dispersions exerts cytostatic effects and apoptotic dismissal of cells," *Toxicology and Applied Pharmacology*, vol. 232, no. 2, pp. 218–225, 2008.

- [97] H. Thrandur, T. S. Awad, K. Kristberg, A. D. Eric, J. M. A. David, and W. Jochen, “Impact of surfactant properties on oxidative stability of β -carotene encapsulated within solid lipid nanoparticles,” *Journal of Agricultural and Food Chemistry*, vol. 57, no. 17, pp. 8033–8040, 2009.
- [98] J. Liu, T. Gong, H. Fu et al., “Solid lipid nanoparticles for pulmonary delivery of insulin,” *International Journal of Pharmaceutics*, vol. 356, no. 1-2, pp. 333–344, 2008.
- [99] H. Bunjes, M. H. J. Koch, and K. Westesen, “Influence of emulsifiers on the crystallization of solid lipid nanoparticles,” *Journal of Pharmaceutical Sciences*, vol. 92, no. 7, pp. 1509–1520, 2003.
- [100] M. Trotta, F. Debernardi, and O. Caputo, “Preparation of solid lipid nanoparticles by a solvent emulsification-diffusion technique,” *International Journal of Pharmaceutics*, vol. 257, no. 1-2, pp. 153–160, 2003.
- [101] T. Wang, N. Wang, Y. Zhang, W. Shen, X. Gao, and T. Li, “Solvent injection-lyophilization of tert-butyl alcohol/water cosolvent systems for the preparation of drug-loaded solid lipid nanoparticles,” *Colloids and Surfaces B*, vol. 79, no. 1, pp. 254–261, 2010.
- [102] C. Olbrich, N. Schöler, K. Tabatt, O. Kayser, and R. H. Müller, “Cytotoxicity studies of Dynasan 114 solid lipid nanoparticles (SLN) on RAW264.7 macrophages—impact of phagocytosis on viability and cytokine production,” *Journal of Pharmacy and Pharmacology*, vol. 56, no. 7, pp. 883–891, 2004.
- [103] Z. Rahman, A. S. Zidan, and M. A. Khan, “Non-destructive methods of characterization of risperidone solid lipid nanoparticles,” *European Journal of Pharmaceutics and Biopharmaceutics*, vol. 76, no. 1, pp. 127–137, 2010.

- [104] S. Chakraborty, D. Shukla, P. R. Vuddanda, B. Mishra, and S. Singh, “Utilization of adsorption technique in the development of oral delivery system of lipid based nanoparticles,” *Colloids and Surfaces B*, vol. 81, no. 2, pp. 563–569, 2010.
- [105] D. Pandita, A. Ahuja, T. Velpandian, V. Lather, T. Dutta, and R. K. Khar, “Characterization and in vitro assessment of paclitaxel loaded lipid nanoparticles formulated using modified solvent injection technique,” *Pharmazie*, vol. 64, no.5, pp. 301–310, 2009.
- [106] R. Li, J. S. Eun, and M.-K. Lee, “Pharmacokinetics and biodistribution of paclitaxel loaded in pegylated solid lipid nanoparticles after intravenous administration,” *Archives of Pharmacal Research*, vol. 34, no. 2, pp. 331–337, 2011.
- [107] R. Mauludin, R. H. Muller, and C. M. Keck, “Development of an oral rutin nanocrystal formulation,” *International Journal of Pharmaceutics*, vol. 370, no. 1-2, pp. 202–209, 2009.
- [108] S. Xie, L. Zhu, Z. Dong et al., “Preparation, characterization and pharmacokinetics of enrofloxacin-loaded solid lipid nanoparticles: influences of fatty acids,” *Colloids and Surfaces B*, vol. 83, no. 2, pp. 382–387, 2011.
- [109] S. Chakraborty, D. Shukla, B. Mishra, and S. Singh, “Lipid-an emerging platform for oral delivery of drugs with poor bioavailability,” *European Journal of Pharmaceutics and Biopharmaceutics*, vol. 73, no. 1, pp. 1–15, 2009.
- [110] Y. Luo, D. Chen, L. Ren, X. Zhao, and J. Qin, “Solid lipid nanoparticles for enhancing vinpocetine’s oral bioavailability,” *Journal of Controlled Release*, vol. 114, no. 1, pp. 53–59, 2006.

- [111] J. K. Vasir, K. Tambwekar, and S. Garg, "Bioadhesive microspheres as a controlled drug delivery system," *International Journal of Pharmaceutics*, vol. 255, no. 1-2, pp. 13–32, 2003.
- [112] S. Xie, B. Pan, M. Wang et al., "Formulation, characterization and pharmacokinetics of praziquantel-loaded hydrogenated castor oil solid lipid nanoparticles," *Nanomedicine*, vol. 5, no. 5, pp. 693–701, 2010.
- [113] C. Han, C. M. Qi, B. K. Zhao et al., "Hydrogenated castor oil nanoparticles as carriers for the subcutaneous administration of tilmicosin: in vitro and in vivo studies," *Journal of Veterinary Pharmacology and Therapeutics*, vol. 32, no. 2, pp. 116–123, 2009.
- [114] D. Pandita, A. Ahuja, V. Lather et al., "Development of lipidbased nanoparticles for enhancing the oral bioavailability of paclitaxel," *AAPS PharmSciTech*, vol. 12, no. 2, pp. 712–722, 2011.
- [115] H. Yuan, J. Chen, Y. Z. Du, F. Q. Hu, S. Zeng, and H. L. Zhao, "Studies on oral absorption of stearic acid SLN by a novel fluorometric method," *Colloids and Surfaces B*, vol. 58, no. 2, pp. 157–164, 2007.
- [116] T. G. Smijs and J. A. Bouwstra, "Focus on skin as a possible port of entry for solid nanoparticles and the toxicological impact," *Journal of Biomedical Nanotechnology*, vol. 6, pp. 469–484, 2010.
- [117] H. L. Karlsson, "The comet assay in nanotoxicology research," *Analytical and Bioanalytical Chemistry*, vol. 398, no.2, pp. 651–666, 2010.
- [118] C. F. Jones and D. W. Grainger, "In vitro assessments of nanomaterial toxicity," *Advanced Drug Delivery Reviews*, vol. 61, no. 6, pp. 438–456, 2009.
- [119] A. C. Silva, E. González-Mira, M. L. García et al., "Preparation, characterization and biocompatibility studies on risperidone-loaded solid lipid nanoparticles (SLN): high

pressure homogenization versus ultrasound,” *Colloids and Surfaces B*, vol. 86, no. 1, pp. 158–165, 2011.

[120] R. H. Müller, D. Rühl, S. Runge, K. Schulze-Forster, and W. Mehnert, “Cytotoxicity of solid lipid nanoparticles as a function of the lipid matrix and the surfactant,” *Pharmaceutical Research*, vol. 14, no. 4, pp. 458–462, 1997.

[121] M. Nassimi, C. Schleh, H. D. Lauenstein et al., “A toxicological evaluation of inhaled solid lipid nanoparticles used as a potential drug delivery system for the lung,” *European Journal of Pharmaceutics and Biopharmaceutics*, vol. 75, no. 2, pp. 107–116, 2010.

[122] V. Meunier, M. Bourrie, Y. Berger, and G. Fabre, “The human intestinal epithelial cell line Caco-2; pharmacological and pharmacokinetic applications,” *Cell Biology and Toxicology*, vol. 11, no. 3-4, pp. 187–194, 1995.

[123] V. Mathur, Y. Satrawala, M. S. Rajput, P. Kumar, P. Shrivastava, and A. Vishvkarma, “Solid lipid nanoparticles in cancer therapy,” *International Journal of Drug Delivery*, no. 2, pp. 192–199, 2010.

[124] M. Harms and C. C. Müller-Goymann, “Solid lipid nanoparticles for drug delivery,” *Journal of Drug Delivery Science and Technology*, vol. 1, no. 21, 2011.

[125] U. H. Cegla, “Long-term therapy over 2 years with ambroxol (Mucosolvan) retard capsules in patients with chronic bronchitis. Results of a double-blind study of 180 patients,” *Praxis und Klinik der Pneumologie*, vol. 42, no. 9, pp. 715–721, 1988.

[126] P. Speiser, Lipid nanopellets as carrier system for drugs for oral administration, 1990.

[127] M. Üner and G. Yener, “Importance of solid lipid nanoparticles (SLN) in various administration routes and future perspectives,” *International Journal of Nanomedicine*, vol. 3, no. 2, 2007.

[128] W. Wei, S. J. Shi, J. Liu et al., “Lipid nanoparticles loaded with 10-hydroxycamptothecin-phospholipid complex developed for the treatment of hepatoma in clinical application,” *Journal of Drug Targeting*, vol. 18, no. 7, pp. 557–566, 2010.

[129] B. Sarmiento, S. Martins, D. Ferreira, and E. B. Souto, “Oral insulin delivery by means of solid lipid nanoparticles,” *International Journal of Nanomedicine*, vol. 2, no. 4, pp. 743–749, 2007.

Polymorphism, crystallinity and hydrophilic–lipophilic balance of stearic acid and stearic acid–capric/caprylic triglyceride matrices for production of stable nanoparticles

Patrícia Severino^{1,2}, Samantha C. Pinho³, Eliana B. Souto^{2,4} and Maria Helena A. Santana¹

¹Departamento de Processos Biotecnológicos, Faculdade de Engenharia Química, Universidade de Campinas, 13083-852 Campinas – SP, Brasil

²Faculdade de Ciências da Saúde, Universidade Fernando Pessoa, 4200-150 Porto - Portugal

³Departamento de Engenharia de Alimentos, Faculdade de Zootecnia e Engenharia de Alimentos, Universidade de São Paulo, 13635- 900 Pirassununga – SP, Brasil

⁴Instituto de Biotecnologia e Bioengenharia, Centro de Genómica e Biotecnologia, Universidade de Trás-os-Montes e Alto Douro, 5001-801 Vila Real - Portugal

Paper published in Colloids and Surfaces B: Biointerface, 86, 125-130, 2011.

Abstract

There is an increasing interest in lipid nanoparticles because of their suitability for several administration routes. Thus, it becomes even more relevant the physicochemical characterization of lipid materials with respect to their polymorphism, lipid miscibility and stability, as well as the assessment of the effect of surfactant on the type and structure of these nanoparticles. This work focuses on the physicochemical characterization of lipid matrices composed of stearic acid or mixtures of stearic acid-capric/caprylic triglycerides, for drug delivery. The lipids were analyzed by Differential Scanning Calorimetry (DSC), Wide Angle X-ray Diffraction (WAXD), Polarized Light Microscopy (PLM) and Hydrophilic-Lipophilic Balance (HLB) in combination with selected surfactants to assess the best solid-to-liquid ratio. Based on the results, selected qualitative and quantitative lipid composition may be useful to obtain stable nanoparticles, since the melting and the tempering processes change crystal ordering favoring the production of solid matrices. The best HLB value obtained for stearic acid-capric/caprylic triglycerides was 13.8, achieved after combining these lipids with accepted surfactants (trioleate sorbitan and polysorbate 80 in the ratio of 10:90). The proposed combinations were shown useful to obtain a stable emulsion to be used as intermediate form for the production of lipid nanoparticles.

Keywords: lipids, stearic acid; capric/caprylic triglycerides; lipid nanoparticles, polymorphism, physicochemical structure; surfactants; hydrophilic-lipophilic balance

1. Introduction

The current increasing interest in lipid nanoparticles [1] relies on the advantages of lipid materials in comparison to others, e.g. including the excellent physical and chemical stability of produced particles that provides greater protection against degradation of drugs [2, 3], and ability to load hydrophobic, hydrophilic and other biomacromolecules (such as peptides and proteins) [4, 5].

Lipids employed for the production of nanoparticles include triglycerides and their mixtures, fatty acids and waxes [6, 7]. It is however required that matrix maintains the solid state at room temperature and for this, the selection of lipids requires the evaluation of their polymorphism, and crystallinity miscibility and physicochemical structure [3]. For large production of lipid nanoparticles, the control of polymorphism is a demand due to its influence on the encapsulation efficiency and on the drug expulsion during storage [8]. The lipid crystallization is also an important characteristic, since the crystalline structures of triglycerides can occur in different polymorphic forms (α , β' , β) [9]. The α -form (hexagonal) is the least stable with a lower melting point and latent heat, whereas the β -form (triclinic) is more stable with higher melting point and higher latent heat. The transformation of α to β' (orthorhombic) and β is irreversible and occurs towards a more hydrodynamic stable system [10, 11].

Pharmaceutical formulations containing lipid nanoparticles prioritize the use of natural lipids [1]. Stearic acid is an endogenous long-chain saturated fatty acid and a primary component of fats in both animal and plant sources, providing better biocompatibility and lower toxicity than the synthesized counterparts [12]. Stearic acid has a melting point higher than body temperature (m.p. 69.6°C), it is biocompatible with human tissues, and neutral with respect to physiological fluids [11]. Its use as pharmaceutical excipient for

drug delivery has also been reported [13]. Medium chain triglycerides (e.g. capric/caprylic triglycerides) are neutral oils having advantages of high stability against oxidation and good solubility [13]. The lipids used in this study are considered non-toxic and are classified as ‘Generally Recognized as Safe’ (GRAS) by the Food and Drug Administration (FDA). Regarding the influence of surfactant on the physicochemical stability of lipid nanoparticles, the amount of emulsifier should be optimized to cover the surface of the particles. Otherwise, it can lead to instabilities (e.g. aggregation and increased size of the particles during shelf-life). Excess can decrease the encapsulation efficiency, induce faster drug release and increase toxicity. The combined use of more than one surfactant can produce mixed films at the interface, contributing for a better surface coverage of particles, and also increases the viscosity to ensure a long term stability of the formulation [14]. The aim of this study was to evaluate the polymorphism and crystallinity of stearic acid, separately, and the binary mixture of stearic acid-capric/caprylic triglycerides (70:30) after fusion and tempering for 1 h at 80°C. The hydrophilic-lipophilic balance (HLB) value for stearic acid and its mixtures with the oil was determined to reach the best combination of surfactants (trioleate sorbitan and polysorbate 80) for the production of a stable emulsion during the course of lipid nanoparticles production.

2. Material and methods

2.1. Material

Capric-caprylic triglycerides (C8-C10) (Crodamol GTCC[®]) and trioate sorbitan (Span 85[®]) were donated as a gift from Croda (Campinas, Brazil); Stearic acid and polysorbate 80

(Tween 80[®]) were obtained from Synth (Diadema, Brazil). Double distilled water was used after filtration in a Millipore system (home supplied).

2.2. Methods

2.2.1. Lipid Screening and Thermal Treatment of Lipid Materials

The solid lipid (i.e., stearic acid) and the binary mixture stearic acid-capric/caprylic triglycerides (70:30) were studied separately. Samples were subject to fusion and tempering. Fusion consisted of melting until 80°C on a thermostatic water bath (Marconi, model MA 127/BD, Piracicaba, Brazil), following tempering by sample incubation in the same bath for 1 h at 80°C [15]. Samples were then kept at room temperature until complete cooling and solidification, to check for the creation of polymorphic forms. Most production processes of nanoparticles require heating; thus, tempering was performed to mimic the production procedure carried out for lipid nanoparticles production.

2.2.2. Differential Scanning Calorimetry (DSC)

Thermal behavior of lipid matrices was assessed by DSC (Mettler Toledo, FP90 Central Processor, São Paulo, Brazil). A volume of sample containing approximately 5-10 mg of lipid mass was weighted in an aluminum pan and sealed hermetically, under inert atmosphere (N₂). The analysis was performed at a heating and cooling rate of 5K/min, using an empty pan as reference. The samples were heated from 10°C up to 100°C, following cooling down to 10°C. The degree of crystallinity of mixture stearic acid-capric/caprylic triglycerides was determined by calculating the crystallinity index (CI) from the heat of fusion using the following equation [16].

$$(\%)CI = \frac{\text{Entalpy MP (J/g)}}{\text{Entalpy LP (J/g)}} 100fM$$

where Enthalpy MP is the fusion enthalpy of the lipid mixture, Enthalpy LP is the fusion enthalpy of the pure lipid, and fM is the factor that takes into account the concentration of lipid, that is solid in the matrix.

2.2.3. Wide Angle X-ray Diffraction (WAXD)

To study the polymorphism and crystalline properties of the lipids and their mixtures, WAXD was carried out in a diffractometer X-ray (Philips, model X'pert, Pennsylvania, USA), using copper anode emitting a wavelength of 0.154056 nm. WAXD measurements were taken from 50° to 330° in 0.015° steps (1s per step). The interlayer spacings were calculated from the reflections using Bragg's equation:

$$d = \frac{\lambda}{\text{sen}2\theta}$$

where λ is the wavelength of the incident X-ray beam and θ is the scattering angle. The parameter d , otherwise called the interlayer spacing, is the separation between a particular set of planes of the crystal lattice structure. Data of the scattered radiation were recorded with a blend local-sensible detector using an anode voltage of 40 kV, a current of 25 mA and a scan rate of 0.5° per minute. The samples were mounted on a thin glass capillary being fastened to a brass pin without any previous sample treatment.

2.2.4. Polarized Light Microscopy (PLM)

PLM is used to check for lipid microstructures and to monitor their melting transitions and fusion. Micrographs of crystallized lipid matrices were examined with a photomicroscope

(LEICA, model Leitz DMRXE, Bensheim, Germany) coupled with a software Motic Images Advanced 3.2. and using cross polarizer. Samples were evaluated 24 h after production and analyzed with increase of 20.000x.

2.2.5. Assessment of Hydrophilic-Lipophilic Balance (HLB) and Phase Separation

The determination the HLB values for the production of stable emulsions was based on the theoretical HLB number obtained from the literature or from the manufacturer for stearic acid-capric/caprylic triglycerides/surfactant combination. The real value of HLB for the tested lipid and surfactant mixtures was determined after Griffin et al. [14], and applying the following equation:

$$\text{HLB} = \frac{\text{Concentration of lipid} \times \text{HLB of lipid}}{100}$$

Seven emulsions were produced, based on different combinations of 2 tested surfactants according to Table 1. Aqueous phase consisted of water (95% v/v) and surfactant (5% m/v). The surfactants used were trioleate sorbitan (HLB 1.8) and polysorbate 80 (HLB 15.0) to obtain different HLB values. The oil phase consisted of stearic acid (7% m/v) and triglyceride mixtures (3% m/v). Then, the aqueous phase and oil phase were heated separately to 80°C. Aqueous phase was poured into oil phase under stirring (Ultra-Turrax[®] T25, USA), 10.000 rpm for 15 min under. Then, the emulsions were cooled down to room temperature during 15 min under mechanical stirring. The emulsions were stored for 24 h at room temperature for further visual and optical microscopic analyses. The visual analysis compared the stability of the emulsions measuring the phase separation with a ruler.

Table 1. HLB values obtained for different blends of lipid and surfactant combinations for 7 emulsions.

Emulsion	Trioleate sorbitan	Polysorbate 80	Oil phase	Aqueous phase	HLB
E1	60	40	10	95	7.08
E2	50	50	10	95	8.40
E3	40	60	10	95	9.72
E4	30	70	10	95	11.04
E5	20	80	10	95	12.36
E6	10	90	10	95	13.68
E7	0	100	10	95	15.00

*Values expressed in percentage (%).

3. Results and discussion

Polymorphic transformations are often shown by long-chain lipid compounds, such as stearic acid. In general, these lipids crystallize in two or three different phases, α and β' , or α , β' and β , respectively. DSC was employed to study the melting temperature and crystallization behaviour of lipids [17]. Stearic acid is the saturated fatty acid, with 18 carbon-chain length, and a high lipophilic character. Its HLB is approximately 15, and is often selected as solid lipid for the production of lipid nanoparticle dispersions. The selection of capric/caprylic triglycerides as liquid lipid was based on their thermodynamic stability and high solubility for many drugs. For the characterization of the bulk stearic acid and mixture of stearic acid-capric/caprylic triglycerides in the ratio of 70:30, respectively, DSC was run before and after tempering by incubation of samples for 1 h in an oven heated at 80°C (Table 2 and 3). The tempering was undertaken to mimic the production procedure of lipid nanoparticles. Although heat exposure during the homogenization step is usually

only about 5 min, here the incubation occurred during 1 h for easier detection of possible effects caused by the temperature. DSC analysis of lipids before and after thermal stress allows anticipating the lipid behavior when processing the raw materials for the production of lipid nanoparticles [18]. Table 1 shows the results obtained for the first heating run. After tempering, stearic acid depicted a melting event at 69.6°C with an endothermic peak at approximately 72.4°C, values that were clearly below those depicted before tempering i.e. 70.1°C and 73.4°C, respectively. Similar results have been reported elsewhere [19, 20].

Table 2. DSC analysis of stearic acid and stearic acid-capric/caprylic triglycerides, before and after tempering the samples for 1 h at 80°C.

Formulation	Onset Temperature (°C)	Melting Peak (°C)	Endset Temperature (°C)	ΔH Melting (J/g)
<i>before tempering</i>				
Stearic acid	70.1	73.4	81.1	187.0
Stearic acid-capric/caprylic triglycerides	64.8	69.4	75.5	136.0
<i>after tempering</i>				
Stearic acid	69.6	72.4	81.2	191.0
Stearic acid-capric/caprylic triglycerides	65.0	69.9	75.8	119.0

Table 3. DSC analysis of crystallization of stearic acid and stearic acid-capric/caprylic triglycerides, before and after tempering the samples for 1 h at 80°C.

Formulation	Onset Temperature (°C)	Melting Peak (°C)	Endset Temperature (°C)	ΔH Melting Enthalpy (J/g)
<i>Before tempering</i>				
Stearic acid	71.9	67.8	61.8	-128.0
Stearic acid-capric/caprylic triglycerides	66.1	64.1	63.8	-91.7
<i>After tempering</i>				
Stearic acid	70.7	66.8	60.5	-132.0
Stearic acid-capric/caprylic triglycerides	66.4	64.1	55.9	-71.1

A decrease of the onset temperature of stearic acid-capric/caprylic triglyceride mixtures was recorded before tempering (64.8°C). Comparing this value with that obtained after tempering (65°C), an increase of the β'/β_i amounts in the lattice of the bulk lipid after thermal stress can be anticipated. The tempering process of stearic acid increased the melting enthalpy from 187 to 191 J/g, whereas the lipid mixture decreased from 136 to 119 J/g, in both cases showing a small difference between both DSC patterns. With regard to stearic acid, the heating run after tempering depicted a higher melting point (70.1°C) with a melting enthalpy of 187 J/g, where the fraction corresponding to the α modification of the lipid was practically absent. After tempering, the input of energy is sufficiently high reflecting lipid changes from a more unstable to a more stable polymorphic form. The

melting and crystallization peaks of stearic acid are wide, suggesting polymorphism. However, the decomposition in more than one peak was not observed. These results are in agreement with the complex polymorphism existing in fatty acids, and particularly in stearic acid, which has at least four polymorphic forms [19].

Concerning the recrystallization temperatures (corresponding to the cooling runs) similar exotherms have been obtained. The results of recrystallization patterns are depicted in Table 3. Also, major differences were observed in the cooling fraction of this curve. In fact, a less pronounced polymorphic form (smaller shoulder) for both curves was registered.

Melting events obtained after tempering were recorded above 40°C, which represents an important feature as it ensures the integrity (solid state) of the particles for pharmaceutical use. Additionally, there is a decrease of the melting enthalpy after the tempering process emphasizing the disorder of the crystal structure. The crystallinity index (CI) of the lipid mixture was 43.61% before tempering, against 50.90% after tempering. If 100% would have been obtained, it would represent a fully crystallized sample. The results show that there is little difference between the two processes, but also tempering has a higher crystallinity of the lipid mixture with less organization of crystals. Analysing the results of crystallization obtained with a rapid cooling rate (5.0 K/min), it is possible to identify the amount and type of the peaks, indicating if it is a pure sample or a mixture. The increase of the melting enthalpy and crystallization is inversely proportional to the amount of liquid lipid mixture. Adding triglycerides in stearic acid resulted in a decrease of the melting enthalpy, affecting the recrystallization during the cooling process. The melting temperature of the lipid mixtures also decreased, indicating greater disorder of the lipid crystal. Generally, the decrease of the onset temperature and melting peak is dependent on the concentration of liquid lipid. A less ordering of lipid matrix is favouring and increasing

the number of imperfections in its structure. Thus, it is able of accommodating a larger amount of drug, minimizing their expulsion during storage, and also modulating the release [21, 22]. Calculating the difference between the melting and onset temperatures measuring the range that melting of lipids occur, and the greater this difference, the greater the disorder of the lipid crystal. For stearic acid this difference was 2.8°C whereas for the lipid mixture was 4.9°C. After tempering, the differences obtained for stearic acid was 3.3°C, versus 4.6°C for the mixture. These results show that the crystalline structures have high susceptibility to clutter under thermal stress.

Regarding the WAXD analysis, the studies of the lamellae arrangement of stearic acid and stearic acid-capric/caprylic triglycerides have also been performed before (Figure 1) and after (Figure 2) tempering the lipid at 80°C for 1 h. The WAXD patterns show that after tempering, the lipid mixture the intensity of the peaks was reduced. The peak width was maintained, although not well defined as before treatment. Small difference has been observed among diffractograms. After tempering, stearic acid shows major reflections, at 21.5 (2 θ), i.e. $d = 0.421$ nm, and another at 24.0 (2 θ), i.e. $d = 0.378$ nm. Before tempering, similar peaks occur at 21.5 (2 θ), i.e. $d = 0.420$ nm, and another at 24.1 (2 θ), i.e. $d = 0.378$ nm. For stearic acid-capric/caprylic triglycerides mixtures after tempering show major reflections, at 21.5 (2 θ), i.e. $d = 0.421$ and 24.0 (2 θ), i.e. $d = 0.378$, after tempering the results are 21.3 (2 θ), i.e. $d = 0.424$ and 23.9 (2 θ), i.e. $d = 0.380$, revealing now only one peak at 22.1 (2 θ), i.e. $d = 0.409$ nm, corresponding to the β' modifications.

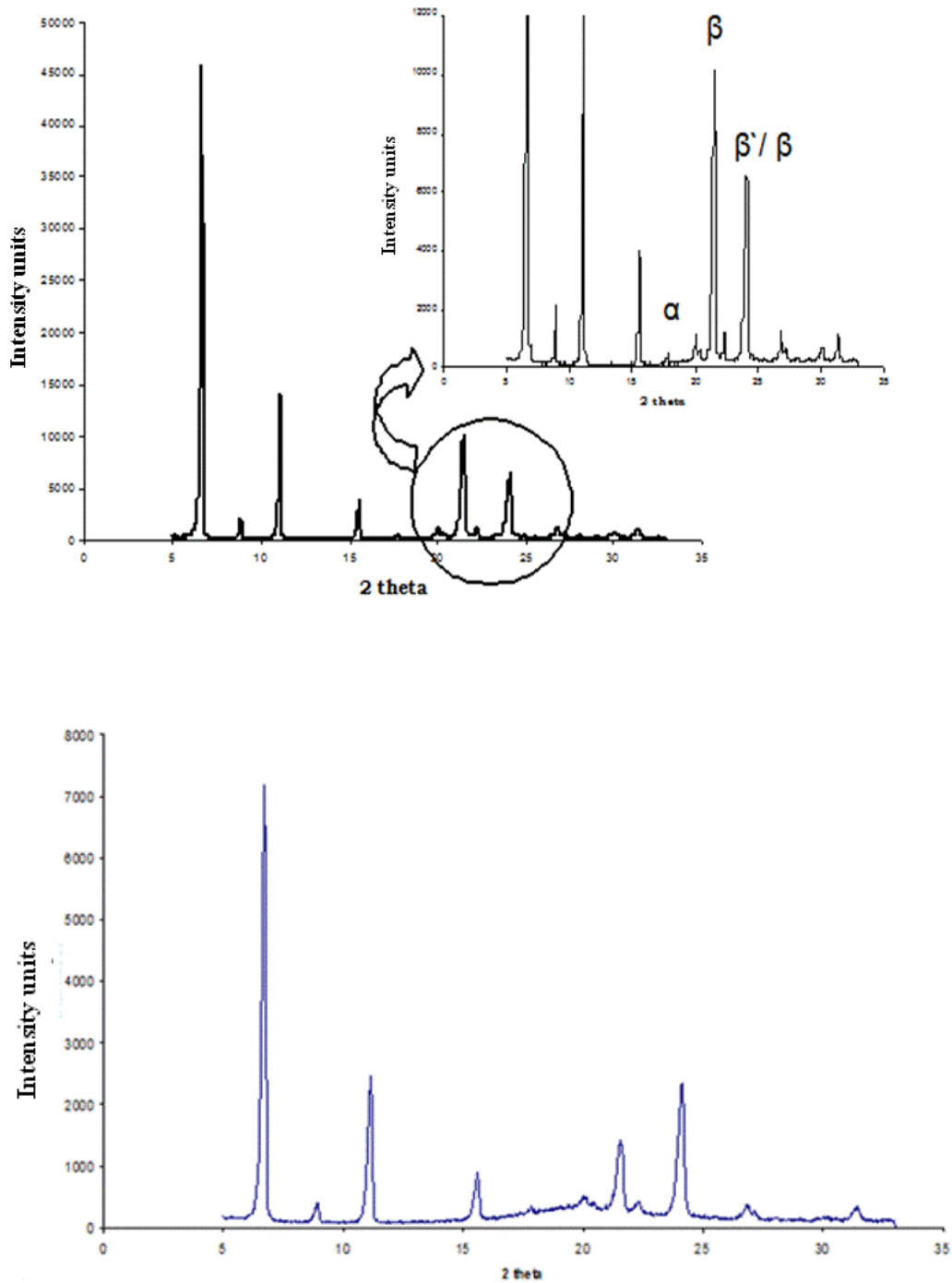


Figure 1. WAXD diffractogram recorded for stearic acid (upper) and stearic acid-capric/caprylic triglycerides (lower) before tempering. Intensity (arbitrary units).

Before tempering, the solid lipid shows little difference in the WAXD reflections. These signals correspond to the β' modifications [23]. The only difference between both curves is the intensity and the width of the peak (resolution of two peaks), which depends on different factors such as the amount of sample mounted on the glass capillary. However, it is clear that the lipid slightly changes its crystallinity by tempering as observed by DSC analysis. It is known that the phase transformations of lipids and their mixtures are monotropic, ($\alpha \rightarrow \beta'$, $\alpha \rightarrow \beta' \rightarrow \beta$, or $\alpha \rightarrow \beta$), implicating only one stable polymorphic form. For monoacid even numbered triglycerides $C_nC_nC_n$ the most stable modification is β , whereas for the $C_nC_{n+2}C_n$ and $C_nC_{n+4}C_n$ the most stable polymorphic form is β' . After tempering, those two peaks were no more recorded, meaning that for this lipid the most stable polymorphic form is β' . These results are in agreement with those obtained with DSC since the recorded melting point after tempering was similar or slightly higher than before tempering, but showing lower melting enthalpy. DSC and WAXD results obtained after tempering are in agreement, as the decrease of the melting and onset temperatures were followed by a decrease of the intensity of WAXD peaks. These results suggest the presence of more structures that favour the encapsulation of drug molecules and increase stability of the particles during storage.

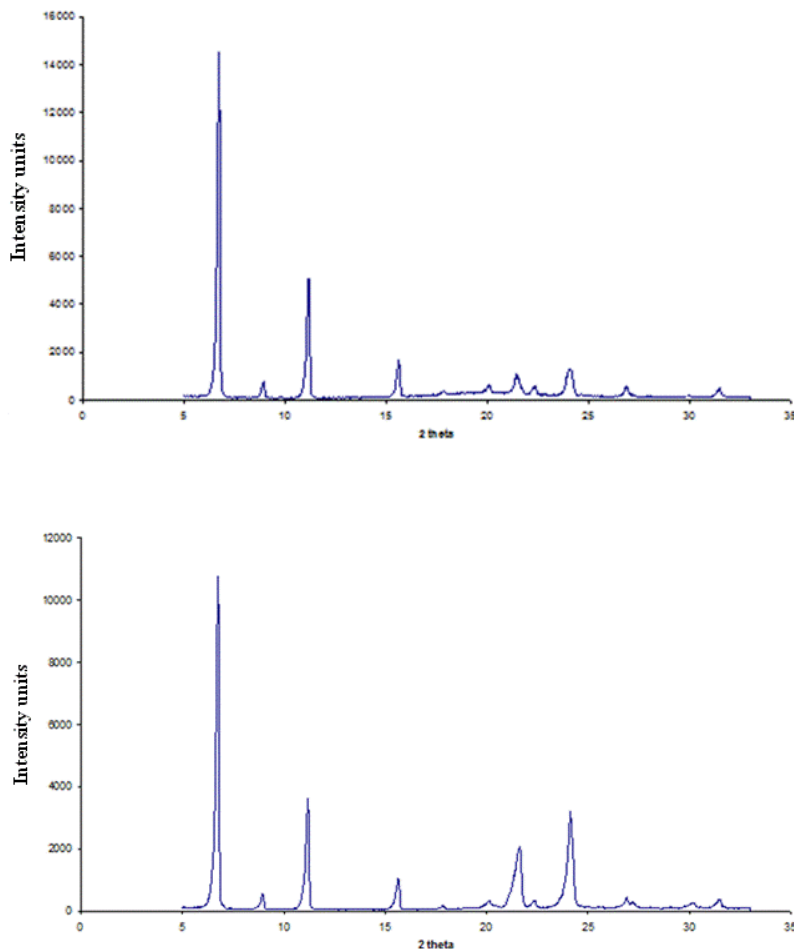


Figure 2. WAXD diffractogram recorded for stearic acid (upper) and stearic acid-capric/caprylic triglycerides (lower) after tempering. Intensity (arbitrary units).

Micrographs show crystalline structures and liquid crystalline states before and after tempering the lipid matrices (Figure 3). Stearic acid (a, b) and stearic acid-capric/caprylic triglycerides (c, d) show irregular forms of crystal with different sizes, confirming the results obtained by DSC and WAXD. Stearic acid-capric/caprylic triglycerides also revealed an amorphous state.

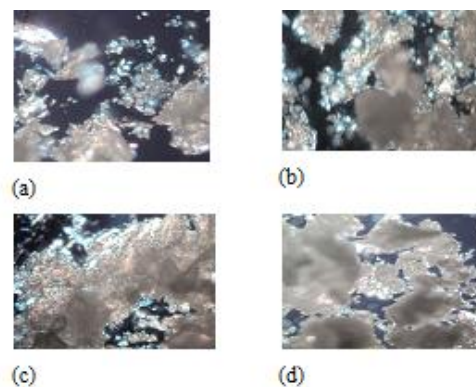


Figure 3. Micrographs obtained by PLM of stearic acid (a) and of stearic acid-capric/caprylic triglycerides (b) before tempering; and of stearic acid (c) and stearic acid-capric/caprylic triglycerides (d) after tempering.

The HLB value obtained for stearic acid was 15.0 and for stearic acid-capric/caprylic triglycerides was 13.8. The mixture of surfactants in different proportions was also performed to provide well defined HLB values. Sorbitan trioleate has a HLB value of 1.8 and polysorbate 80 of 15, when used in the ratio 10:90, respectively. Because of their similar chemical structure, polysorbate 80 is often used in combination with sorbitan trioleate for the production of stable emulsions. In the majority of cases, the most stable emulsions are usually formed when both emulsifying agents are of the same hydrocarbon chain length [24]. To anticipate the effect of the long term stability of selected combinations of stearic acid-capric/caprylic triglycerides mixtures, the effect of HLB on the risk of phase separation was checked for 7 emulsions (Figure 4). Phase separation profoundly decreased when HLB value increased above 12. After 24 h stearic acid-capric/caprylic triglycerides mixtures with a HLB value of 13.8 showed greater stability, similar to those reported for the theoretical value. By PLM formulation E6 (composed by 10% trioleate sorbitan; 90% polysorbate 80; 10% oil phase and 95% aqueous phase) was

shown homogeneous with respect to stability, and no foaming was observed upon mechanical stress.

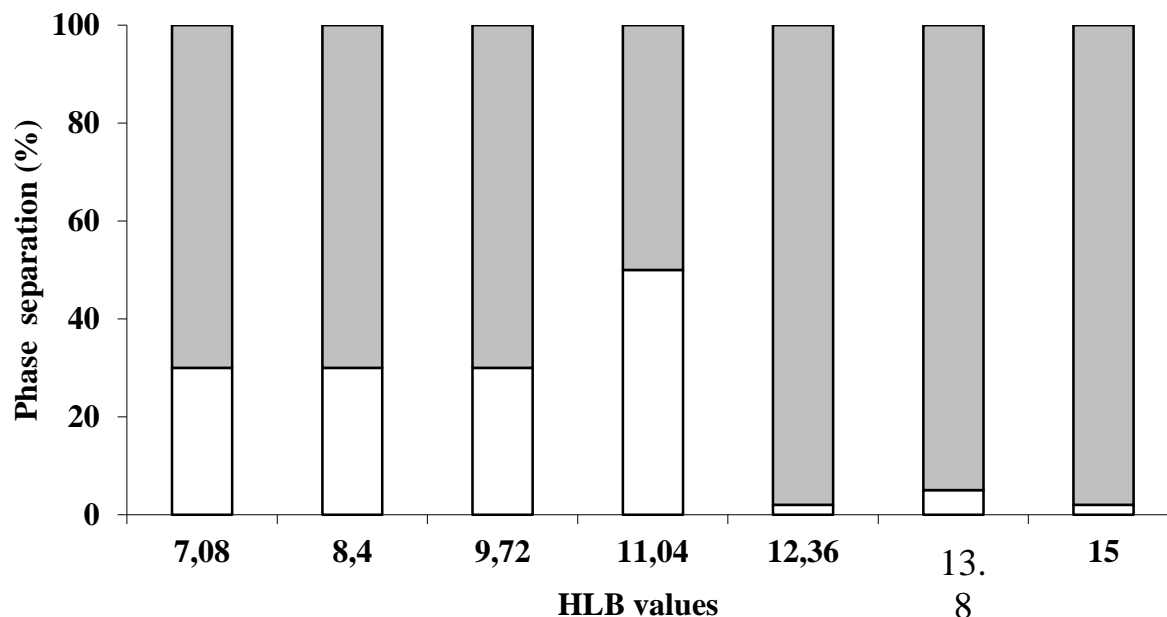


Figure 4. Stability of stearic acid-capric/caprylic triglycerides emulsion, after 24 h.

4. Conclusions

The polymorphic behaviour of stearic acid has been assessed by means of DSC and WAXD to evaluate the usefulness of these proposed solid lipid and its mixtures for the production of lipid nanoparticles. Stearic acid consists of a very small amount of α -form which tends to disappear under thermal stress due to its high thermodynamic instability. To enhance long term stability of emulsions a suitable surfactant/co-surfactant combination needs to be reached. Analysis of HLB values allows anticipating the best ratio in parallel with appropriate solid to liquid lipid ratio. In the present study, DSC and WAXD analyses for several mixture concentrations of solid and liquid lipid have been run. Emulsions with 30% of oil regarding to the lipid matrix were prepared. The HLB value of 13.8, promotes more

homogeneous emulsions, with no foaming or phase separation during 24 h storage. This has been attributed to the perfect interaction of hydrophilic and lipophilic emulsifiers on the o/w interface of emulsion.

Acknowledgment

The authors wish to acknowledge the sponsorship of the FAPESP (*Fundação de Amparo a Pesquisa*) and CAPES (*Coordenação de Aperfeiçoamento de Pessoal de Nível superior*).

References

- [1] A.A. Attama, B.C. Schicke and C.C. Muller-Goymann, Further characterization of theobroma oil-beeswax admixtures as lipid matrices for improved drug delivery systems. *Eur. J. Pharm. Biopharm.*, **64** (2006), pp. 294–306.
- [2] A.O. Hassan and A.H. Elshafeey, Nanosized particulate systems for dermal and transdermal delivery. *J. Biomed. Nanotechnol.*, **6** (2010), pp. 621–633.
- [3] E.B. Souto and R.H. Muller, Lipid nanoparticles: effect on bioavailability and pharmacokinetic changes. *Handb. Exp. Pharmacol.*, (2010), pp. 115–141.
- [4] B. Heurtault, P. Saulnier, B. Pech, J.E. Proust and J.P. Benoit, Physico-chemical stability of colloidal lipid particles. *Biomaterials*, **24** (2003), pp. 4283–4300.
- [5] S. Martins, A.C. Silva, D.C. Ferreira and E.B. Souto, Improving oral absorption of Salmon calcitonin by trimyristin lipid nanoparticles. *J. Biomed. Nanotechnol.*, **5** (2009), pp. 76–83

- [6] A.J. Almeida and E. Souto, Solid lipid nanoparticles as a drug delivery system for peptides and proteins. *Adv. Drug Deliv. Rev.*, **59** (2007), pp. 478–490.
- [7] Y.P. Fang, Y.K. Lin, Y.H. Su and J.Y. Fang, Tryptanthrin-loaded nanoparticles for delivery into cultured human breast cancer cells, MCF7: the effects of solid lipid/liquid lipid ratios in the inner core. *Chem. Pharm. Bull. (Tokyo)*, **59** (2011), pp. 266–271
- [8] E.B. Souto, S. Doktorovová and P. Boonme, Lipid nanocarriers-based semisolids: review on materials and end product formulations. *J. Drug Deliv. Technol.*, **21** (2011), pp. 43–54
- [9] K. Jores, W. Mehnert, M. Drechsler, H. Bunjes, C. Johann and K. Mader, Investigations on the structure of solid lipid nanoparticles (SLN) and oil-loaded solid lipid nanoparticles by photon correlation spectroscopy, field-flow fractionation and transmission electron microscopy. *J. Control. Release*, **95** (2004), pp. 217–227.
- [10] A. Kovacevic, S. Savic, G. Vuleta, R.H. Muller and C.M. Keck, Polyhydroxy surfactants for the formulation of lipid nanoparticles (SLN and NLC): effects on size, physical stability and particle matrix structure. *Int. J. Pharm.*, **406** (2011), pp. 163–172.
- [11] R.E. Timms, Physical-properties of oils and mixtures of oils. *J. Am. Oil Chem. Soc.*, **62** (1985), pp. 241–249.
- [12] R.E. Timms, Physical Properties of Oils and Mixtures of Oils, (2005).
- [13] A. Fundaro, R. Cavalli, A. Bargoni, D. Vighetto, G.P. Zara and M.R. Gasco, Non-stealth and stealth solid lipid nanoparticles (SLN) carrying doxorubicin: pharmacokinetics

and tissue distribution after i.v. administration to rats. *Pharmacol. Res.*, **42** (2000), pp. 337–343

[14] K. Hippalgaonkar, S. Majumdar and V. Kansara, Injectable lipid emulsions-advancements, opportunities and challenges. *AAPS PharmSciTech*, **11** (2010), pp. 1526–1540

[15] W.C. Griffin, Classification of surface active agents by HLB. *J. Soc. Cosmet. Chem.*, **1** (1949), pp. 311–326.

[16] E.B. Souto, W. Mehnert and R.H. Muller, Polymorphic behaviour of Compritol888 ATO as bulk lipid and as SLN and NLC. *J. Microencapsul.*, **23** (2006), pp. 417–433.

[17] V.B. Junyaprasert, V. Teeranachaideekul, E.B. Souto, P. Boonme and R.H. Muller, Q10-loaded NLC versus nanoemulsions: stability, rheology and in vitro skin permeation. *Int. J. Pharm.*, **377** (2009), pp. 207–214

[18] V. Jenning, A.F. Thunemann and S.H. Gohla, Characterisation of a novel solid lipid nanoparticle carrier system based on binary mixtures of liquid and solid lipids. *Int. J. Pharm.*, **199** (2000), pp. 167–177

[19] A.C. Teixeira, A.R. Garcia, L.M. Ilharco, A.M. Goncalves da Silva and A.C. Fernandes, Phase behaviour of oleanolic acid, pure and mixed with stearic acid: Interactions and crystallinity. *Chem. Phys. Lipids*, **163** (2010), pp. 655–666.

- [20] T. Inoue, Y. Hisatsugu, R. Ishikawa and M. Suzuki, Solid-liquid phase behavior of binary fatty acid mixtures. 2. Mixtures of oleic acid with lauric acid, myristic acid, and palmitic acid. *Chem. Phys. Lipids*, **127** (2004), pp. 161–173.
- [21] R.H. Muller, M. Radtke and S.A. Wissing, Nanostructured lipid matrices for improved microencapsulation of drugs. *Int. J. Pharm.*, **242** (2002), pp. 121–128.
- [22] R.H. Muller, M. Radtke and S.A. Wissing, Solid lipid nanoparticles (SLN) and nanostructured lipid carriers (NLC) in cosmetic and dermatological preparations. *Adv. Drug Deliv. Rev.*, **54** 1 (2002), pp. S131–155.
- [23] K. Sato, Crystallization of fats and fatty acids, N. Garti, K. Sato, Editors , *Crystallization and Polymorphism of Fats and Fatty Acids. Surfactant Science Series*, Marcel Dekker Inc., New York (1988), pp. 267–303.
- [24] T. Schmidts, D. Dobler, C. Nissing and F. Runkel, Influence of hydrophilic surfactants on the properties of multiple W/O/W emulsions. *J. Colloid Interface Sci.*, **338** (2009), pp. 184–192.

Optimizing SLN and NLC by 2² full factorial design: Effect of homogenization technique

Patrícia Severino^{1,2}, Maria Helena A. Santana¹, Eliana B. Souto^{2,3}

¹*Biotechnological Processes Development Laboratory, School of Chemical Engineering, State University of Campinas-UNICAMP, Campinas, SP, Brazil*

²*Faculty of Health Sciences, Fernando Pessoa University (FCS-UFP), Rua Carlos da Maia, 296, P-4200-150 Porto, Portugal*

³*Institute of Biotechnology and Bioengineering, Centre of Genomics and Biotechnology, University of Trás-os-Montes and Alto Douro (CGB-UTAD/IBB), P.O. Box 1013, P-5001-801, Vila Real, Portugal*

Paper published in Materials Science & Engineering C, 32, 1375–1379 2012.

Doi:10.1016/j.msec.2012.04.017

Abstract

Solid lipid nanoparticles (SLN) and nanostructured lipid carrier (NLC) have been employed in pharmaceuticals and biomedical formulations. The present study focuses on the optimization of the production process of SLN and NLC by High Shear Homogenization (HSH) and High Pressure Homogenization (HPH). To build up the surface response charts, a 2^2 full factorial design based on 2 independent variables was used to obtain an optimized formulation. The effects of the production process on the mean particle size, polydispersity index (PI) and zeta potential (ZP) were investigated. Optimized SLN were produced applying 20,000 rpm HSH and 500 bar HPH pressure and NLC process 15,000 rpm HSH and 700 bar HPH pressure, respectively. This factorial design study has proven to be a useful tool in optimizing SLN (~100 nm) and NLC (~300 nm) formulations. The present results highlight the benefit of applying statistical designs in the preparation of lipid nanoparticles.

Keywords: Solid Lipid Nanoparticle (SLN), Nanostructured Lipid Nanoparticle (NLC), High Pressure Homogenization, High Shear Homogeneization and factorial design.

1. Introduction

The introduction of a new biomaterial on the pharmaceutical market is coined by different phases of research and development. During development, several adjustments in formulation, process and product presentation are available. During development, adjustments in formulation, processing and product presentation are possible. These steps are relevant because many processes are limited to a small scale and, in practice, scaling up is not a linear process. For large scale production it is essential to guarantee high product quality, economy of production and reduction of production time [1].

Pharmaceutical and biomedical products [2] employ solid lipids, such as triglycerides (tristearine, tripalmitine, and trimiristine) [3], fatty acids (stearic acid and palmitic acid) [4], waxes (carnauba and cetyl palmitate) [5], but also liquid lipids e.g. medium chain triglycerides, oleic acid, isopropyl myristate [6].

Lipid nanoparticles were initially produced in 1991, opening an exciting research area for many pharmaceutical applications [7]. In the pharmaceutical field, lipid nanoparticles can be used for all routes of administration because of their small particle size, ranging from 50 to 1000 nm [8–10]. A variety of techniques have been developed for lipid nanoparticle production [11]. The most promising production process is considered to be the High Pressure Homogenization (HPH) which can be employed at low or high temperatures [12,13]. HPH has been used for more than fifty years for the production of parenteral nutrition, such as Intralipid[®] and Lipofundin[®] [14]. The advantages of this technique include the possibilities of scaling up, lack of organic solvents and the production of small particles diameter [13,15] with a low polydispersity index (PI), usually below 0.2 [16]. The sequential use of High Shear Homogenization (HSH) followed by HPH, can modulate nanoparticles size for different routes of administration. The present paper reports the

optimization of the production process for SLN (using cetyl palmitate as solid lipid) and for NLC (using stearic acid as solid lipid and capric/caprylic triglycerides as liquid lipid) by means of a factorial design, evaluating the mean particle size, PI and zeta potential (ZP) as the dependent variables.

2. Material and methods

2.1. Materials

Cetyl palmitate (Crodamol[®] CP), capric/caprylic triglycerides (C8–C10) (Crodamol[®]GTCC) and trioleate sorbitan (Span[®] 85) were donated as a gift from Croda Industrial Specialities (Campinas, Brazil). Stearic acid and polysorbate 80 (Tween[®] 80) were obtained from Synth (Diadema, Brazil).

2.2. Methods

2.2.1. Production of lipid nanoparticles

SLN (10% (w/w) Crodamol[®] CP, 3.5% (w/w) Tween[®] 80 and 1.5% (w/w) Span[®] 85 and NLC (7.0% (w/w) stearic acid, 3.0% (w/w) Crodamol[®] GTCC, 4.65% (w/w) Tween[®] 80 and 0.35% (w/w) Span[®] 85) [17] were produced by HSH using the Ultra-Turrax[®] (IKA, model T25, impeller 10 G, Germany). For all formulations, an aqueous surfactant solution of Tween[®] 80 and Span[®] 85 were slowly added to the lipid phase, at 5 to 10 °C above the lipid melting temperature. The formulation was mixed for 1 min applying increasing intensities 5000; 8000; 10,000; 15,000 and 20,000 rpm. An external water bath heated at approximately 80 °C was used to maintain the sample temperature. The obtained oil/water (o/w) nanoemulsion was subsequently cooled down to room temperature; the lipid

recrystallized forming lipid nanoparticle suspensions. The obtained SLN and NLC were used for subsequent studies. For the production applying the HPH, the hot o/w nanoemulsion was further processed using a high pressure homogenizer (GEA Niro Soavi, model NS1001L2K, PANDA 2 K, Italy) at 80 °C for three cycles. The hot o/w nanoemulsion was cooled to room temperature leading to the lipid phase recrystallization and finally the lipid nanoparticles were formed. The volume of the formulations subjected was 200 mL.

2.2.2. Experimental factorial design

The influence of the HSH intensity and HPH pressure on the SLN and NLC properties was evaluated using a 2^2 factorial design with triplicate of central point for estimating the experimental error, composed of 2 variables which were set at 2-levels each.

The mean particle size, PI and ZP were the dependent variables. The design required a total of 7 experiments for each formulation. Each factor, the lower and higher values of the lower and upper levels, was represented by a (-1) and a (+1) and the central point was represented by (0) as summarized in Table 1. These were chosen on the basis of the tested lower and upper values for each variable according to preformulation studies and literature research. A factorial design approach was applied to maximize the yield of production on the basis of the production possibility curves, requiring a minimum of experiments to optimize SLN and NLC formulations. The data were analyzed using STATISTICA 7.0.

Table 1. Initial 2-level full factorial design, providing the lower (-1), upper (+1) and (0) central point level values for each variable.

Variables	Levels		
	-1	0	+1
Ultra-Turrax [®] intensity	10.000	15.000	20.000
HPH pressure	500	700	900

2.2.3. Particle size and zeta potential analysis

The particle size of SLN and NLC was determined through Photon Correlation Spectroscopy (PCS) (Dynamic Light Scattering, DLS, Zetasizer Nano NS, Malvern Instruments, Malvern, UK). PCS is a non-invasive technique to obtain the mean particle size and polydispersity index (PI) in the submicron region [18], and uses electrophoretic mobility to determine the surface electrical charge (zeta potential, ZP) of particles. The samples were diluted with ultra-purified water to weaken the opalescence before measuring the particle mean diameter and PI. ZP of lipid nanoparticles was also measured in purified water adjusting conductivity (50 $\mu\text{S}/\text{cm}$) with potassium chloride solution (0.1%, weight/volume). The ZP was calculated from the electrophoretic mobility using the Helmholtz–Smoluchowski equation included in the software of the system [19].

3. Result and discussion

SLN produced particles by HSH with size ranging between 1000 nm and 2000 nm, as shown in Fig. 1 (a).

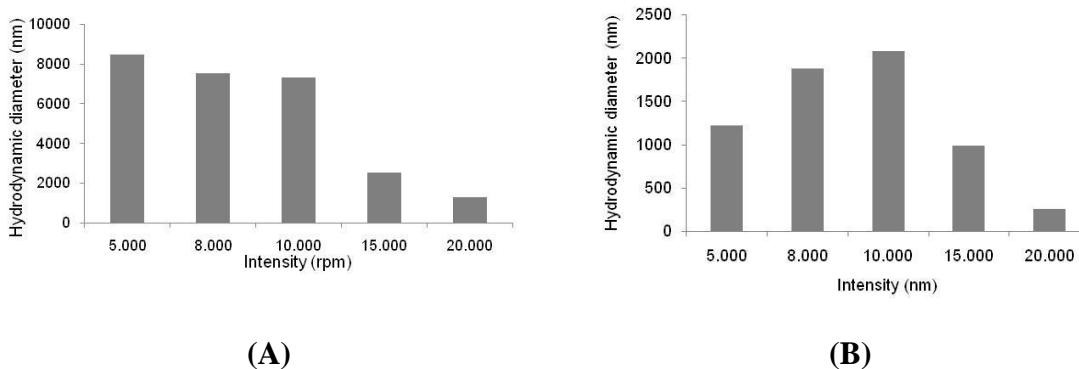


Figure 1. Influence of Ultra-Turrax® intensity on the particle size of the pre-emulsion to produce (A) SLN and (B) NLC.

Fig. 1 (b) shows the NLC results applying 8000 to 10,000 rpm, obtaining particles with size larger (1500 to 2000 nm). When using 5000, 15,000 and 20,000 rpm NLC were smaller. In this case, the PI of the particles was approximately 0.5.

Table 2 shows influence of pressure and number of homogenization cycles used for the production of SLN. Fig. 2 shows surface response charts of experimental design and Fig. 3 Pareto chart of the standardized effects for SLN.

Polynomial equations were generated to establish the relationship between the factors and the mean particle size, PI and ZP. The proposed model was realized by each variable effect and interactions (stirring intensity and pressure). For SLN, PI results were not shown statistically relevant, no model was obtained for this parameter. The p value obtained by stirring intensity was 0.11800, pressure was 0.244161 and interaction was 0.977497. The pressure and interaction were reported to be not significant. The linear model for the particle size and ZP is shown by the following equations:

$$\text{Particle size (nm)} = -8.9750P$$

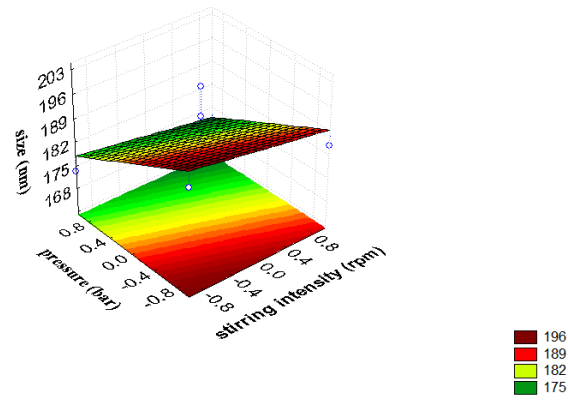
$$\text{Zeta potential (mV)} = 183.8 - 3.2750It + 0.1750It.P$$

where, P is the pressure of HPH and It is intensity of HSH. From the obtained results (mean size of 180 nm and ZP of -53 mV), an optimal SLN formulation may be produced by 20,000 rpm with HSH and 500 bar under HPH.

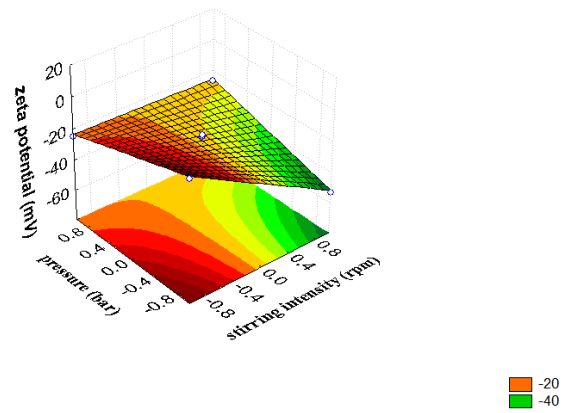
Table 2. Influence of pressure and number of homogenization cycles used for the production of SLN.

Pressure (bar)	Number of cycles	Mean			ZP		
		diameter (nm)	SD	PI	SD	(mV)	SD
500	1	55.20	40.65	0.44	0.03	-29.23	8.41
700	1	83.12	51.33	0.30	0.03	-20.90	4.98
900	1	123.90	107.25	0.39	0.08	-23.97	4.66
500	2	92.41	51.33	0.47	0.20	-12.83	5.42
700	2	124.48	28.33	0.79	0.04	-15.15	15.82
900	2	107.60	50.03	0.69	0.11	-1.60	0.13
500	3	61.51	107.25	0.42	0.14	-22.83	2.02
700	3	67.74	107.25	0.35	0.15	-19.60	0.92
900	3	96.60	29.56	0.75	0.23	-12.60	19.06

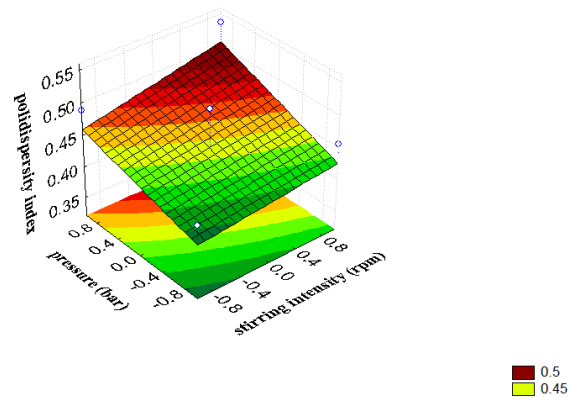
SD: Standard Deviation; PI: Polydispersity Index; ZP: Zeta Potential



A

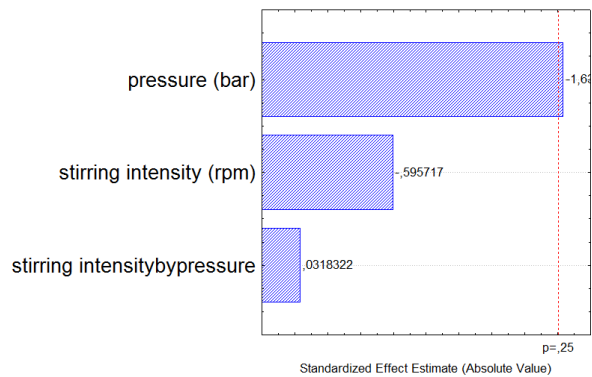


B

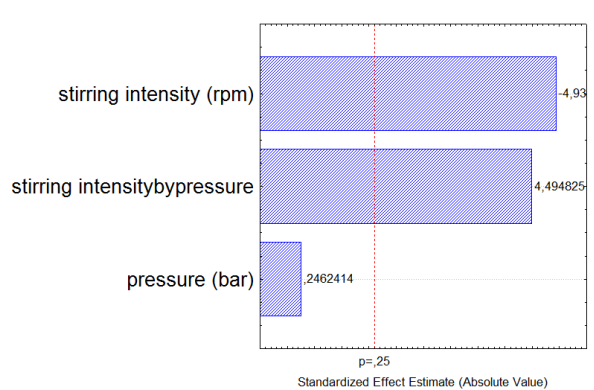


C

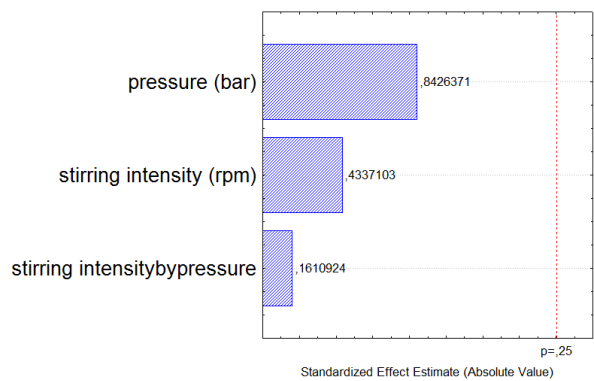
Figure 2. Surface response charts of experimental design SLN (A) particle size; (B) zeta potential; (C) polydispersity index.



A



B



C

Figure 3. Pareto chart of the standardized effects for SLN (A) particle size; (B) zeta potential; (C) polydispersity index.

Table 3 shows the influence of pressure and number of homogenization cycles used for the production of NLC.

Table 3. Influence of pressure and number of homogenization cycles used for the production of NLC.

Pressure (bar)	Number of cycles	Mean diameter (nm)	SD	PI	SD	ZP (mV)	SD
500	1	133.75	50.82	0.43	0.06	-30.10	15.08
700	1	147.24	118.21	0.42	0.10	-20.70	0.90
900	1	76.09	70.18	0.59	0.11	-21.40	1.71
500	2	187.45	118.21	0.51	0.02	-19.87	3.32
700	2	76.95	25.20	0.54	0.01	-19.66	5.24
900	2	81.43	26.02	0.57	0.02	-20.70	3.20
500	3	126.49	70.18	0.55	0.05	-20.60	3.51
700	3	84.13	70.18	0.54	0.02	-15.23	7.54
900	3	124.42	50.95	0.79	0.17	-19.03	0.97

SD: Standard Deviation; PI: Polydispersity Index; ZP: Zeta Potential

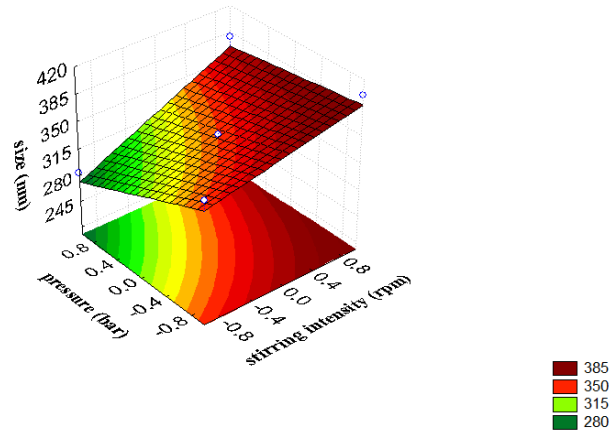
Fig. 4 shows the surface response charts of experimental design and Fig. 5 Pareto chart of the standardized effects for NLC. For the NLC formulation, also polynomial equations were generated to establish the relationship between the factors and the mean particle size, PI and ZP. The p values obtained by stirring intensity were 0.052523, pressure was

0.096310 and interaction was 0.239273. The interaction was reported to be not significant. The proposed model was realized by each variable effect and interactions (stirring intensity and pressure), and the linear models obtained are the following:

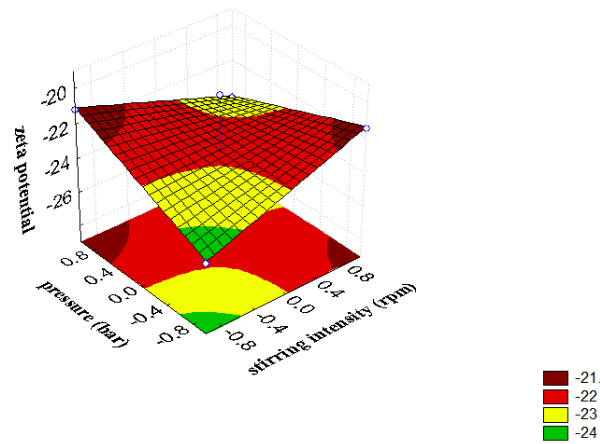
$$\text{Particle size (nm)} = -343.3 + 34.25I_t - 24.4P$$

$$\text{Polydispersity index (IP)} = 343.3 + 34.25I_t - 24.4P + 13.55P$$

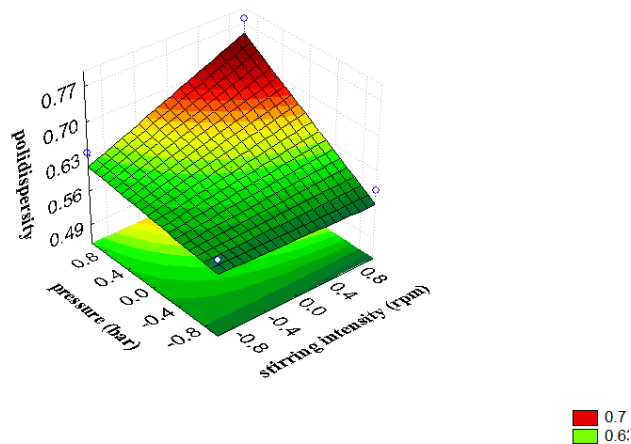
where P is pressure of HPH and I_t is intensity of HSH. From the obtained results, an optimal NLC formulation may be produced by 15,000 rpm HSH and 700 bar HPH pressure because it shows higher stability, ZP (-28 mV) and acceptable PI (0.587).



A

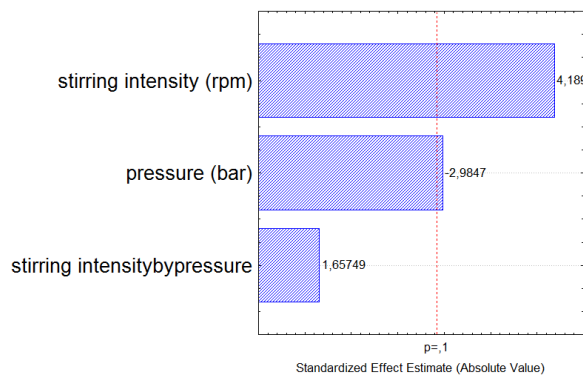


B

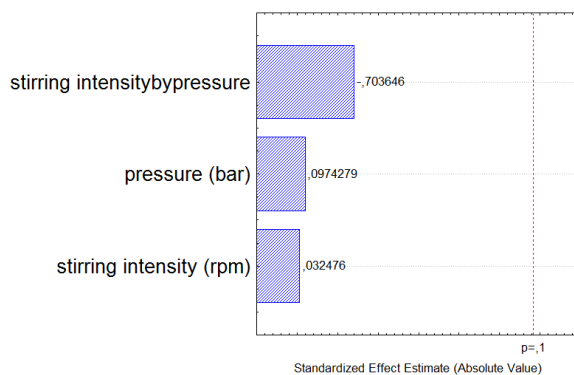


C

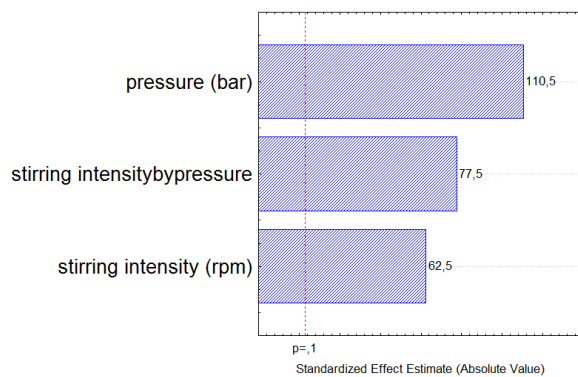
Figure 4. Surface response charts of experimental design NLC (A) particle size; (B) zeta potential; (C) polydispersity index.



A



B



C

Figure 5. Pareto chart of the standardized effects for NLC (A) particle size; (B) zeta potential; (C) polydispersity index.

4. Discussion

In the field of pharmaceutical dosage forms, to design a new formulation it is of paramount importance to identify the influencing parameters, since these might affect the properties of the final dosage form.

The use of experimental designs is nowadays a common method of simultaneously analyzing the influence of different variables on the properties of the drug delivery system being studied [20]. To evaluate the optimum experimental conditions for SLN and NLC production by HSH and HPH for each independent experiment, we have employed a factorial design to assess the influencing factors that are involved in the characteristics of lipid nanoparticles, such as lipid, surfactant, particle size, drug loading, PI and ZP [21,22]. Varshosaz et al. [23] used a fractional factorial design to examine which variables affect the physicochemical properties of amikacin-SLN. Study was continued by a statistical central composite design to minimize particle size and maximize the encapsulation efficiency of the drug in SLN. Three quantitative factors, including the amount of lipid phase, ratio of drug to lipid, and volume of aqueous phase, were reported as the most important variables on the studied responses. The optimized particle size was 149 ± 4 nm and the encapsulation efficiency $88\pm 5\%$. PI was lower than 0.3.

In the present work, the results obtained with HSH showed different properties for SLN and NLC formulations (Fig. 1). A non-hierarchical model was applied since stirring intensity was found not to be statistically significant. For SLN applying higher stirring intensity (20,000 rpm) produced smaller particles, whereas larger particles were obtained at lower intensities (5000, 8000 and 10,000 rpm) with a PI around 0.3. For NLC, a smaller particle size was obtained when using the lowest and highest intensities (5000, 15,000 and 20,000 rpm).

With respect to the ZP (i.e. the electrical charge at the SLN and NLC surface), it reflects the long-term physical stability and the particle adhesive properties. Higher ZP values, either positively or negatively charged, mean that lipid nanoparticles will have greater long-term stability. The electrostatic repulsion between particles with the same electrical charge avoids the occurrence of aggregation [24]. In SLN, increasing intensity of HSH produced particles with lower dispersity of ZP values (0 mV). The ZP values ranged between -24 mV to 0 mV, and showed that the excess of energy promotes lower stability. NLC showed a weak variation from -13 mV to -5 mV. Usually, particle aggregation is less likely to occur for charged particles with pronounced ZP ($>|20|$) due to the electrostatic repulsion between particles with the same electrical charge [25]. Thus, some physical instability of particle dispersions may be anticipated when produced by HSH because of the risk of higher PI, since higher ZP values, being positive or negative, tend to stabilize particle suspensions.

The scaling up process was performed in one step by HPH. This technique minimizes the amount of drug, in case of expensive or limited available drugs, when performing a formulation screening (lipid composition, surfactant type and concentration). Table 2 shows the values of size, ZP and PI for SLN and NLC formulations after 3 cycles in HPH using different pressures. For the SLN formulation, the pressure influenced the size of the particles. Smaller particles were obtained with high pressure, being attributed to the additional energy input leading to higher kinetic energy of the droplets with subsequent disruption. The best size (with a PI ca. 0.30) was obtained with smaller pressures (500 to 700 bar). The ZP observed was practically the same (~ -25 mV) on the number cycle, except in SLN using 2 cycles with 900 bar. HPH is more efficient than HSH in reducing the

size and in producing more stable particles. These results are promising for applications of SLN for encapsulation and controlled release of drugs.

The results are in agreement with the literature [26], where HPH using 500 bar was reported to produce monodispersed particle suspensions, and the increasing number of homogenization cycles could contribute for particle aggregation and higher polydispersity. In the present case, increased pressure up to 1000 bar with a cycle reduced the particle size down to 37 nm. The increasing number of homogenization cycles, while maintaining the same pressure at 1000 bar, caused only a small increase in the diameter. HPH can form small particles with high kinetic energy which can result in aggregation after the homogenization process. ZP values were negative in all cases due to the chemical nature of the lipid used (i.e. stearic acid). Moreover, ZP values were influenced by the homogenization process. In the case of HSH, the absolute value was lower than that obtained with HPH. The HPH processing promotes higher particle stability. As expected, the PI values were also influenced by the type of procedure. Ultra-Turrax® produced a pre-emulsion with high PI (about 0.9) independently on the formulation, while the PI after HPH was lower (around 0.4).

The number of experiments required for a 2-level factorial design is 2^k , where k stands for the total number of analyzed variables. In this case, a total of 7 experiments were performed in each formulations (SLN and NLC), where 2 is the number of analyzed variables. A 2^7 factorial design was developed to provide considerable amount of useful information about the main effects and interactions of the selected variables (Table 1) on mean particle size, PI and ZP.

Results of SLN formulation show the mean particle size of the developed formulations varying between 167 nm and 192 nm, whereas ZP ranged from -50 mV to -1 mV. The

lowest value of PI was 0.347 for 15,000 rpm for HSH and 700 bar for HPH (Fig. 2). At lower levels of intensity and pressure smaller PI was obtained of particles. The average size was reduced with higher HSH intensity and HPH pressure. The results from ZP measurements showed a wide variation in this study. PI was not shown to be significantly influenced by the tested parameters, neither did the interaction between variables ($\text{value} \leq 0.25$) (Fig. 3 (a)).

On the other hand, ZP and the mean particle diameter were influenced by the pressure applied during HPH ($p \geq 0.25$). NLC formulation showed that the mean particle size of the developed formulations varied from 283.8 nm to 401.1 nm, whereas ZP ranged between -28 and -20 mV (Fig. 4). The lowest value of PI was 0.585 for 15,000 rpm of HSH and 700 bar HPH. In this case, particle size, ZP and PI showed only little variation. The results were obtained with 90% confidence. PI and mean particle size were shown to be dependent on the pressure, and stirring intensity ($p \leq 0.1$). Table 3 shows the values of size, PI and ZP with their standard deviations for NLC obtained after 3 cycles in HPH using different pressures. The same results obtained with SLN were also observed in NLC, with respect to the pressure and risk of particle aggregation. The ZP resulting from HPH was higher in absolute value compared to the Ultra-Turrax[®] and to the SLN formulation.

The influence of each independent variable (intensity and pressure) and their interactions on the NLC formulation were also assessed using Pareto charts (Fig. 5). ZP (Fig. 5 (b)) was not significantly dependent on the analyzed variables, but it was influenced by the interaction between both independent variables (stirring intensity and pressure) and the interaction among variables ($p \leq 0.1$).

5. Conclusions

This study reports an approach to use a 2-level 2-factor factorial design in the optimization of SLN and NLC formulations produced by HSH and HPH. The derived polynomial equations and Pareto Charts proved to be satisfactory in predicting the dependent variable values for the preparation of optimum SLN and NLC with desired mean particle size, PI and ZP. Optimal parameters for SLN were obtained using 20,000 rpm HSH and 500 bar HPH pressure and for NLC 15,000 rpm HSH and 700 bar HPH pressure. The present results highlight the benefit of applying statistical designs in the preparation of lipid nanoparticles. The design demonstrated the correlation between various production parameters.

Acknowledgments

The authors wish to acknowledge the sponsorship of the FAPESP (Fundação de Amparo a Pesquisa) and CAPES (Coordenação de Aperfeiçoamento de Pessoal de Nível superior). The authors wish to acknowledge Fundação para a Ciência e Tecnologia do Ministério da Ciência e Tecnologia, under the reference ERA-Eula/0002/2009.

References

- [1] S.A. Galindo-Rodriguez, F. Puel, S. Briancon, E. Allemann, E. Doelker, H. Fessi, Eur. J. Pharm. Sci. 25 (2005) 357–367.
- [2] Y. Gao, R. Yang, Z. Zhang, L. Chen, Z. Sun, Y. Li, Nanotoxicology 5 (2011) 636–649.
- [3] M.K. Rawat, A. Jain, S. Singh, J. Pharm. Sci. 100 (2011) 2366–2378.
- [4] S. Xie, L. Zhu, Z. Dong, X. Wang, Y. Wang, X. Li, W. Zhou, Colloids Surf., B 83 (2011)

382–387.

[5] V.V. Kumar, D. Chandrasekar, S. Ramakrishna, V. Kishan, Y.M. Rao, P.V. Diwan, *Int. J. Pharm.* 335 (2007) 167–175.

[6] J. Pardeike, A. Hommoss, R.H. Muller, *Int. J. Pharm.* 366 (2009) 170–184.

[7] E.B. Souto, R.H. Muller, *Handb. Exp. Pharmacol.* (2010) 115–141.

[8] M.L. Bondi, E.F. Craparo, G. Giammona, F. Drago, *Nanomedicine (Lond)* 5 (2010) 25–32.

[9] E.B. Souto, R.H. Muller, *J. Microencapsul.* 23 (2006) 377–388.

[10] H. Ali, A.B. Shirode, P.W. Sylvester, S. Nazzal, *Colloids Surf., A* 353 (2009) 43–51.

[11] S.A. Wissing, O. Kayser, R.H. Muller, *Adv. Drug Deliv. Rev.* 56 (2004) 1257–1272.

[12] R. Shegokar, K.K. Singh, R.H. Muller, *Int. J. Pharm.* 416 (2011) 461–470.

[13] W. Mehnert, K. Mader, *Adv. Drug Deliv. Rev.* 47 (2001) 165–196.

[14] R. Becker, B. Kruss, R.H. Muller, K. Peters, *Patent, U. S., Ed.: Hamburg, DE, 1997.*

[15] M. Muchow, P. Maincent, R.H. Müller, *Drug Dev. Ind. Pharm.* 34 (2008) 1394–1405.

[16] A. Lippacher, R.H. Muller, K. Mader, *Int. J. Pharm.* 214 (2001) 9–12.

[17] P. Severino, S.C. Pinho, E.B. Souto, M.H. Santana, *Colloids Surf., B* 86 (2011) 125–130.

[18] D.M. Luykx, R.J. Peters, S.M. van Ruth, H. Bouwmeester, *J. Agric. Food Chem.* 56 (2008) 8231–8247.

[19] S.R. Deshiikan, K.D. Papadopoulos, *Colloid Polym. Sci.* 276 (1998) 117–124.

[20] J. Araujo, E. Gonzalez-Mira, M.A. Egea, M.L. Garcia, E.B. Souto, *Int. J. Pharm.* 393 (2010) 167–175.

[21] G. Abdelbary, R.H. Fahmy, *AAPS PharmSciTech* 10 (2009) 211–219.

- [22] J. Varshosaz, M. Minayian, E. Moazen, J. Liposome Res. 20 (2010) 115–123.
- [23] J. Varshosaz, S.Ghaffari, M.R. Khoshayand, F. Atyabi, S. Azarmi, F. Kobarfard, J. Liposome Res. 20 (2010) 97–104.
- [24] S. Feng, G. Huang, J. Control. Release 71 (2001) 53–69.
- [25] E.B. Souto, S.A. Wissing, C.M. Barbosa, R.H. Müller, Eur. J. Pharm. Biopharm. 58 (2005) 83–90.
- [26] J. Liu, W. Hu, H. Chen, Q. Ni, H. Xu, X. Yang, Int. J. Pharm. 328 (2007) 191–195.

Capítulo 3

Development potential solid lipid nanoparticles carrier for proteins

Patrícia Severino^{1,2}, Tatiana Andreani^{2,4}, Alessandro Jäger³, Amélia M. Silva^{4,5}, Eliana B. Souto^{2,4}, Maria Helena A. Santana¹

¹School of Chemical Engineering, University of Campinas, UNICAMP, Campinas, São Paulo, Brazil.

²Health Sciences, Fernando Pessoa University, Rua Carlos da Maia, Porto, Portugal.

³Institute of Macromolecular Chemistry, Academy of Sciences of the Czech Republic, v.v.i., Heyrovsky Sq. 2, 162 06, Prague, Czech Republic.

⁴Department of Biology and Environment, University of Trás-os-Montes e Alto Douro, P.O. Box 1013, 5000-911 Vila Real, Portugal

⁵Centre for Research and Technology of Agro-Environmental and Biological Sciences, Vila Real, Portugal

Article in submission

Abstract

Insulin was used to as the hydrophilic model protein to developed novel solid lipid nanoparticles (SLN). It was prepared by double emulsion (w/o/w) the purpose to improve bioavailability and protect degradation of protein. Softisan[®] 100 was selected as lipid material due low melting point evicting degradation of protein in production. The surfactants (Tween[®] 80, Span[®] 80 and Lipoid[®] S75) were chosen by theoretical calculations, therefore it was studied the influence of the surfactant of ratio Span[®]80/Lipoid[®]S75 and efficiency of encapsulation (EE) of insulin on the SLN by 2² factorial design with triplicate of central point. The dependents variables evaluated were size, polydispersity index (PI), zeta potential (ZP), EE. SLN was evaluated by effect of toxicity in cells HEPG-2 and Caco-2, stability *in vitro* and shape by SEM. In addition, matrix lipid was evaluated by Differential Scanning Calorimetry (DSC) and Wide Angle X-ray Diffraction (WAXD). Results showed particle size width 294.6 nm to 627.0, PI 0.425 to 0.750, ZP was about -3 mV, and EE was 38.39 % to 81.20 %. Studies of DSC and WAXD showed less ordered structures of crystals were formed in SLN. SLN was more compatible in Caco-3 than HepG-2 cells and citotoxicity was dependent of concentration. The morphological structure was spherical. The colloidal carrier development in this report is promising to vehicle label and hydrophilic drugs in all routes of administration.

Keywords: solid lipid nanoparticles, double emulsion method, protein, citotoxicity.

1. Introduction

Proteins, monoclonal antibodies and hormones development by biotechnology has increasing for treatment diseases. In 2011, according Pharmaceutical Research and Manufacturers Association 901 medicines and vaccines were development for more than 100 diseases (1). These actives have great potential for pharmaceutical therapy; however environmental factors may cause physicochemical instability, damage of structure, decrease biological action, decrease half life and variable bioavailability (2).

Nanotechnology as a promising strategy for labels drugs in different routes of administration for medicine. Solid lipid nanoparticle (3), polymeric nanoparticle (4), and liposome (5) are examples of particles for drug delivery of label drugs and promoting their stability in pharmaceutical formulation. Solid lipid nanoparticles are attractive colloidal system, composed by biodegradable and biocompatibility excipients (6, 7) that promoting stability of drug (8), controlled release profile (9), improve bioavailability (10), easy scale up (11) and evicting use organic solvents (12).

In this work was produced SLN by double emulsion method, studying the concentration of surfactant and protein model, insulin, delineating the region of study of a 2^2 factorial design with triplicate at the central point for analysis of the combined effect the serial processing, the properties of the particles (size, polydispersity index (PI), zeta potential (ZP) and efficiency encapsulation (EE)). The study was completed with the thermal analysis by Differential Scanning Calorimetry (DSC), Wide Angle X-Ray Diffraction (WAXD), the effect of toxicity in cells HepG-2 and Caco-3, *in vitro* stability and Transmission Electron Microscope.

2. Material e methods

2.1. Material

Glycerides of hydrogenated coconut (Softisan[®] 100) was gift by Sasol. Polysorbate 80 (Tween[®] 80) and Coomassie blue were obtained by Sigma. Mono/oleate sorbitan oleate (Span[®] 80) was donated by Croda, soya lecitin hydrogenated (Lipoid[®] S75) were donated as a gift from Lipoid; insulin (Humalog[®] mix 25) was purchased by Libbs. Penicillin, streptomycin, L-glutamine, hank's balanced salt solution HBSS were purchased by Gibco. Alamar blue[®] was obtained by Invitrogen. Double distilled water was used after filtration in a Millipore system (home supplied).

2.2. Methods

2.2.1. SLN preparation

The method double emulsion (w/o/w) was chosen to avoid high temperatures and high shear energy that may degrade the protein. The model protein used was insulin. To produced, the internal aqueous phase (IP) was composed by insulin and water in pH = 5.4. The lipid phase (LP) was composed by 500 mg Softisan[®] 100, 5 mL glycerol, Span[®] 80/ Lipoid[®] S75.

IP and LP were heated, separately, 10 °C above the lipid phase transition. The IP was added in LP and homogenized with high shear homogenization (Ultra-Turrax[®], IKA, T25, German) for 10 minutes, intensity of 10,000 rpm and maintaining heating. The external aqueous phase (EP) cooled (0.25 g Tween[®] 80 and 40 mL water) was added in emulsion (w/o) previously formed. It was maintained by high shear homogenization for 2 minutes at

10,000 rpm. Then, it was transferred to magnetic stirring (Tecnal, TE-0851, Brazil), and added to another part of the EP and kept in agitation and cooled for 20 minutes.

2.2.2. Factorial design

The influence of surfactants on the properties of double emulsion has been studied by theoretical calculations, Hydrophilic Lipophilic Balance (HLB), and from the data obtained was used in the development of the formulation (13). Then, HLB was calculated from Equation 1.

$$HLB = \frac{HLB(I) \times \frac{\Phi\left(\frac{a}{o}\right)}{a} \times wt\%(I) + HLB(II) \times wt\%(II)}{\frac{\Phi\left(\frac{a}{o}\right)}{a} \times wt\%(I) + wt\%(II)} \quad \text{Equation 1}$$

where HLB(I) is the HLB value of the internal emulsifier used for the primary w/o emulsion, $\phi(w/o)/w$ is the w/o fraction in the multiple emulsion, wt%(I) is the per cent by weight of emulsifier I in the w/o emulsion, HLB(II) is the HLB value of emulsifier II and wt% (II) is the per cent by weight of emulsifier II in the multiple emulsion (13).

The influence of the surfactant of ratio Span[®] 80/Lipoid[®] S75 and EE of insulin on the SLN was evaluated using a 2² factorial design with triplicate of central point for estimating the experimental error, composed of 2 variables which were set at 2-levels each.

The mean particle size, PI, ZP and EE were the dependent variables. The design required a total of 7 experiments. Each factor, the lower and higher values of the lower and upper levels, were represented by a (-1) and a (+1) and the central point was represents by (0) as summarized in Table 1. These were chosen on the basis of the tested lower and upper values for each variable according to pre-formulation studies and literature research. The data were analyzed using Statistic 7.0.

Table 1. Factorial design 2² with triplicate of central point.

Variables	Level		
	(-1)	(0)	(+1)
Span [®] 80/ Lipoid [®] S75	1:1	2:1	3:1
Insulin	1.75 mg	3.5 mg	5.25 mg

2.2.3. Particle size, polydispersity index, and zeta potential analysis

The sample was evaluated with respect to the hydrodynamic mean size, PI, and ZP. The mean size was determined by Dynamic Light Scattering (DLS; Zetasizer Nano NS, Malvern, UK). The samples were diluted with ultra purified water to weaken the opalescence before particle size measurements. ZP was analyzed in NaCl 0.9 % adjusting conductivity to 50 µS/cm. The ZP was calculated from the electrophoretic mobility using the Helmholtz–Smoluchowski equation. The analysis was performed using the software included in the system.

2.2.4. Encapsulation efficiency (EE)

The protein encapsulated into SLN was dosed by the method of Bradford, adapted by Robyt e White, 1990 (14). The preparation of the calibration curve consisted in aqueous solution of albumin at a concentration of 0.001 g/mL and an aqueous solution of Coomassie blue at a concentration of 0.1 g/mL. The reading was held in spectrophotometer at a

wavelength of 595 nm. The calibration curve was performed with concentrations of 0, 10, 15, 20, 25, 30, 40, 50, 70, 90, 110, 140, 170, 200, 230, 270, 310, 350, 400, 400, 450, 500, 600 mg/mL. To determine the EE of SLN samples were ultra filtration (Amicon, Beverly, USA) using ultrafiltration membranes (Millipore, NMWL 30,000, Billerica, USA) and 500 uL of the supernatant was added to a solution of Coomassie blue, followed by agitation. Then EE was calculated from Equation 2.

$$EE (\%) = \frac{(\text{total of protein IP}) - (\text{total of protein supernatant})}{(\text{total of protein IP})} \times 100 \quad \text{Equation 2}$$

2.2.5. *Differential Scanning Calorimetry (DSC)*

Thermal behavior of lipid matrice (softisan[®] 100 after and before tempering process) (6, 7) and SLN empty and loading insulin were assessed by DSC (NETZSCH DSC 200 F3 Maia, USA). A volume of sample containing approximately 5 - 10 mg of sample mass was weighed in an aluminium pan and sealed hermetically, under inert atmosphere (N₂). The analysis was performed at a heating and cooling rate of 5 K/min, using an empty pan as reference. The samples were heated up from 10 to 100 °C, following cooling down to 10 °C.

2.2.6. *Wide Angle X-ray Diffraction (WAXD)*

To study the polymorphism and crystalline properties of softisan[®] 100 matrice (after and before tempering) and empty SLN (6, 7). WAXD was carried out in a diffractometer X-Ray (Philips, model X'pert, Pennsylvania, USA), using copper anode which delivered X-ray of wavelength, $\lambda = 0.154056$ nm. WAXD measurements were taken from 5° to 33° in 0.015°

steps (1s per step). The interlayer spacings were calculated from the reflections using Bragg's equation:

$$d = \frac{\lambda}{\text{sen}2\theta} \quad \text{Equation 3}$$

where λ is the wavelength of the incident X-ray beam and θ is the scattering angle. The parameter d , otherwise called the interlayer spacing, is the separation between a particular set of planes of the crystal lattice structure. Data of the scattered radiation were recorded with a blend local sensible detector using an anode voltage of 40 kV, a current of 25 mA and a scan rate of 0.5° per minute. The samples were mounted on a thin glass capillary being fastened to a brass pin without any previous sample treatment.

2.2.7. Citotoxicity essay HepG-2 and Caco-3 cells

The biocompatibility of SLN formulation could be assessed performing the alamar blue[®] assay (15). Alamar blue[®] (resazurin) is a sensitive oxidation-reduction indicator, after cells reduction it fluoresces and changes color. The reduction is mediated by mitochondrial enzymes (16, 17). Firstly, cell culture HepG-2 and Caco-3 was produced separately in flasks. Each culture was added complete medium containing 2 mL penicillin and streptomycin, 1 ml L-glutamine, 87 mL DMEM and fetal bovine serum and incubated at 37 °C for one week. Then, the supernatants were removed and added 1 mL of trypsin, maintained at 37 °C for 10 minutes in order to disaggregate and spread cells, followed by addition of 2 ml of complete medium and homogenized. After, subculture was performed on cell counts of Neubauer camera. After this time, each well was added 100 mL of cells being $5 \cdot 10^3$ cells/well and waited 24 hours. Then removed the complete medium and added 100 μ L of SLN in 4 different dilutions (1 %, 2 %, 5 % and 10 % SLN solubilized in

medium without serum), in each well and incubated for 24 hours. After 36 hours was added 100 mL, in each well, alamar Blue[®] and incubated for 4 hours, then held a reading in a microplate reader (Multiskan EX, Labsystems) at wavelengths 570 nm and 620 nm. New readings took place after 4, 5 and 7 days of exposure.

2.2.8. *In vitro* Stability

Dynamic light scattering experiments (DSL) were performed using an ALV-setup with an ALV-6000 correlator in the cross-correlation mode detector and a 30 mW He-Ne laser with wavelength $\lambda = 632$ nm. The correlation functions were analyzed by numerical inverse Laplace transformation using the REPES program (18), which calculates the distribution of relaxation times, $A(\tau)$, from the measured intensity autocorrelation function, $g^2(t)$. From the centers of gravity of the peaks in $A(\tau)$, the diffusion coefficient D is obtained using $D = \frac{\Gamma}{q^2}$

where Γ is the relaxation rate ($\Gamma = \tau^{-1}$) and q the modulus of the scattering vector at angle θ , given by $q = 4\pi n \sin(\theta/2)/\lambda$, with n the refractive index of the sample and λ the wavelength of the laser light in vacuum. The hydrodynamic radius, R_H , is calculated (19, 20) using the Stokes-Einstein equation (Equation 4).

$$R_H = \frac{k_B T}{6\pi\eta D} \quad \text{Equation 4}$$

where k_B is Boltzmann's constant, T the absolute temperature, and η the temperature-dependent viscosity of water included in the Repes program used for analysis. The stability of the SLN was monitored after placing them in contact with human serum albumin (HSA) solution. Typically, $6.25 \mu\text{g.mL}^{-1}$ of the SLN was placed in contact with the model blood

plasma protein HSA at concentration of $45 \text{ mg}\cdot\text{mL}^{-1}$ in PBS. The dynamic light scattering experiments were performed periodically up to 24 h in order to monitor the stability of the system (especially the size and distribution of the SLN).

2.2.9. Transmission Electron Microscope (TEM) analysis

The morphology of SLN cationic was performed using a Transmission Electron Microscope (LEO 906 E, Leo Electron). SLN was placed on a copper grid, and then a drop of 1 % uranyl acetate was added and dry for observation.

2.2.10. Scanning electron microscopy (SEM) analysis

In order to verify the result of TEM, SLN empty was cooled with liquid nitrogen (N_2) and lyophilized (Liobras, L101, Brazil) for 48 hours. After that, SLN was gold coated and analyzed by SEM (LEO, LEO 440i).

3.0 Results and discussion

The compatibility of ingredients of emulsion and optimum HLB is essential to obtain stable formulation. The double emulsion HLB is the sum of HLB values all surfactants. It is not feasible to choose surfactant for double emulsion using HLB values for the lipid phase because it is adding lipophilic surfactant in oil phase. To produce stable SLN by double emulsion, lipophilic surfactant (Span[®] 80) migrates to external surface (o/w) and joining with hydrophilic surfactant (Lipoid[®] S75 and Tween[®] 80) resulting droplets (13, 21). Lecithin is important to maintain stable formulation, forming particles with smaller sizes, favorable penetration in skin applications and help drugs to into cells (22). Span[®] 80 and

Tween[®] 80 are widely employed in pharmaceutical formulations. Span[®] 80, Tween[®] 80 and lecithin have HLB 4.3, 15 and range 4 to 8, respectively. The sum HLB (Equation 1) obtained was 7.9, according Frenkel et al., 1983 (23) is possible forming stable double emulsion with HLB < 10 because is not occur phase inversion in w/o emulsion.

In this study evaluated particle size, ZP, PI and EE obtained with design factorial, the statically analyses were obtained using 95 % confidence, according Table 2. Results showed particle size width 294.6 nm to 627.0 nm, PI was 0.425 to 0.750. ZP obtained was about -3 mV, and EE was 38.39 % to 81.20 %.

Table 2. Results of design factorial for SLN loading insulin.

Essay/ Factor	1	2	Size (nm)	PI	ZP (mV)	EE (%)
1	-1	-1	389.4	0.636	-3.85	38.39
2	+1	-1	367.2	0.578	-3.56	40.60
3	-1	+1	627.0	0.750	-3.57	76.96
4	+1	+1	294.6	0.455	-3.55	81.20
5	0	0	389.2	0.425	-3.44	65.01
6	0	0	375.6	0.577	-3.01	63.66
7	0	0	464.0	0.492	-3.56	70.31

Figure 1 represents Pareto charts, observing that surfactant ratio and interaction surfactant ratio and insulin were significant in relation size (Figure 1 a). Surfactant ratio, amount of insulin and interaction were not significant for PI and ZP (Figure 1b e 1 c). Therefore, amount of insulin was significant for EE (Figure 1d).

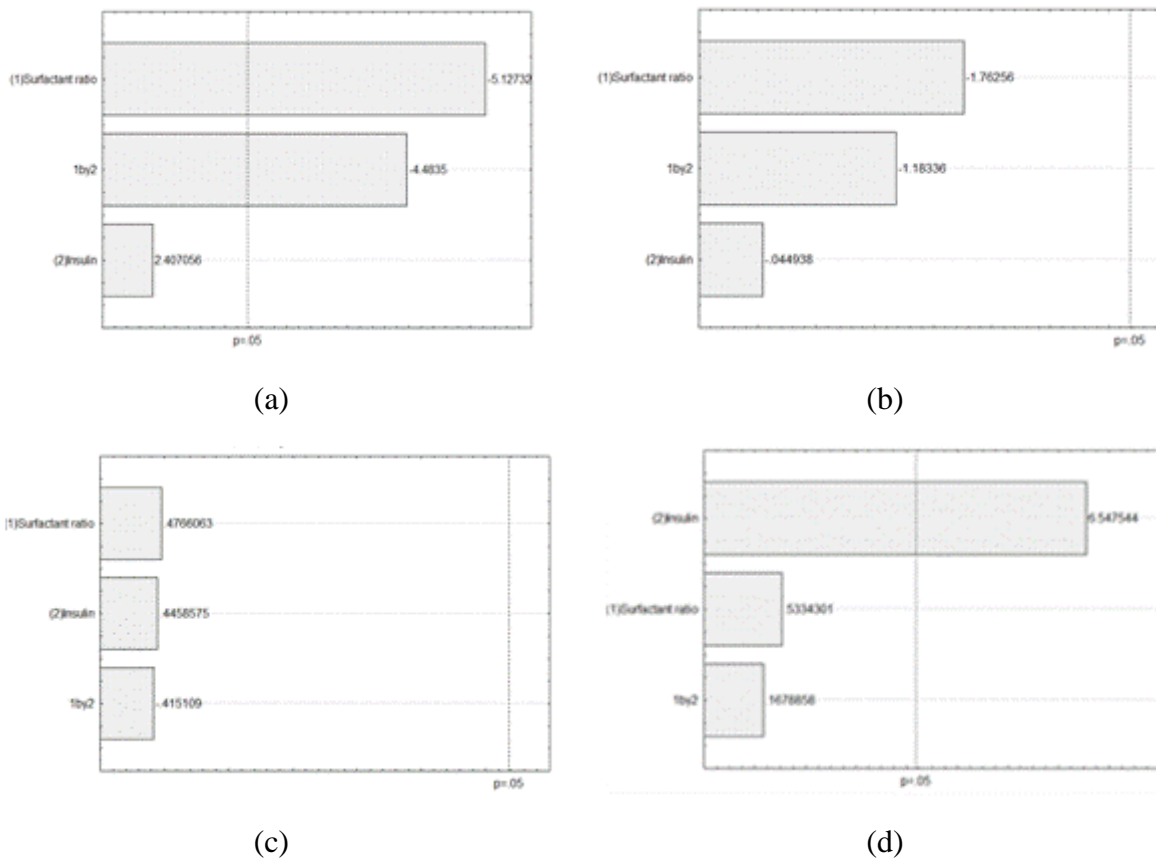


Figure 1. Pareto chart of the standardized effects for SLN (a) size, (b) polidispersity index, (c) zeta potential, (e) encapsulation efficiency.

Figure 2 shows surface response charts of experimental design of the standardized effects size, PI, ZP and EE for SLN. Observing that decrease amount of surfactant ratio was obtained higher values of size of SLN. The same results were obtained about PI. ZP showed little variation (-3.5 mV to -3.7 mV). EE was lower using little amount of insulin.

It was expected that ZP stay near to 0 mV because the lipid and surfactants used to development formulation no have charge. ZP shows the physical stability the formulation over time and adhesiveness properties. It is know that higher ZP (>|20|) avoid aggregation. Additionally, formulation development in central point of factorial design was added 0.4 % DOTTAP in EP, the results of size, PI, EE, ZP were 330.5 ± 1.935 nm, 0.277 ± 0.022 and

66.65 % \pm 2.54, 22.00 \pm 2.56 mV, respectively. DOTAP was favorable to promoting physical stability and potential carrier for protein therapy.

Yang et al., 2011 (24) produced gel-core-solid lipid nanoparticle (SLN) by double emulsion loading insulin as model protein. And, the researches obtained similar results in relation EE, about 57.36%. Suggesting SLN could be a promising drug delivery system.

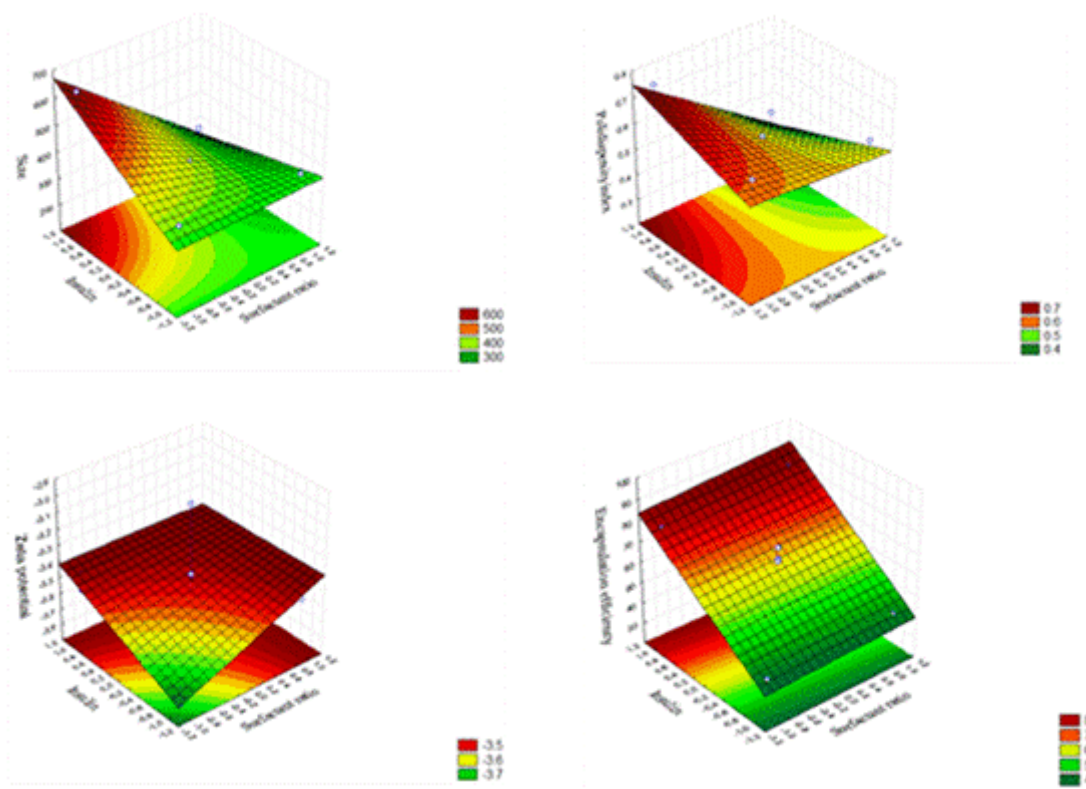


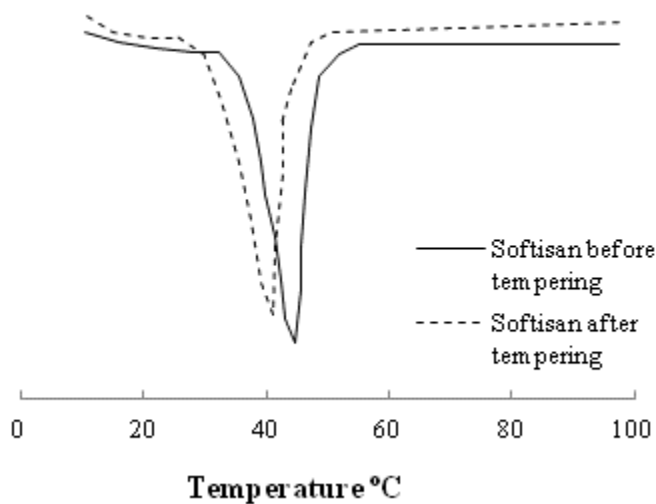
Figure 2. Surface response charts of experimental design of SLN.

Lipids show crystalline characteristics. Cooling (recrystallization) and heating (fusion) cause transitions in polymorphism estate (6, 7). For structural characterization is a used DSC and WAXD analysis. These techniques are complementary (25). Tempering treatment is important to predict thermal characteristics of lipids (6, 7). In SLN, the crystalline forms influence in stability and EE.

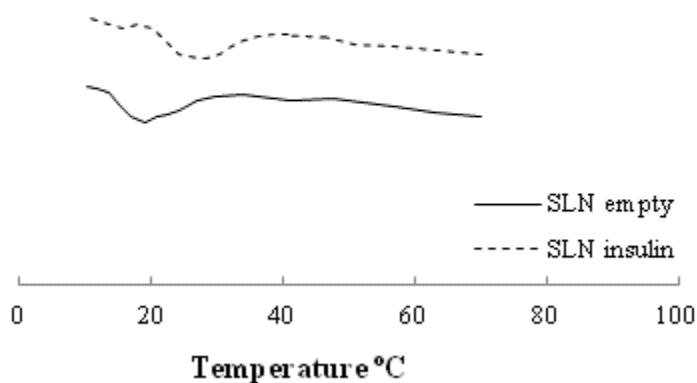
Figure 3 (a) shows the thermogram obtained with Softisan[®] 100 before and after tempering. Before tempering occur fusion the lipid in 42.4 °C and effect of heat 103 J/g, the onset temperature was 36.1 °C and endset was 48.4 °C. After tempering was obtained fusion temperature 39.1 °C and effect of heat of 105 J/g, that started in 30.4 °C and finished in 43.5 °C. The melting event occurs between differences the melting and the onset temperatures. The difference obtained was 6.3 °C before tempering and 8.7 °C after tempering, the thermal treatment increase crystal disorder. Figure 3 (b) shows the result of the thermogram SLN empty. In curve heating is an endothermic peak observable in onset temperature 26.7 °C and effect of heat of 0.78 J/g, being located at a temperature of 30.4 °C, this effect also extends to 36.6 °C, temperature endset. In cooled no effect was observed.

Figure 3 (b) represents the thermogram of SLN loading insulin. For this sample it is possible to verify the effect of protein denaturation, endotherm beginning at a temperature of 25.6 °C with enthalpy of 0.89 J/g. This effect has two temperature peaks at 30.1 °C and 32 °C. It was not observable any significant effect in cooling curve in all samples. Observing that enthalpy is lower in SLN that bulk lipid, it can be explained the interaction between lipid and surfactants or the large of surface of SLN (25, 26).

Results indicate that the crystal structure of Softisan[®] 100 was changed by SLN preparation, acquiring less ordered structure. Similar results were obtained by Shi et al., 2012 (27) and Severino et al., 2011 (28)



(a)



(b)

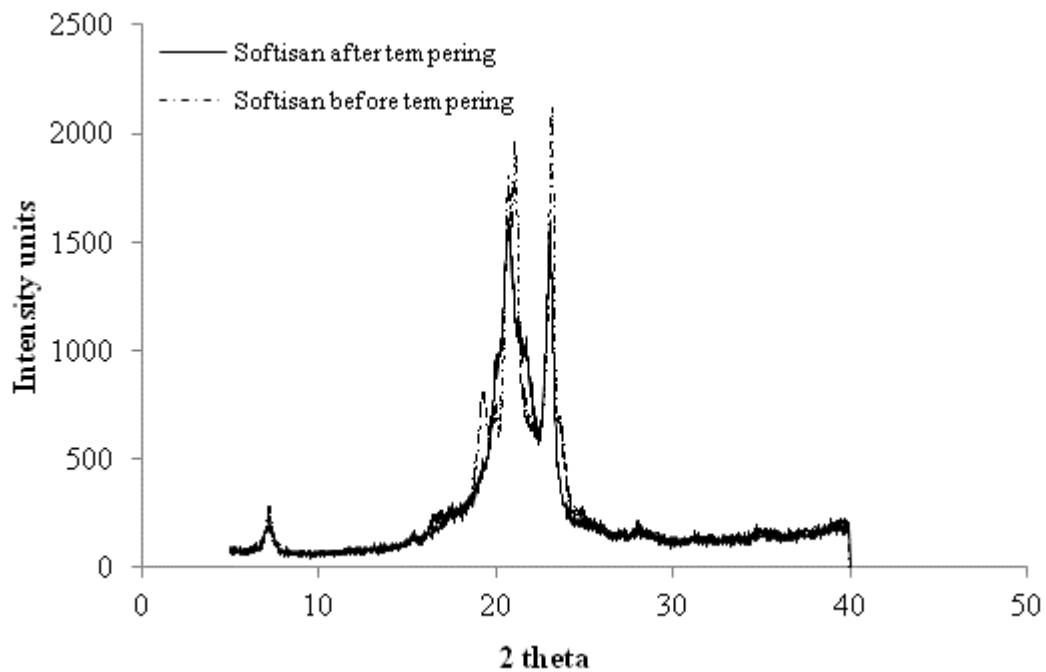
Figura 3. DSC thermograms (a) Softisan before and after tempering; (b) SLN empty and loading insulin.

WAXD is used to study the crystallinity of the of lipid molecules. Softisan[®] 100 is blend of triglyceride (C10-C18). For triglycerides lines around 15 - 25° (2 θ) are denominated “short spacing” and corresponding distances between carbon chains of fatty acids. Triglycerides crystallize in four polymorphics forms called sub- α , α , β' e β . Characterizing thermal stability and carbon chain packing (29). WAXD diffraction studies of Softisan[®] 100 after

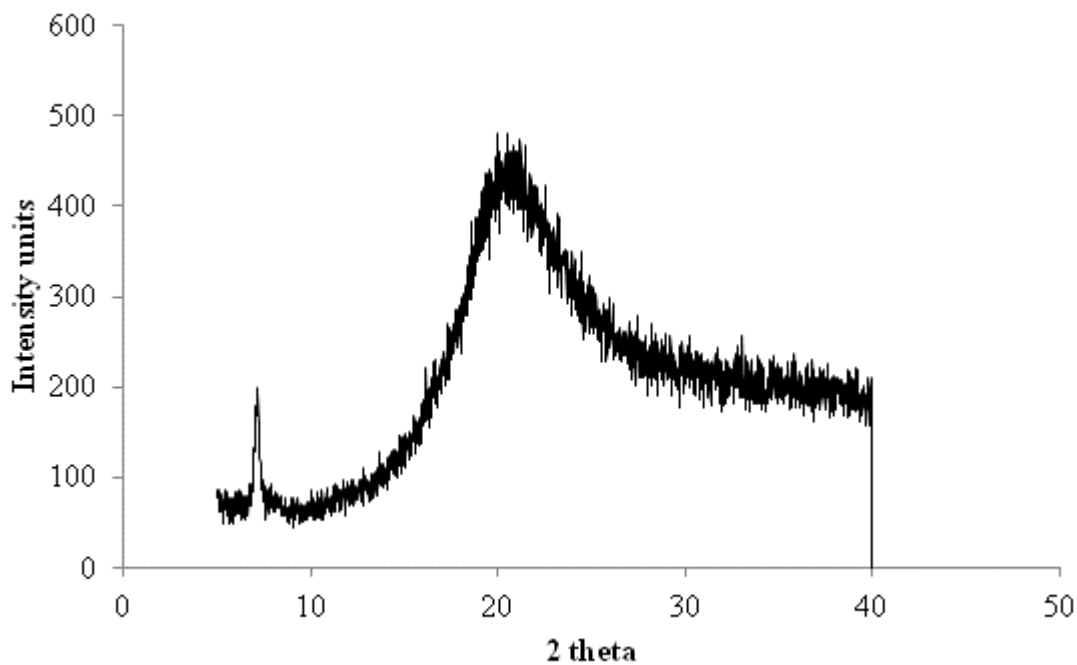
and before tempering show peaks 20.66 (2θ) and 23.33 (2θ), Figure 4 (a). Before thermal treatment decrease intensity of peaks, indicating lower cristallinity. Figure 4(b) shows difratogram of SLN, observing changes sharp peaks compared bulk material. The intensity of peaks decreases forming one peak, indicating amorphous characteristic of SLN.

Results of DSC and WAXD analyses showed that before tempering, increase melting temperature and decrease peak WAXD intensity. Obtained structure less organized that favorable stability of storage and EE. Severino et al., 2011 (7), Jia et al., 2012 (30), Silva et al., 2011 (26) studying lipid cristallinity to produce SLN and obtained similar results with different lipids.

Tests of cell viability were carried out with the empty SLN containing 11.90 mg lipid/mL water. In these cellular assays alamar blue[®] was employment as a marker, samples were blue when oxidized and it is rose when reduced. The blue color indicates cells died, and rose color cell viability. In cell count was obtained 55.104 cell/ml HepG-2 and to Caco-3 was 155.104 cells/mL. Figure 5 shows the results of cell growth obtained with cells in Caco-3 (Figure 5 a) and cells HepG-2 (Figure 5 b) showed that increasing the concentration of SLN is reduced cell growth. Since cell growth was lower in HepG-2 cells compared with Caco-3.

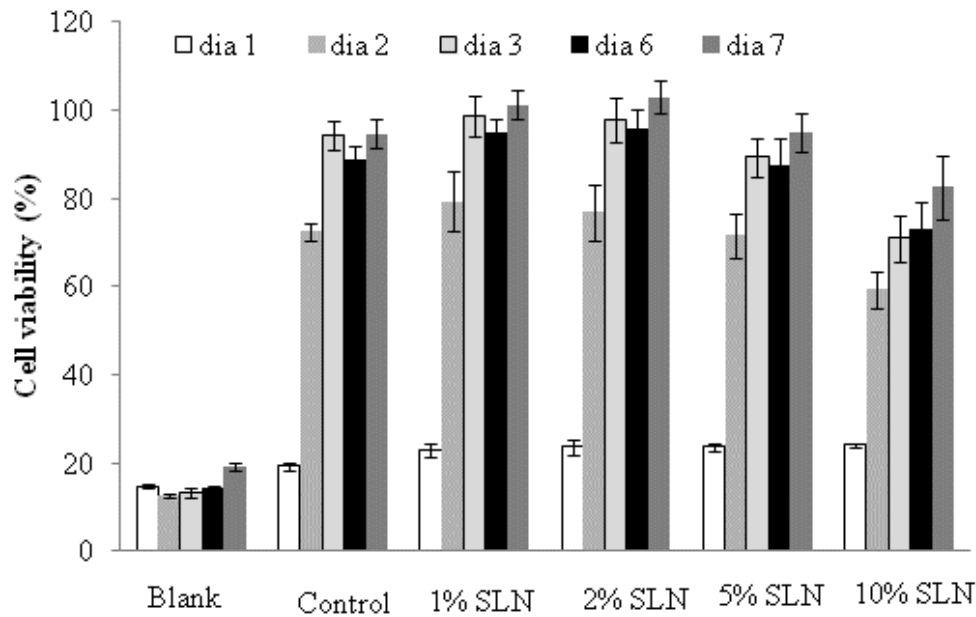


(a)

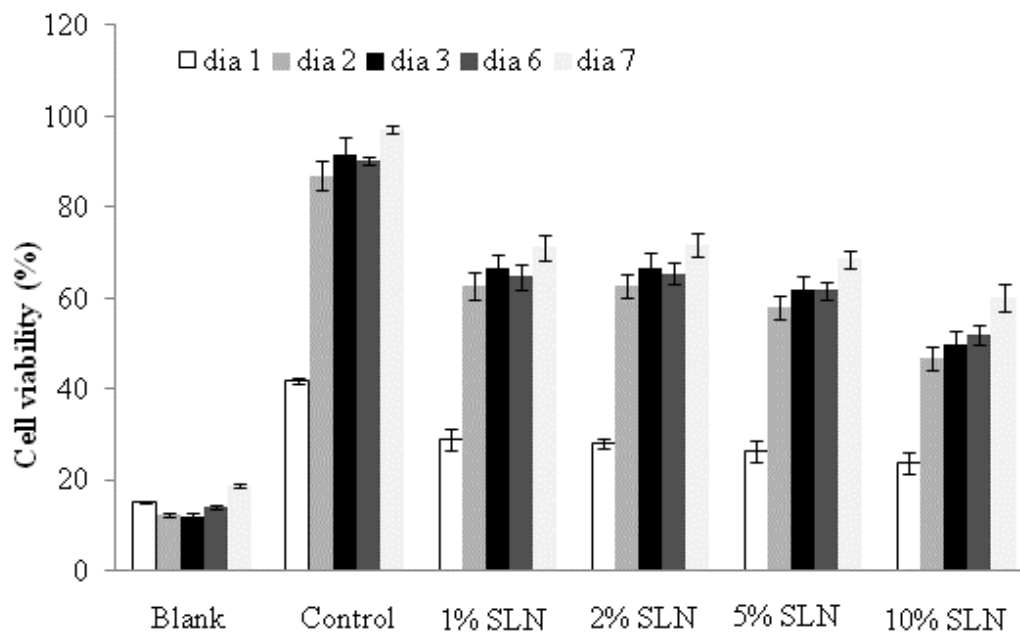


(b)

Figure 4. WAXD diffractogram (a) Softisan[®] 100 before and after tempering, (b) WAXD diffractogram SLN.



(a)



(b)

Figure 5. Cell viability determined by alamar blue[®] assay, after exposition to blank and SLN formulations (concentration 1%, 2%, 5% and 10%) prepared by double emulsion technique. (a) Caco-3 e (b) HepG-2. The results are average values (n=3), compared blank and control cells (unexposed to SLN).

These results suggest SLN was more compatible with Caco-3, indicating tolerance in gastrointestinal tract. Similar have been related by Silva et al., 2011 (26), Xu et al., 2009 (31), Müller et al., 1997 (32), Tabatt et al., 2004 (33) using cells essays to study biocompatibility SLN, indicating efficient colloidal system for drug delivery.

The serum albumins are of particular interest for their ability to anchor both hydrophilic and hydrophobic surfaces and participate in a cascade of protein adhesion at surfaces presented (34). Therefore nanoparticles stability in the serum is a criterion for their usefulness as drug carrier *in vivo* (35-37). The stability of the SLN was monitored when in contact with the model protein HSA in PBS (up to 24 h). The experiments were performed in the presence of 45 mg.mL⁻¹ of HSA which is nearly the amount found in the blood plasma. These experiments were performed by monitoring the system in contact with dynamic light scattering over time. The dynamic light scattering results are given in Figure 7. The DLS experiments revealed that the SLN are stable for up to 24 h in the presence of HSA since no NP aggregates where detected. However, regardless the NLS stability during the experiment the hydrodynamic radius (R_h) increases from 86 nm to 105 nm in 24h (Figure 8) clearly demonstrates the increase in HSA adsorption in the nanoparticle surface in time. Since our SLN particles surface coverage consisting of the hydrophilic polysorbate and previously experiments with human plasma showed protein fouling process in this surfaces the HSA adsorption can not be avoided (38). Finally, in the Figure 6 one may notice the development of a small amount of large aggregates after 24 hours. This was experimentally evidenced to be related to the aggregation of protein molecules themselves rather than the nanoparticles since the same behavior was observed at nanoparticle-free HSA solutions (not shown here).

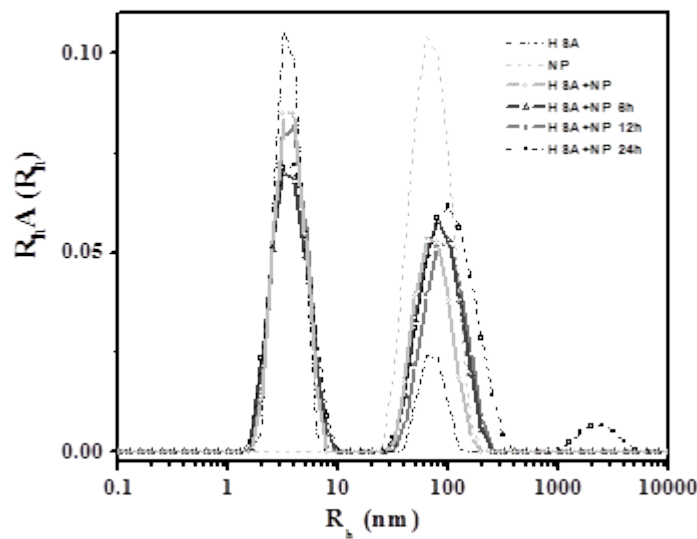


Figure 6. Distribution of R_h for SLN ($6.25 \mu\text{g.mL}^{-1}$) in presence of 45 mg.mL^{-1} HSA dissolved in PBS at various times during 24 hours.

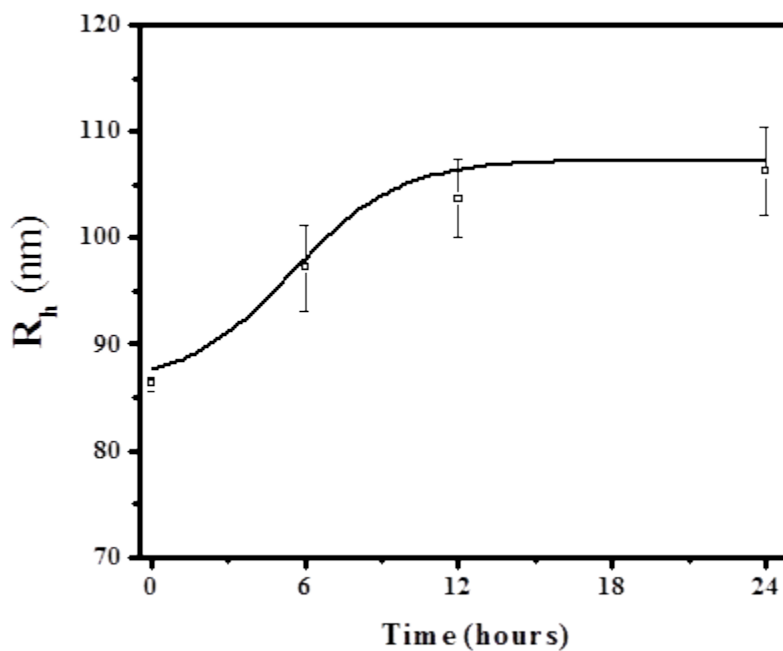


Figure 7. R_h vs. time of the SLN in presence of 45 mg.mL^{-1} HSA dissolved in PBS. Microscopy images analyzed by TEM and SEM of empty SLN are presented in Figure 8. SLN showed spherical morphology.

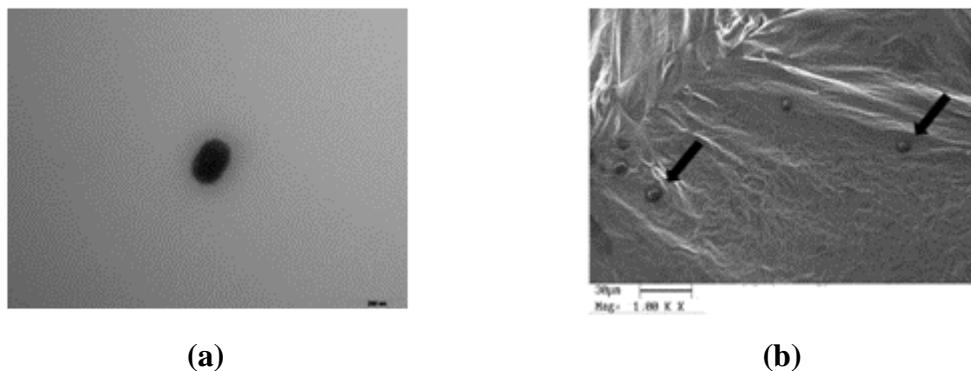


Figure 8. (a) Transmission electron micrograph (TEM) (b) Scanning electron micrograph (SEM).

4.0. Conclusion

Results obtained showed that SLN are promising to vehicle label and hydrophilic drugs. The method of production demand low costs. SLN showed citotoxicity dependent concentration and less toxic in Caco-3 culture cells. SLN are stable for up to 24 h in the presence of HSA since no NP aggregates where detected. SLN presented spherical morphology. This carrier is promising to of administration label drugs.

Acknowledgement

The authors wish to acknowledge the sponsorship of the FAPESP (Fundação de Amparo a Pesquisa do Estado de São Paulo) and CAPES (Coordenação de Aperfeiçoamento de Pessoal de Nível Superior).

5.0. References

1. PhRMA. Medicines in Development - Biotechnology. Washington, DC2011.

2. Frokjaer S, Otzen DE. Protein drug stability: a formulation challenge. *Nat Rev Drug Discov*2005;4(4):298-306.
3. Yang R, Gao R, Li F, He H, Tang X. The influence of lipid characteristics on the formation, in vitro release, and in vivo absorption of protein-loaded SLN prepared by the double emulsion process. *Drug Dev Ind Pharm* 2011;37(2):139-48.
4. Zhang X, Sun M, Zheng A, Cao D, Bi Y, Sun J. Preparation and characterization of insulin-loaded bioadhesive PLGA nanoparticles for oral administration. *Eur J Pharm Sci*2012;45(5):632-8.
5. SJ P, SG C, E D, JS P. Encapsulation enhancement and stabilization of insulin in cationic liposomes. *Int J Pharm*2011;415(1-2):267-72.
6. Severino P, Pinho SC, Souto EB, Santana MH. Polymorphism, crystallinity and hydrophilic-lipophilic balance of stearic acid and stearic acid-capric/caprylic triglyceride matrices for production of stable nanoparticles. *Colloids Surf B Biointerfaces*2011;86(1):125-30.
7. Severino P, Pinho SC, Souto EB, Santana MHA. Crystallinity of Dynasan®114 and Dynasan®118 matrices for the production of stable Miglyol®-loaded nanoparticles *J Therm Anal Calorim* 2011.
8. Helgason T, Awad TS, Kristbergsson K, Decker EA, McClements DJ, Weiss J. Impact of Surfactant Properties on Oxidative Stability of beta-Carotene Encapsulated within Solid Lipid Nanoparticles. *Journal of Agricultural and Food Chemistry*2009;57(17):8033-40.
9. Zhang J, Smith E. Percutaneous permeation of betamethasone 17-valerate incorporated in lipid nanoparticles. *J Pharm Sci* 2011;100(3):896-903.

10. Xie S, Pan B, Shi B, Zhang Z, Zhang X, Wang M, et al. Solid lipid nanoparticle suspension enhanced the therapeutic efficacy of praziquantel against tapeworm. *Int J Nanomedicine*2011;6:2367-74.
11. Das S, Chaudhury A. Recent advances in lipid nanoparticle formulations with solid matrix for oral drug delivery. *AAPS PharmSciTech*2011;12 (1):62-76.
12. Severino P, Souto EB, Pinho SC, Santana MH. Hydrophilic coating of mitotane-loaded lipid nanoparticles: Preliminary studies for mucosal adhesion. *Pharm Dev Technol*2011;In press.
13. Schmidts T, Dobler D, Nissing C, Runkel F. Influence of hydrophilic surfactants on the properties of multiple w/o/w emulsions. *J Colloid Interface Sci*2009;338(1):184-92.
14. Robyt JF, White BJ. *Biochemical Techniques - Theory and Practices*. Chicago: Waveland; 1990.
15. de Ven HV, Vermeersch M, Shunmugaperumal T, Vandervoort J, Maes L, Ludwig A. Solid lipid nanoparticle (SLN) formulations as a potential tool for the reduction of cytotoxicity of saponins. *Pharmazie*2009;64(3):172-6.
16. Hamid R, Rotshteyn Y, Rabadi L, Parikh R, Bullock P. Comparison of alamar blue and MTT assays for high through-put screening. *Toxicol In Vitro*2004;18(5):703-10.
17. O'Brien J, Wilson I, Orton T, Pognan F. Investigation of the Alamar Blue (resazurin) fluorescent dye for the assessment of mammalian cell cytotoxicity. *Eur J Biochem*2000;267(17):5421-6.
18. Štěpánek P. Static and dynamic properties of multiple light scattering. *J Chem Phys* 1993;99:6384-93J.
19. Štěpánek P. *Dinamic Light Scattering; the method and some applications*. Press OU, editor. New York1993.

20. Štěpánek P, Koňák Č. *Advances in Colloid and Interface Science*. 1984;21:195-274.
21. Schmidts T, Dobler D, Schlupp P, Nissing C, Garn H, Runkel F. Development of multiple W/O/W emulsions as dermal carrier system for oligonucleotides: effect of additives on emulsion stability. *Int J Pharm*2019;398(1-2):107-13.
22. Teskac K, Kristl J. The evidence for solid lipid nanoparticles mediated cell uptake of resveratrol. *Int J Pharm* 2010;390(1):61-9.
23. Frenkel M, Shwartz R, Garti N. Multiple emulsions: I. Stability: Inversion, apparent and weighted HLB. *Journal of Colloid and Interface Science*1983;94(1983):174-8.
24. Yang R, Gao RC, Cai CF, Xu H, Li F, He HB, et al. Preparation of gel-core-solid lipid nanoparticle: a novel way to improve the encapsulation of protein and peptide. *Chem Pharm Bull (Tokyo)*2011 Sep;58(9):1195-202.
25. Bunjes H, Unruh T. Characterization of lipid nanoparticles by differential scanning calorimetry, X-ray and neutron scattering. *Adv Drug Deliv Rev*2007 Jul 10;59(6):379-402.
26. Silva AC, González-Mira E, García ML, Egea MA, Fonseca J, Silva R, et al. Preparation, characterization and biocompatibility studies on risperidone-loaded solid lipid nanoparticles (SLN): high pressure homogenization versus ultrasound. *Colloids Surf B Biointerfaces*2011;86(1):158-65.
27. Shi F, Zhao JH, Liu Y, Wang Z, Zhang YT, Feng NP. Preparation and characterization of solid lipid nanoparticles loaded with frankincense and myrrh oil. *International Journal of Nanomedicine*2012;7:2033-43.
28. Severino P, Pinho SC, Souto EB, Santana MHA. Polymorphism, crystallinity and hydrophilic-lipophilic balance of stearic acid and stearic acid-capric/caprylic triglyceride

matrices for production of stable nanoparticles. *Colloids and Surfaces B-Biointerfaces*2011;86(1):125-30.

29. Gibon V, Durant F, Deroanne C. Polymorphism and intersolubility of some palmitic, stearic and oleic triglycerides: PPP, PSP and POP *Journal of the American Oil Chemists' Society*1986;63(8):1047-55.

30. Jia L, Shen J, Zhang D, Duan C, Liu G, Zheng D, et al. In vitro and in vivo evaluation of oridonin-loaded long circulating nanostructured lipid carriers. *Int J Biol Macromol*2012;50(3):523-9.

31. Xu Z, Chen L, Gu W, Gao Y, Lin L, Zhang Z, et al. The performance of docetaxel-loaded solid lipid nanoparticles targeted to hepatocellular carcinoma. *Biomaterials*2009;30(2):226-32.

32. Muller RH, Ruhl D, Runge S, SchulzeForster K, Mehnert W. Cytotoxicity of solid lipid nanoparticles as a function of the lipid matrix and the surfactant. *Pharmaceutical Research*1997;14(4):458-62.

33. Tabatt K, Sameti M, Olbrich C, Muller RH, Lehr CM. Effect of cationic lipid and matrix lipid composition on solid lipid nanoparticle-mediated gene transfer. *European Journal of Pharmaceutics and Biopharmaceutics*2004;57(2):155-62.

34. Peters Jr. in *All About Albumins: Biochemistry, Genetics and Medical Applications*. Academic Press, San Diego1996.

35. Rodriguez-Emmenegger C, Jäger A, Jäger E, Stepanek P, Alles AB, Guterres SS, et al. Polymeric nanocapsules ultra stable in complex biological media. *Colloids Surf B Biointerfaces*2011;83(2):376-81.

36. C. Rodriguez-Emmeneger, A. Jäger, E. Jäger, P. Stepánek, A. Bollogna-Alles, S. S. Guterres, et al. *Colloids Surf, B*2011;83:376-81.

37. Giacomelli FC, Štěpánek P, Giacomelli C, Schmidt V, Jäger A, Jäger E, et al. Soft Matter 2011.
38. Göppert TM, Müller RH. Plasma protein interactions of Tween 80- and poloxamer 188-stabilized SLN. Journal of Drug Targeting 2003;11(4):225-31.

Capítulo 3

Development Cationic Lipid carrier for transfection cell

Patrícia Severino^{1,2}, Marcelo Szymanski², Marianna Favaro², Adriano R. Azzoni², Eliana B. Souto³, Maria Helena A. Santana¹.

¹*Faculdade de Engenharia Química, Departamento de Engenharia de Materiais e Bioprocessos (DEMBio), Universidade Estadual de Campinas, Unicamp, Campinas, SP, Brazil.*

²*Centro de Biologia Molecular e Engenharia, Genética, Departamento de Genética e Evolução, Instituto de Biologia, Universidade Estadual de Campinas, Campinas, SP, Brazil.*

³*Faculdade de Ciências da Saúde, Universidade Fernando Pessoa, Porto, Portugal*

Article in submission

Abstract

The aim of present work is to produced a cationic solid lipid nanoparticle (SLN). The cationic SLN was produced by double emulsion method, and it was composed of softisan[®] 100, cetyltrimethylammonium bromide (CTAB), tween[®] 80, span[®] 80, glycerol and lipoid[®] S75 loading model protein. The formulation was characterized by size (z-ave), polispersity index (PI), zeta potential (ZP), stability of storage, stability after lyophilization, effect of toxicity and ability to transfection in HeLa cells, release profile *in vitro* and morphology. SLN was stable for 30 days and showed minimal change after lyophilization. It exhibited relatively lower release, spherical morphology and it was able to transfect, but toxicity is still an obstacle. Results suggest that NLS are most promising for delivery of proteins or acid nucleic.

1. Introduction

New perspectives for treatment and prevention of untreatable diseases are emerging with gene therapy (1). Non viral transfection agents have recently been investigated for *in vitro* and *in vivo* applications in gene delivery (2). Nano-vector has been focused due to biocompatibility, safety (3), less immunogenic, relatively easy to produce on a large scale, and able to be modified (1, 4, 5), although low transfection efficiencies (3). Cationic lipid nanocarriers as liposomes (6), emulsions (7), and solid lipid nanoparticles (2, 8, 9) are used to transfection of proteins and nucleic acids.

Cationic SLN are promising to produced non viral vector because are easy to produce in large scale, low cost and reduced time production (10). Vighi et al., 2012 (8), Vighi et al., 2010 (11), Olbrich et al., 2001 (12), Rudolph et al., 2012 (13) and others researches showed that cationic SLN were able to transfect cells.

For transfection in cells are necessary cationic surface properties. It can be produced adding benzalkonium chloride (14), cetylpyridinium chloride (15), cetyltrimethylammonium bromide (CTAB), Dimethyldioctadecylammonium (DDAB) and (N-[1-(2,3-Dioleoyloxy)propyl]-N,N,N-trimethylammonium methyl-sulfate) (DOTAP) (16), hexadecyl-PTA iodide and octadecyl-PTA iodide (17, 18). Therefore, it determine physical and chemical characteristics, increase bioavailability of active delivery, intracellular penetration, destination in blood circulation, rate of clearance and targeting ability (19-21).

Our group, Severino et al., 2012 (22) has development SLN by double emulsion method. A 2^2 factorial design with triplicate at the central point was used to evaluate ideal concentration of surfactant and model protein. The properties of the size (z-ave), polydispersity index (PI), zeta potential (ZP), efficiency of encapsulation (EE), thermal analysis (Differential Scanning Calorimetry (DSC) and Wide Angle X-Ray Diffraction

(WAXD)), the effect of toxicity in cells HepG-2 and Caco-3, *in vitro* stability and morphology. Results showed promising.

The purpose of this study was to continue the investigation of SLN adding CTAB as cationic lipid. The cationic SLN was produced with protein models and characterized by z-ave, PI, ZP, EE, stability of storage, stability after lyophilization, effect of toxicity and ability to transfect in HeLa cells, and morphology.

2. Material e methods

3.1. Material

Glycerides of hydrogenated coconut (Softisan[®] 100) was gift by Sasol. Polysorbate 80 (Tween[®] 80) and Coomassie blue were obtained by Sigma. Mono/oleate sorbitan oleate (Span[®] 80) was donated by Croda, soya lecitin hydrogenated (Lipoid[®] S75) were donated as a gift from Lipoid; Cetyltrimethylammonium bromide (CTAB) was obtained by Vetec. F-12 medium and fetal bovine serum were obtained by Gibco. Double distilled water was used after filtration in a Millipore system (home supplied).

3.2. Methods

3.2.2. SLN preparation

SLN was produced according Severino et al., 2012 (22). The method double emulsion (w/o/w) was chosen to avoid high temperatures that may degrade the protein. For the production of internal aqueous phase (IP) (insulin and water) and the lipid phase (LP) (490 mg Softisan[®] 100, 10 mg CTAB, 5 mL glycerol, 0.22g Span[®] 80, 0.10g Lipoid[®] S75) were, separately, heated to 10 °C above the lipid phase transition. The IP was added in LP and

homogenized with high shear homogenization (Ultra-Turrax[®], IKA, T25, German) for 10 minutes, intensity of 10.000 rpm and maintaining heating. A part of external aqueous phase (EP) cooled (0.25 g Tween[®] 80 and 40 mL water) was added in emulsion (w/o) previously formed. It was maintained by high shear homogenization for 2 minutes at 10.000 rpm. Then, it was transferred to magnetic stirring (Tecnal, TE-0851, Brazil), and added to another part of the EP and kept in agitation for 20 minutes.

3.2.3. Particle size, polydispersity, and zeta potential analysis

The SLN was evaluated with respect to the hydrodynamic mean size, PI, and ZP. The mean size was determined by Dynamic Light Scattering (DLS; Zetasizer Nano NS, Malvern, UK). The samples were diluted with ultrapurified water to weaken the opalescence before particle size measurements. ZP was analyzed in NaCl 0.9% adjusting conductivity to 50 $\mu\text{S}/\text{cm}$. The ZP was calculated from the electrophoretic mobility using the Helmholtz–Smoluchowski equation. The analysis was performed using the software included in the system.

3.2.4. Encapsulation efficiency (EE)

The protein encapsulated into SLN was dosed by the method of Bradford, adapted by Robyt e White, 1990 (23). The preparation of the calibration curve consisted in aqueous solution of albumin at a concentration of 0.001 g/mL and an aqueous solution of *Coomassie blue* at a concentration of 0.1 g/mL. The reading was held in spectrophotometer at a wavelength of 595nm, with a quartz cuvette. The calibration curve was performed with concentrations of 0, 10, 15, 20, 25, 30, 40, 50, 70, 90, 110, 140, 170, 200, 230, 270, 310, 350, 400, 400, 450, 500, 600 mg/mL. To determine the EE of SLN samples were ultra

filtration (Amicon, Beverly, USA) using ultrafiltration membranes (Millipore, NMWL 30,000, Billerica, USA) and 500 uL of the supernatant was added to a solution of Coomassie blue, followed by agitation. Then EE was calculated from Equation 2.

$$EE (\%) = \frac{(\text{total of protein IP}) - (\text{total of protein supernatant})}{(\text{total of protein IP})} \times 100 \quad \text{Equation 2}$$

3.4.5. Stability testing

SLN was stored in amber flask at 4°C. Particle size was monitored z-ave, PI and ZP. It was analysed in time zero, 24 hours, 15 and 30 days.

3.4.6. Stability after liofilization

Approximately 5.0 g of formulation were placed in a flask and frozen at - 80 ° C, after the samples were lyophilized for 48 hours using a vacuum pump followed by a steam condenser. After lyophilization, the formulation was reconstituted Milli'Q in water and sonicator 60 min. (Cole-Parmer, 8890, Illinois, USA). The average z-ave, PI, ZP and EE were determined.

3.4.6. In vitro release experiment

The protein release from SLN was performed using a bag method. The dialysis bag retains SLN and allows the free protein into dissolution media. The bags were soaked in Milli-Q water for 12 h before use. Two milliliters of SLN were poured into the bag with two ends fixed by clamps. The bags were placed in a flask and 200 mL phosphate buffer (pH 7.4) receiving phase was added. The flask was placed into a thermostatic shaker (New Brunswick, USA) 37 °C at rate of 140 times per min. At predetermined time intervals, 1

mL samples were withdrawn and centrifuged 20.000 rpm for 20 min (Eppendorf, 5417R, USA). The supernatant was assayed for protein release and it was determined by the method of Bradford. All samples were analyzed in triplicate.

3.4.7. WST-1 citotoxicity test

The citotoxicity of cationic SLN in HeLa cells was assessed by Cell Proliferation Reagent WST-1 (Roche Applied Science, USA) following manufacturer's instructions. WST is a colorimetric assay for quantification of cell proliferation and cytotoxicity based on the cleavage of the tetrazolium salt WST-1 by mitochondrial dehydrogenases in viable cells. Firstly, cell culture HeLa was cultivated in flasks with complete medium (F-12 nutrient mixture containing 10% (v/v) fetal bovine serum, growth medium) and incubated (37 °C, 5% CO₂). Then, the supernatants were removed and washed with PBS, after that 6 mL of trypsin, maintained at 37 °C for 5 minutes in order to disaggregate and spread cells. Cell culture HeLa was centrifuged for 5 minutes and 1,000 rpm, the supernatant was removed and added 9 mL PBS and 1 mL FBS and homogenous. Then, 1 ml cell culture HeLa was diluted in 9 ml of PBS and cell counts of Neubauer camera resulting in 3.4×10^5 cells/mL. After this time, each well was added 5×10^3 cells/well and waited 36 hours. Then, removed the complete medium and added 100 µL of SLN in 4 different dilutions (1%, 2%, 5% and 10% SLN), in each well and incubated for 24 hours. After that, 15 µl WST was added in each well and incubated for 2 hours then held a reading in a microplate reader (SpectraMax Plus 384 UV/Vis cuvette/microplate reader Molecular Devices, EUA) at wavelengths 440 nm.

3.4.8. Culture and transfection of HeLa cells

HeLa cells were grown in F-12 (Ham) nutrient mixture containing 10% (v/v) fetal bovine serum (growth medium). All cell cultures were performed in 75 cm² culture flasks and incubated in 5% CO₂ humidified environment at 37°C. Following growth up to confluence, cells were trypsinized and seeded in 24 well culture plates (5 x 10⁴ cells per well). The cells were incubated for 48 hours (to a 70% confluence) and then transfected with pDNA:protein complexes formed as described previously in the presence of SLN (concentration 1%, 2%, 5% and 10%). In the present work we used as model protein the human Dynein light chain Lc8 with an N-terminal His₆-tag kindly provided by Toledo and collaborators (24). The medium containing the transfection solution remained on the cell containing wells for 4 hours. Afterwards, cells were extensively washed with PBS and collected with Cell Lysis Reagent from Lusing the luciferase Assay System (Promega, USA). HeLa cells protein extract were concentrated with 12.5% trichloroacetic acid (TCA). Pelleted samples were resuspended in SDS-PAGE loading buffer and denatured at 94° for 5 min.

3.4.8. Western blot analysis

Transfection samples were resolved SDS-PAGE and were transferred to a 0.45-µm Potran BA 85 Nitrocellulose membrane (Whatman, Dassel, Germany) by a Semi-Dry Transfer Cell (BioRad, CA, USA). The transferred membrane was incubated with the specific anti His₆-tag antibody at a dilution of 1:4000 for 16 hours followed by incubation with a secondary antibody linked to an alkaline phosphatase (goat anti-rabbit IgG-AP, Souza-Cruz, Brazil) at a dilution of 1:8000 for another 2 hours. *Western blots* were developed with BCIP/NBT Color Development Substrate (Promega, Madison, Wisconsin, USA) following the manufacturer's instructions.

3.4.9. Transmission Electron Microscope (TEM) analysis

The morphology of SLN was performed using a Transmission Electron Microscope (LEO 906 E, Leo Electron). SLN was placed on a copper grid, and then a drop of 1 % uranyl acetate was added and dry for observation.

4. Results and discussion

Preliminary studies for development this SLN without charge was realized by Severino et al., 2012 (22). Tween[®] 80 was used because are known it increase ability of intracellular penetration and evicting aggregates in emulsion (25-27). Span[®] 80 and Tween[®] 80 were used to obtain exact Hydrophilic Lipophilic balance (HLB). Therefore, the blend of surfactants (polysorbate and sorbitan monooleate) promote more stability (28, 29). Lecithin was used to maintain more stable lipid droplets in formulation. This formulation to produce stable cationic SLN with a z-ave of 125.4 ± 3.9 nm, 0.213 ± 0.023 PI, 50.8 mV ± 3.72 ZP. Insulin loading SLN was z-ave of 103 ± 1.7 nm, 0.219 ± 0.006 PI, 34.8 mV ± 1.0 ZP, 79% ± 6.8 EE.

Stability is an important characteristic for pharmaceutical products. The stability test, SLN was stored in amber glass flask at 4 °C. Particle size, PI, ZP and EE was measurements for 30 days are given in Table 1. In this period SLN and insulin loaded SLN showed minimal changes. The results obtained are acceptable that cationic SLN are more stable than non charge or negative charge. Long stability of SLN are demonstrate by others groups (30-33). The process of lyophilization was studied to evaluate reconstituted of SLN. It is important after reconstituted the formulation maintain their physicochemical properties. The

formulation development in present work showed promising to storage in lyophilized form, according Table 2. Howard et al., 2012 (34) obtained similar results with SLN that exhibited stability, minimal change in the particle size and drug expulsion.

Table 1. Particle size, polydispersity index, zeta potential and entrapment efficiency of SLN formulations, (n = 3). SLN: empty SLN; I-SLN: insulin loaded SLN.

Time	Sample	z-ave (nm)	PdI	ZP (mV)	EE (%)
24 hours	SLN	127.4 ± 0.550	0.223 ± 0.005	+29.4 ± 2.45	-
	I-SLN	110.6 ± 3.989	0.234 ± 0.093	+22.4 ± 1.06	75.4 ± 2.5
15 days	SLN	158.5 ± 3.415	0.395 ± 0.007	+23.6 ± 2.5	-
	I-SLN	133.0 ± 5.99	0.372 ± 0.032	+20.5 ± 0.45	70.9 ± 3.4
30 days	SLN	178 ± 4.405	0.465 ± 0.012	+24.1 ± 3.33	-
	I-SLN	139.3 ± 2.004	0.353 ± 0.017	+16.9 ± 2.25	65.9 ± 4.2

Table 2. Stability of SLN after liophilization (n = 3). SLN: empty SLN; I-SLN: insulin loaded SLN.

Sample	z-ave (nm)	PdI	ZP (mV)	EE (%)
SLN	203.0 ± 2.740	0.407 ± 0.029	+14.44 ± 0.079	-
I-SLN	169.9 ± 3.041	0.440 ± 0.057	+23.89 ± 0.590	75.89 ± 5.7

Figure 1 shows protein release profiles of protein and insulin loading SLN (I-SLN). A burst protein free protein release. I-SLN obtained depicted a controlled release, attributed to encapsulation.

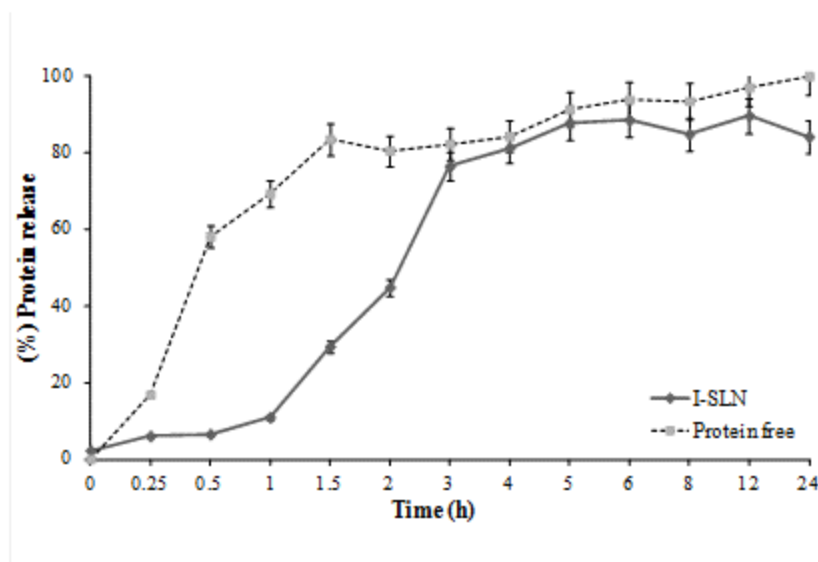


Figure 1. Release profile of protein vs time by double emulsion method (Protein-free: aqueous solution of protein; I-SLN: insulin loaded SLN). The results are average values (n=3).

Cytotoxicity of cationic SLN in HeLa cells was determined by means of WST-1 cytotoxicity test, after incubation of cells for 24 h. The formulation reduced the viability of HeLa in a concentration dependent manner are given Figure 2. And, it showed toxicity dependent concentration due to cationic molecule. It is known CTAB and others cationic molecules are toxicity (12, 35), but it is necessary to carry nucleic acid and proteins for intracellular cell (16, 36).

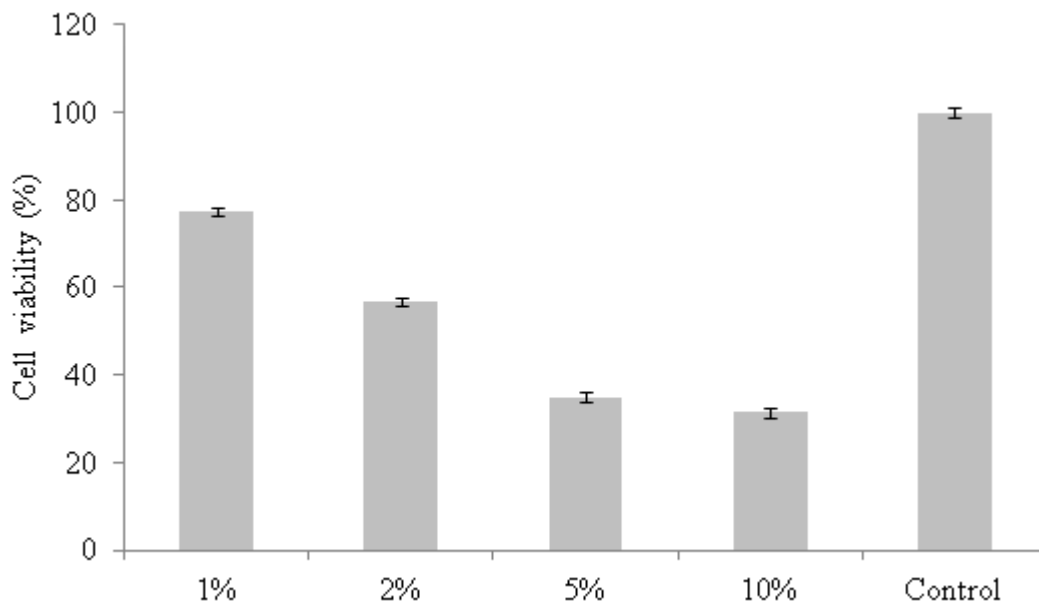


Figure 2. Cell viability determined by WST-1 assay SLN empty after exposition to SLN formulations (concentration 1%, 2%, 5% and 10%) and control prepared by double emulsion technique. The results are average values (n=6).

This essay was realized to study the transfection efficacy of cationic SLN loading model protein by Western blot technique. As shown in Figure 3, SLN was able to promote transfection in HeLa cells. Wangyang et al., 2009 (37) produced SLN with CTAB. Results showed able to tranfection DNA in A549 cell line and the HeLa cell line.

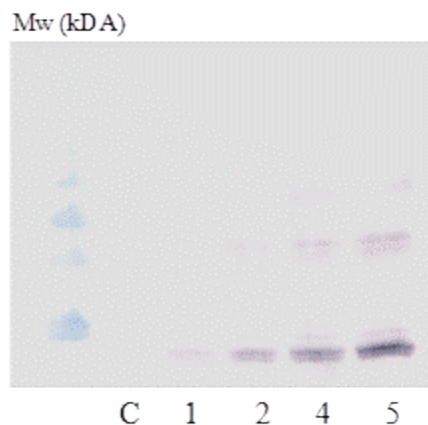


Figure 3. SLN loading Lc8 incubated for 4 h and detected western blot technique. C: control; 1: SLN concentration 1 %, 2: SLN concentration 2 %, 3: SLN concentration 5 %, 4: SLN contraction 10 %. The results are average values (n=3).

Microscopy images analyzed by TEM of empty SLN are presented in Figure 4. SLN showed spherical morphology.

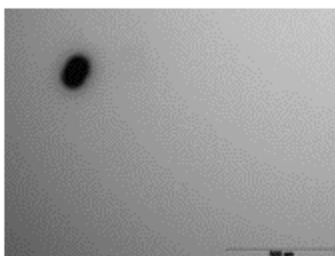


Figure 4. Transmission electron microscopy images of SLN.

5. Conclusion

Results of this study show that cationic solid lipid nanoparticles can be successfully prepared by the double emulsion method as potential protein delivery systems. The production is easy, fast and demand low cost. Therefore, SLN showed stable for 30 days and after lyophilization process. In vitro studies SLN obtained a controlled release and it

was able to the transfection in HeLa cells, but cytotoxicity was an obstacle in non viral protein/gene delivery.

Acknowledgement

The authors wish to acknowledge the sponsorship of the FAPESP (Fundação de Amparo a Pesquisa do Estado de São Paulo) and CAPES (Coordenação de Aperfeiçoamento de Pessoal de Nível Superior).

References

1. Jiang Z, Sun C, Yin Z, Zhou F, Ge L, Liu X, et al. Comparison of two kinds of nanomedicine for targeted gene therapy: premodified or postmodified gene delivery systems. *Int J Nanomedicine*2012;7:2019-31.
2. Tabatt K, Sameti M, Olbrich C, Muller RH, Lehr CM. Effect of cationic lipid and matrix lipid composition on solid lipid nanoparticle-mediated gene transfer. *Eur J Pharm Biopharm*2004 Mar;57(2):155-62.
3. Liu Z, Zhong Z, Peng G, Wang S, Du X, Yan D, et al. Folate receptor mediated intracellular gene delivery using the charge changing solid lipid nanoparticles. *Drug Deliv*2009 Aug;16(6):341-7.
4. Boulaiz H, Marchal JA, Prados J, Melguizo C, Aranega A. Non-viral and viral vectors for gene therapy. *Cell Mol Biol (Noisy-le-grand)*2005;51(1):3-22.
5. Torchilin VP. Multifunctional nanocarriers. *Adv Drug Deliv Rev*2006 Dec 1;58(14):1532-55.

6. Brgles M, Santak M, Halassy B, Forcic D, Tomasic J. Influence of charge ratio of liposome/DNA complexes on their size after extrusion and transfection efficiency. *Int J Nanomedicine*2012;7:393-401.
7. Bozelli JC, Jr., Sasahara ET, Pinto MR, Nakaie CR, Schreier S. Effect of head group and curvature on binding of the antimicrobial peptide tritrpticin to lipid membranes. *Chem Phys Lipids*2012 May;165(4):365-73.
8. Vighi E, Montanari M, Ruozi B, Iannucelli V, Leo E. The role of protamine amount in the transfection performance of cationic SLN designed as a gene nanocarrier. *Drug Deliv*2012 Jan;19(1):1-10.
9. Choi SH, Jin SE, Lee MK, Lim SJ, Park JS, Kim BG, et al. Novel cationic solid lipid nanoparticles enhanced p53 gene transfer to lung cancer cells. *Eur J Pharm Biopharm*2008 Mar;68(3):545-54.
10. Severino P, Santana MH, Souto EB. Optimizing SLN and NLC by 2² full factorial design: Effect of homogenization technique. *Materials Science and Engineering C* 2012;32:1375-9.
11. Vighi E, Ruozi B, Montanari M, Battini R, Leo E. pDNA condensation capacity and in vitro gene delivery properties of cationic solid lipid nanoparticles. *Int J Pharm*2010 Apr 15;389(1-2):254-61.
12. Olbrich C, Bakowsky U, Lehr CM, Muller RH, Kneuer C. Cationic solid-lipid nanoparticles can efficiently bind and transfect plasmid DNA. *J Control Release*2001 Dec 13;77(3):345-55.
13. Rudolph C, Rosenecker J. Formation of Solid Lipid Nanoparticle (SLN)-Gene Vector Complexes for Transfection of Mammalian Cells In Vitro. *Cold Spring Harb Protoc* 2012;In press.

14. Severino P, Souto EB, Pinho SC, Santana MH. Hydrophilic coating of mitotane-loaded lipid nanoparticles: Preliminary studies for mucosal adhesion. *Pharm Dev Technol*2011 Sep 29.
15. Taveira SF, Araujo LM, de Santana DC, Nomizo A, de Freitas LA, Lopez RF. Development of cationic solid lipid nanoparticles with factorial design-based studies for topical administration of doxorubicin. *J Biomed Nanotechnol*2012 Apr;8(2):219-28.
16. Carbone C, Tomasello B, Ruozi B, Renis M, Puglisi G. Preparation and optimization of PIT solid lipid nanoparticles via statistical factorial design. *Eur J Med Chem*2012 Mar;49:110-7.
17. Cortesi R, Bergamini P, Ravani L, Drechsler M, Costenaro A, Pinotti M, et al. Long-chain cationic derivatives of PTA (1,3,5-triaza-7-phosphaadamantane) as new components of potential non-viral vectors. *Int J Pharm*2012 Jul 15;431(1-2):176-82.
18. Tabatt K, Sameti M, Olbrich C, Muller RH, Lehr CM. Effect of cationic lipid and matrix lipid composition on solid lipid nanoparticle-mediated gene transfer. *European Journal of Pharmaceutics and Biopharmaceutics*2004 Mar;57(2):155-62.
19. Juillerat-Jeanneret L, Schmitt F. Chemical modification of therapeutic drugs or drug vector systems to achieve targeted therapy: looking for the grail. *Med Res Rev*2007 Jul;27(4):574-90.
20. Doktorovova S, Shegokar R, Martins-Lopes P, Silva AM, Lopes CM, Muller RH, et al. Modified Rose Bengal assay for surface hydrophobicity evaluation of cationic solid lipid nanoparticles (cSLN). *Eur J Pharm Sci*2012 Apr 11;45(5):606-12.
21. Doktorovova S, Shegokar R, Rakovsky E, Gonzalez-Mira E, Lopes CM, Silva AM, et al. Cationic solid lipid nanoparticles (cSLN): structure, stability and DNA binding capacity correlation studies. *Int J Pharm*2011;420(2):341-9.

22. Severino P, Andreani A, Jäger A, Santana MHA, Silva AM, Souto EB. Development potential solid lipid nanoparticles carrier for vehicle protein (Submitted). 2012.
23. Robyt JF, White BJ. Biochemical Techniques - Theory and Practices. Chicago: Waveland; 1990.
24. Toledo MA, Janissen R, Favaro MT, Cotta MA, Monteiro GA, Prazeres DM, et al. Development of a recombinant fusion protein based on the dynein light chain LC8 for non-viral gene delivery. *J Control Release* 2012;159(2):222-31.
25. Liu CH, Yu SY. Cationic nanoemulsions as non-viral vectors for plasmid DNA delivery. *Colloids Surf B Biointerfaces* 2012 Sep 1;79(2):509-15.
26. Choi WJ, Kim JK, Choi SH, Park JS, Ahn WS, Kim CK. Low toxicity of cationic lipid-based emulsion for gene transfer. *Biomaterials* 2004 Dec;25(27):5893-903.
27. del Pozo-Rodriguez A, Delgado D, Solinis MA, Gascon AR, Pedraz JL. Solid lipid nanoparticles: formulation factors affecting cell transfection capacity. *Int J Pharm* 2007 Jul 18;339(1-2):261-8.
28. Griffin WC. Classification of Surface Active Agents by HLB. *J Soc Cosmet Chem* 1949;1:311-26.
29. Griffin WC. Calculation of HLB values of Nonionic Surfactants. *J Soc Cosmet Chem* 1954;5:249-56.
30. Wang Y, Zhu L, Dong Z, Xie S, Chen X, Lu M, et al. Preparation and stability study of norfloxacin-loaded solid lipid nanoparticle suspensions. *Colloids Surf B Biointerfaces* 2012 Oct 1;98:105-11.
31. Siddiqui A, Patwardhan GA, Liu YY, Nazzal S. Mixed backbone antisense glucosylceramide synthase oligonucleotide (MBO-asGCS) loaded solid lipid nanoparticles:

in vitro characterization and reversal of multidrug resistance in NCI/ADR-RES cells. *Int J Pharm*2010 Nov 15;400(1-2):251-9.

32. Doktorovova S, Shegokar R, Rakovsky E, Gonzalez-Mira E, Lopes CM, Silva AM, et al. Cationic solid lipid nanoparticles (cSLN): structure, stability and DNA binding capacity correlation studies. *Int J Pharm*2012 Nov 28;420(2):341-9.

33. Liu J, Gong T, Wang C, Zhong Z, Zhang Z. Solid lipid nanoparticles loaded with insulin by sodium cholate-phosphatidylcholine-based mixed micelles: preparation and characterization. *Int J Pharm*2007 Aug 1;340(1-2):153-62.

34. Howard MD, Lu X, Jay M, Dziubla TD. Optimization of the lyophilization process for long-term stability of solid-lipid nanoparticles. *Drug Dev Ind Pharm*2012 Jan 12.

35. Nassimi M, Schleh C, Lauenstein HD, Hussein R, Hoymann HG, Koch W, et al. A toxicological evaluation of inhaled solid lipid nanoparticles used as a potential drug delivery system for the lung. *Eur J Pharm Biopharm*2012 Jun;75(2):107-16.

36. Simberg D, Weisman S, Talmon Y, Barenholz Y. DOTAP (and other cationic lipids): chemistry, biophysics, and transfection. *Crit Rev Ther Drug Carrier Syst*2004;21(4):257-317.

37. Yu W, Liu C, Ye J, Zou W, Zhang N, Xu W. Novel cationic SLN containing a synthesized single-tailed lipid as a modifier for gene delivery. *Nanotechnology*2009 May 27;20(21):215102.

Conclusões finais

Analisando os resultados obtidos com a produção das NLS para encapsulação de proteínas, pode-se concluir que:

- As misturas lipídicas (Dynasan[®]114, Dynasan[®]118, Miglyol[®]812, Miglyol[®]840 e Crodamol[®] GTCC e ácido esteárico) estudadas por calorimetria diferencial de varredura, difração de raios-X e microscopia de luz polarizada mostraram promissoras para produção das NLS. Ressaltando que os melhores resultados foram obtidos utilizando a concentração 70% de lipídio sólido e 30% de lipídio líquido;
- As NLS produzidas com Dynasan[®]114, Dynasan[®]118, Miglyol[®]812, Miglyol[®]840 apresentaram tamanho, índice de polidispersidade e potencial zeta promissores para encapsulação de proteínas.
- As NLS produzidas com ácido esteárico e Crodamol[®] GTCC foram estabilizadas empregando o estudo de Equilíbrio Hidrofílico Lipofílico (EHL). A melhor proporção de EHL foi de 13.8 da mistura de tensoativos (Tween[®] e Span[®]).
- O aprimoramento da produção das NLS por planejamento fatorial foi efetivo para otimizar as variáveis do processo. Os resultados apresentados destacam o benefício da aplicação de modelos estatísticos na preparação de uma formulação.
- As NLS produzidas pelo método de emulsão múltipla foram desenvolvidas estudando as variáveis de tensoativo e eficiência de encapsulação da proteína modelos por planejamento fatorial. O método de produção apresentou prático, rápido e de baixo custo. A caracterização mostrou que as NLS apresentam tamanho adequado para

Conclusões finais

administração parenteral, baixa toxicidade em células de HepG-2 e Caco-3, estabilidade por 24 horas na presença de albumina e morfologia esférica.

- A adição de CTAB nas NLS promoveu a mudança da carga superficial para positiva, sendo capaz de transfectar em culturas de células HeLa. As NLS foram estáveis por 30 dias de estocagem e após a liofilização. A formulação obteve uma mais lenta que a proteína livre e morfologia esférica.

Os resultados obtidos com a produção das NLS mostraram satisfatórios para encapsulação de proteínas. As NLS até aqui desenvolvidas obtiveram características físico-químicas promissoras para serem administradas pela via oral e parenteral. Além disso, os resultados obtidos com o desenvolvimento das nanopartículas foram promissores para continuidade dos estudos e serve como alternativa para o desenvolvimento de um produto eficaz de proteger a proteína de degradação e aumentar a biodisponibilidade.

Sugestões para próximos trabalhos

Encapsular proteínas terapêuticas e ácidos nucleicos nas nanopartículas lipídicas e realizar a caracterização;

Avaliação da eficiência de transfecção e citotoxicidade em células HeLa;

Avaliação da resposta imunológica em células dendríticas e;

Avaliação da resposta imunológica *in vivo*.